On Random Sampling for Compliance Monitoring in Opportunistic Spectrum Access Networks

Sean Rocke

A Dissertation
Submitted to the Faculty
of the
WORCESTER POLYTECHNIC INSTITUTE
in partial fulfillment of the requirements for the
Degree of Doctor of Philosophy
in
Electrical and Computer Engineering

April 2013

APPROVED:

Professor Alexander M. Wyglinski Primary Advisor ECE Department WPI	Professor Kaveh Pahlavan Committee Member ECE Department WPI
Professor Donald R. Brown III Committee Member ECE Department WPI	Dr. Kim I. Mallalieu Committee Member ECE Department UWI

Abstract

In the expanding spectrum marketplace, there has been a long term evolution towards more market–oriented mechanisms, such as Opportunistic Spectrum Access (OSA), enabled through Cognitive Radio (CR) technology. However, the potential of CR technologies to revolutionize wireless communications, also introduces challenges based upon the potentially non–deterministic CR behaviour in the Electrospace. While establishing and enforcing compliance to spectrum etiquette rules are essential to realization of successful OSA networks in the future, there has only been recent increased research activity into enforcement.

This dissertation presents novel work on the spectrum monitoring aspect, which is crucial to effective enforcement of OSA. An overview of the challenges faced by current compliance monitoring methods is first presented. A framework is then proposed for the use of random spectral sampling techniques to reduce data collection complexity in wideband sensing scenarios. This approach is recommended as an alternative to Compressed Sensing (CS) techniques for wideband spectral occupancy estimation, which may be difficult to utilize in many practical congested scenarios where compliance monitoring is required.

Next, a low–cost computational approach to online randomized temporal sensing deployment is presented for characterization of temporal spectrum occupancy in cognitive radio scenarios. The random sensing approach is demonstrated and its performance is compared to CS–based approach for occupancy estimation. A novel frame–based sampling inversion technique is then presented for cases when it is necessary to track the temporal behaviour of individual CRs or CR networks. Parameters from randomly sampled Physical Layer Convergence Protocol (PLCP) data frames are used to reconstruct occupancy statistics, taking account of missed frames due to sampling design, sensor limitations and frame errors.

Finally, investigations into the use of distributed and mobile spectrum sensing to collect spatial diversity to improve the above techniques are presented, for several common monitoring tasks in spectrum enforcement. Specifically, focus is upon techniques for achieving consensus in dynamic topologies such as in mobile sensing scenarios.

Acknowledgements

The undertaking of a Ph.D represents an exceptional opportunity for growth and transformation, in addition to the many challenges faced in this achievement. This Ph.D journey can be similarly characterized, and therefore expressions of gratitude need to be given to all those, without whom it would not have been possible to reach to this point.

First, I would like to thank God, through whose blessings, and guidance over the years I have been able to reach this far and to continue to this point. I am further, deeply grateful to my advisor, Professor Alexander M. Wyglinski who has been instrumental in embarking upon this Ph.D at WPI. He was from the moment we met in Cambridge and he invited me to visit WPI in 2009, through the challenges to acquire funding, and through all the many hurdles faced during the program at WPI. His support, eternal optimism, humor, energy, ambition, and vision have been inspirational to me as much as his guidance and insights have been crucial to my progress. It truly has been a pleasure having him as a supervisor.

I am extremely grateful to my thesis committee members: Professor Kaveh Pahlavan, Professor Donald R. Brown III, and Dr. Kim. I. Mallalieu for all the encouragement, insights, feedback and suggestions offered during this Ph.D journey. Their interactions with me have helped me tremendously in shaping my perspectives about the Ph.D process as well as with my dissertation.

I sincerely thank the financial support provided by the U.S. Department of State's Fulbright Program as well as RA support offered through Toyota ITC, and the TA support provided through WPI. I additionally thank the staff of LASPAU and the IIE for their assistance with managing Fulbright students in settling and progressing in their academic programs. At Toyota, I would also like to thank Rama Vuyyuru and Onur Altintas with whom I have further had the pleasure of collaborating with on research while preparing this dissertation. I also express my gratitude to staff at WPI for various forms of assistance provided during my time at WPI: Colleen Sweeney, Robert Brown, Cathy Emmerton, Stacie Murray, Tom Thomsen, Shannon Cotter, Regina Roberto and Jeannette Dalida.

I also thank all of those friends who I have had the opportunity to share this journey with. At WPI, I would like to thank my lab mates in the Wireless Innovation Laboratory

for their friendship: Zhu Fu, Dr. Srikanth Pagaradai, Travis Collins, Dr. Si Chen, Jingkai Su, Travis Collins, Le Wang, Harika Velamala, Amit Sail and Di Pu. I would also like to thank my colleagues at the University of the West Indies, (UWI), who have been extremely supportive during this process: Professor Stephan Gift, Professor Brian Copeland, Gene Francis, Elizabeth Nyack, Gail Hosein, Azim Abdool, Dr. Cathy–Ann Radix, Dr. Musti Sastry, Dr. Akash Pooransingh, Ravi Deonarine, Mark Lessey, Dr. Richelle Adams, Aniel Maharajh and the other participants of the UWI Friday research support group meetings. I also express my thanks to two men I hold dearly as my brothers: Jeevan Persad and David Williams. You have offered so much, so many times, to support and encourage me during this process. Thank you.

Last, but most importantly, I acknowledge that this would never be possible without the love, support and patience of my family. I express my heart–felt thanks to my beloved wife, Camira; my beautiful daughter, Alexis; my loving sister, Renee; my wonderful mother, Judy; and my understanding aunt, Roslyn. Theirs has truly been the biggest sacrifice of all, over this Ph.D as well as during my life. I also express my thanks to my mother–in–law and father–in–law, Barbara and Roopnarine, for their support of my wife and daughter while I have been away. It truly helped to put my mind at ease allowing me to do what was necessary while separated from them. I also say thank you from the bottom of my heart to my aunts and uncles, Pearl & Steve, Winston & Norma, and Marcia & Raymond as well as my cousins Stacy and Sharon for helping me to be comfortable while here at WPI.

Contents

List of Figures

List of Tables

List of Acronyms

ASA	Authorized Shared Access.
BRSS	block–static random spectral sensing.
CR	Cognitive Radio.
CRSS	Collaborative/Distributed Random Spectral Sampling.
CS	Compressed Sensing.
DRSS	dynamic random spectral sensing.
DSA	Dynamic Spectrum Access.
DTV	Digital Television.
EMC	Electromagnetic Compatibility.
FBRTS	Frame–Based Random Temporal Sampling.
FBSE	filter bank spectral estimator.
KBVC	Knowledge–Based Vehicular Communications.
MAC	Medium Access Control.
MRSS	Mobile Random Spectral Sampling.
NCSS	Non–Contiguous Spectral Sampling.
NUSS	Non–Uniform Spectral Sampling.
OSA	Opportunistic Spectrum Access.
PAR	Project Authorization Request.
PLCP	Physical Layer Convergence Protocol.
PU	Primary User.
RAT	Radio Access Technology.
RF	Radio Frequency.

RSS	Random Spectrum Sensing.
SDR	Software–Defined Radio.
SRSS	static random spectral sensing.
SU	Secondary User.
TVWS	Television White Space.
USRP	Universal Software Defined Radio Platform.
VDSA	Vehicular Dynamic Spectrum Access.
WLAN	Wireless Local Area Network.

Chapter 1

Introduction

1.1 Aim

The aim of this research is to investigate random sampling techniques for extraction of wideband wireless spectrum occupancy characteristics from measured data across a geography of interest. The techniques will ultimately be used to statistically quantify the behaviour of existing signals in time, frequency, and space, in order to facilitate monitoring for compliance enforcement of emerging wireless technologies.

1.2 Motivation

In a world that is dependent on information, reliable wireless communications is a vital component of modern civilization. Everyday operations such as financial transactions, public safety operations, educational activities, national defense, and social interactions require some form of wireless communications in order to enable information exchange, which in turn requires access to Radio Frequency (RF) spectrum. In the last few years there has consequently been considerable debate into the ability of current spectrum management approaches to support the growing demand for wireless communications services [1]. Through recent measurement campaigns such as [2–12], there has been evidence to suggest that current spectrum allocation and assignment practices have facilitated artificially–induced spectrum shortage situations in which spectrum has been allocated and assigned but is

underutilized.

Coupled with the increasing demand for multimedia communications services, the artificially induced spectrum shortage has led many to investigate Dynamic Spectrum Access (DSA) techniques, introducing new challenges for spectrum management. DSA encompasses mechanisms for real–time adjustment of spectrum utilization based upon changing circumstances such as changes of the radio's state (*e.g.*, operational mode, battery life, location), changes in environmental and external constraints (*e.g.*, RF spectrum, propagation, operational policies) as well as changing objectives (*e.g.*, efficiency targets, quality of service, graceful degradation guidelines, maximization of radio lifetime) [13].

In support of emerging wireless technologies such as DSA there have been numerous technical enablers. Research into wideband radio front ends and antenna systems, Software–Defined Radio (SDR) systems, as well as the application of theories from diverse fields including economics, networking, artificial intelligence, and signal processing, among others have facilitated the development of CR technology. While it's precursor, SDR, focuses upon increased ability to reconfigure radio interfaces through the use of software radio components, CRs add *awareness*, *agency*, and *intelligent adaptation* elements to SDRs reconfigurability capabilities [14].

CR technology consequently creates numerous opportunities for advanced wireless communications technologies, beyond DSA. In a recent report aimed at quantifying the benefits of CRs [14], several proposed new applications enabled by CRs were identified, including: dynamic spectrum access, self-organizing networks, cognitive jamming systems, cognitive gateways/bridges, real–time spectrum markets, synthetic (cooperative) MIMO, cognitive spectrum management, and cognitive routing. Additionally, identified performance metrics improved through CR deployment included: improving spectrum utilization and efficiency, improving interoperability between legacy and emerging systems, improving link reliability, less expensive radios, enhancing SDR techniques, extended battery life and extended coverage, among others.

However, despite the potential of CR–enabled DSA technologies to revolutionize wireless communications, CRs employing DSA techniques possess the ability to sense, learn and adapt to the RF environment. These characteristics introduce various challenges for

service providers, regulators, and policy–makers. There is growing consensus that current spectrum management practices are ill–suited to address the needs of spectrum governance of emerging wireless network environments (*e.g.*, [15–23]).

Establishing and enforcing compliance to spectrum etiquette rules are essential elements required for realization of successful DSA networks in the future. While several initiatives have been underway to establish appropriate operating parameters for DSA networks, initiatives for addressing the enforcement aspects are not as developed [24]. Perhaps the most compelling concern is the potentially non–deterministic CR behaviour in the Electrospace. Such situations can arise in various ways, such as [25]:

- CR learning algorithms can introduce changing responses to a set of inputs which may be difficult to enumerate or track.
- CRs introduce possibilities for errors through valid software changes or invalid changes due to malicious code, which both can result in the device violating transmission rules.
- CR frequency and waveform agility can introduce scenarios where there is in–band conformance but out–of–band interference, which may be difficult to track.

Furthermore, the shift towards more market–oriented paradigms for spectrum access [21–23, 26–30] has resulted in considerable research into more flexible spectrum access models and access architectures. Consequently management strategies for spectrum allocation, assignment and enforcement are increasingly being shifted away from being traditionally the role of the regulator[1]. In the current communications ecosystem, spectrum management responsibility in vertical service structures, (*e.g.*, cellular, paging) is the Service Provider's. However, in horizontal structures, (*e.g.*, WiFi, secondary markets), the responsibility for spectrum management currently falls upon the primary licensee (if applicable), when in–fact there should also be consideration of the role of the secondary licensee. The introduction of CRs introduces new problems since each CR is in fact now a (possibly non–deterministic) secondary licensee.

[1]Evidence in support of this is the increasing spectrum management decentralization with more responsibility being pushed to Service Providers, Service Users and other stakeholder entities (*e.g.*, Frequency Coordinators and Guard Band Managers [30] as well as White Space Database Administrators [31–33])

To address these issues, both technology and policy interventions are required [15–20]. The extensive debates on the policy impact of CR use for DSA is representative of the complexity of the situation. While the role of spectrum management in this emerging landscape is currently evolving, two key questions naturally arise [25]:

1. *What are the rights of the license holder to prevent unauthorized use by an opportunistic device?*

2. *What kind of assurance can be provided that the interference will exist for only a finite and precise duration, within any protected region?*

In answering these questions, the current debate within the community has highlighted the need for appropriate interference metrics, a suitable interference measurement and analysis system, a viable system deployment strategy, as well as operational mechanisms for data access and arbitration. To support these elements, stakeholders recognize the need for technology–enabling infrastructure to provide secure device operations. Traditional security includes enforcement of spectrum access policies which has historically been primarily accomplished through *equipment authorization*, *software certification*, and *monitoring* mechanisms by the regulator [15–23, 25, 34–37].

In current systems, enforcement of secure device operation is already challenging and resource intensive. Even with more decentralized management models, the envisioned CR–enabled environments introduce new challenges due to the increasing system dynamics and potentially render current approaches ill–suited for future scenarios. Therefore, more flexible security enforcement mechanisms should be contemplated [15–20, 25]. Equipment authorization and software certification are very challenging areas requiring inputs from many sectors to converge on a suitable set of mechanisms and is outside of the scope of this work. This dissertation therefore focuses upon measurement mechanisms for compliance enforcement in DSA scenarios.

Compliance enforcement at the policy level traditionally entails the specification of acceptable transmitter operational parameters such as center frequency, signaling bandwidth, power spectral density, antenna gain, allowable times of operation, and geographic region

for operation, among others[2]. Following definition, suitable thresholds must be established to mitigate effects of harmful operation, (*e.g.*, interference, denial of service). Because of the flexibility offered by DSA, policy definition in terms of fixed parameters may be insufficient for several reasons [25]:

1. Operational parameters should be contextually reflective of real–time spectrum usage, taking account of location and the condition of RF environment.

2. Operational parameters should account for the impact of the transmitter on the surrounding region. Many RF environments typically have complex geometries, possibly with many users which may be mobile.

3. Even with current improvements in propagation models, current approaches are still insufficient for extrapolation in interference analysis in envisioned DSA environments.

Therefore, there is increasing consensus that in situ measurements in support of interference analysis should be facilitated through the deployment of monitoring stations which provide multiple measurements within the operational area of interest (*e.g.*, [24, 25, 34–39]). An example scenario involving a heterogeneous multi–agent wireless spectrum sensing network with fixed and mobile monitoring nodes is illustrated in Fig 1.1.

1.3 Current State of the Art

Assessing the current state–of–the–art in spectrum monitoring requires contemplation of the multi–faceted approach to security enforcement. This involves consideration of initiatives in DSA system deployment, regulation and policy development, standardization development, academic research and recent work on spectrum monitoring initiatives by regulators,service providers and users. The current status of work addressing these aspects are discussed in this section.

Global DSA system deployment is still mostly in the early stages. A key reason for this, is the need for enabling regulatory environments for DSA development and operation.

[2]Technology and service-specific parameters such as transmission delays, bit error rates, and dropped network availability can also be specified.

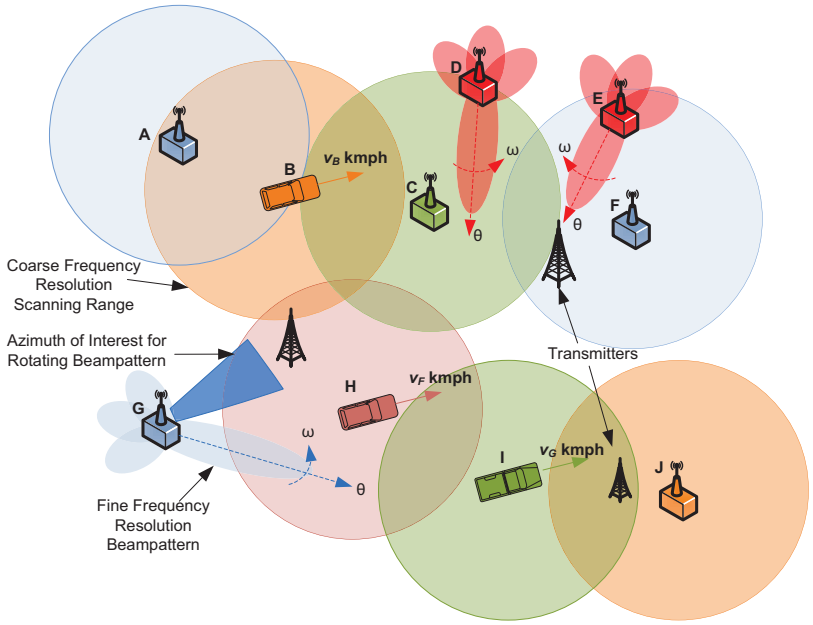

Figure 1.1: An example scenario involving a heterogeneous multi–agent wireless spectrum sensing network with fixed and mobile monitoring nodes. Different colors indicate different sensing configurations such as sampling ratios and sub–band measurements in progress. Some nodes may possess beamforming capabilities which can be used for localization and other enforcement functions not considered in this dissertation.

Following the initial phase of extensive research into DSA operation, over the last few years there has been increasing work in various jurisdictions to provide the enabling mechanisms for DSA. The most advanced jurisdictions at the time of this writing, are the USA and the UK, where there have been extensive regulatory interventions and investigation into using Television White Space (TVWS) to satisfy the anticipated spectrum demand, and achieve greater technical, functional and economic spectrum efficiency [40–43]. In other jurisdictions such as Europe, Canada, Japan, and Singapore, further investigations are underway relating to TVWS deployments. Presently, most regulation and policy development has focussed upon spectrum usage right specification relying upon traditional monitoring mechanisms for security enforcement, given the currently limited deployment. However, in lieu of future development, it is recognised that new approaches are needed for management of future wireless networks [15–20, 24, 25, 35].

Standardization development is also crucial to DSA deployment, as it provides a frame-

work for technology development, analysis and operation. Several standards have been introduced in support of DSA operation. The most advanced are ECMA–392 in 2009 [44] and IEEE Standard 802.22 [45] which provide Medium Access Control (MAC)/PHY–layer specifications for TVWS home and regional area networks, respectively. Other MAC/PHY–layer standards currently under development include IEEE 802.11af [46] for Wireless Local Area Network (WLAN) operation in TVWS, IEEE 802.19 [47] specifying standards for inter–standard TVWS coexistence and IEEE 1900.7 [48] for dynamic spectrum access radio systems supporting fixed and mobile operation in white space frequency bands. However, currently these standards are still in the early stages of development. Additionally, while the MAC/PHY–layer standards, (*i.e.*, or equivalent specifications), specify protocols and operating parameters for using the standards, this by no means offer a guarantee of compliance.

Furthermore, with the exception of IEEE 802.19, the current monitoring mechanisms in standardization initiatives focus upon measurement approaches specifically aimed at white space detection for usage, as opposed to the requirements for evaluating compliance. IEEE 802.19 is in the early stages of development but monitoring mechanisms are aimed at coexistence for primarily IEEE standards and therefore offers limited scope as well. IEEE has also been working on the 1900 series standards supporting deployment and analysis of DSA systems. These focus upon general principles for dynamic spectrum access networks including Terminology Definition [13], Interference and Coexistence Analysis [49], Distributed Resource Optimization Architectures [50], Policy Languages and Architectures [51] and Spectrum Sensing Interfaces and Data Structures for DSA [52]. The scope of these standards also does not currently provide specific guidelines for monitoring for compliance enforcement[3].

Standardization work in monitoring mechanisms for DSA compliance has been based upon related academic research work on spectrum sensing. While the current literature illustrates various ways to deal with user detection under different sensing performance requirements (*e.g.*, energy detection, cyclostationary detection, waveform sensing) [54–57], sensing wide spectrum bands, a key requirement for DSA compliance monitoring [35], is

[3]The initial proposal for the 1900 series also included a Project Authorization Request (PAR) for 1900.3 with the goal of investigating approaches for assessing the spectrum access behavior of radio systems employing DSA methods, which was approved, but the responsible Working Group (WG) was later disbanded [53].

still a difficult task. Many techniques have been proposed for wideband sensing such as compressed sensing [58, 59], multi–resolution sensing [60, 61], and collaborative sensing [62, 63], as well as combinations of these [64–66]. However, these approaches focus upon primary and secondary user detection for CR communications, and not on monitoring for compliance evaluation. In [58, 67, 68] there has been some work in signal estimation, but again, the focus was upon user detection for CR communication, as opposed to spectrum monitoring for compliance. Wideband sensing approaches are also still challenged with the detection of intermittent use, particularly in low–occupancy scenarios. Additionally, current approaches do not differentiate between primary services and differing/heterogeneous secondary usage. Finally, in many of the approaches in the literature, spectrum sensing are channel–oriented and are thus ill–suited[4] for modeling the impact of heterogeneous Radio Access Technology (RAT) on spectrum occupancy in proposed spectrum sharing models in the literature.

Recently, however, there has been increased research into spectrum security issues in DSA networks. Research into spectrum security has focussed upon the impact of malicious spectrum users in DSA environments, (*e.g.*, due to primary user emulation attacks [69–71], denial of service attacks [72–74], spectral honeypot attacks [75, 76]), and has demonstrated the relatively low barriers required for exploitation if security measures are not in place, (*e.g.*, [75, 77–79]). Many existing proposals for spectrum sharing and management introduce security leakages, and consequently potential unfairness, spectrum unavailability, malicious behaviour in DSA networks. Identification, recording and reporting of such behaviour still remains an open research issue [75, 77–79]. This is even more challenging for monitoring in real–time [80]. The literature to–date, however, focuses upon development of mechanisms for DSA spectrum management for deployment within the network, in a similar manner to existing standardization activities. While the techniques for identification, recording, and reporting are related to the needs of compliance monitoring, application to spectrum management within the network, still does not directly address the issue of compliance enforcement.

In most jurisdictions, from regulator and service provider perspectives, spectrum mon-

[4]Currently most channel–oriented approaches in the literature do not account for coexistence scenarios where secondary networks with different channel specifications operate.

itoring techniques are principally either of two different approaches [35]: 1) Attempting to sense every transmission in the band under observation; or 2) Periodic sensing with statistical estimation of occupancy. Service provider monitoring mechanisms have focused upon restricting access to their networks based upon their assigned access to the Electrospace. These have naturally been limited in geographical extent, as well as licensed sub–band scope, based upon the service provider's infrastructural investments, and are typically specific to the technology deployed, (*e.g.*, GSM, UMTS, DAB). Consequently, such measurement approaches tend to be very technology–specific, since radio resource management mechanisms are based upon measurement of key performance indicators for use in resource optimization for the specific technology [81].

From the regulator perspective, there has been a historic lack of monitoring technology innovation which has been primarily attributed to the requirement for policy–makers to provide the enabling infrastructure for security monitoring, which is not the typical focus of regulatory agencies [25]. Regulator investment in monitoring networks generally consist of a mixture of fixed and mobile monitoring nodes, which are deployed based upon traditional spectrum management approaches [24, 35], which have increasingly been considered to be inadequate for the dynamic characteristics of DSA networks [15–20, 24, 25, 35]. Recently, there has however been increased work in development of monitoring infrastructures for DSA. Proposed approaches are primarily based upon either: 1) Spectrum sensing mechanisms or 2) Geolocation database mechanisms.

Figure 1.2: RFeye Spectrum Monitoring Solution [38, 39].

Perhaps the most advanced work which utilizes spectrum sensing is RFeye [38, 39]. RFeye, developed by CFRS [38], was designed for continuous remote spectrum monitoring. System deployments can potentially provide real–time access to Electrospace usage data in

addition to direction finding and radio geolocation for pinpointing suspicious or unauthorized transmitters. The RFeye node, (Fig 1.2), currently offers flexible system deployment in various applications including security and surveillance, regulatory enforcement, as well as military spectrum operations. This currently represents the most advanced work to–date in development of spectrum monitoring infrastructure. Infrastructure development is underway in various jurisdictions including the UK, Canada and the Netherlands [24, 38].

Another promising approach for compliance monitoring which leverages regulatory developments involves the use of geolocation databases storing data to determine the availability of white space for secondary service usage [31–33, 82–84]. This can be accomplished through use of the geolocation database contents which are currently being used for spectrum management in DSA scenarios. For example, Spectrum Bridge has developed its Authorized Shared Access (ASA) technology which relies upon geolocation databases for direct spectrum allocation and managed shared access to spectrum, (Fig 1.3). This approach represents the state–of–the art in spectrum management deployments aimed at DSA operation. Secondary Users (SUs) receive only information on a subset of accessible channels based upon ASA optimization [82].

However, such database approaches focus upon protection of the primary services, and rely upon mostly slowly–varying Primary User (PU) information coupled with access restriction mechanisms achieved by limiting the channel lists provided to SUs for DSA. There is still a need to account for the impact of the more dynamic and stochastic secondary services, particularly in such scenarios, for example in interference characterization. The current FCC approach only requires that SU devices request channel availability for the SUs current position [40, 41]. There is no requirement for SU registration prior to spectrum usage, as currently proposed by the OFCOM regulatory regime [40–43]. Also as currently specified, the databases would be primarily derived from nominal licensing data available from the regulator (*e.g.*, [85]) as opposed to actually measured and estimated occupancy statistics, and are currently limited to the Digital Television (DTV) bands. Even with the OFCOM requirement for SU registration, no guarantee is offered to ensure compliance. The lack of reliable feedback therefore makes the current database approaches ill–suited to accounting for secondary spectrum usage.

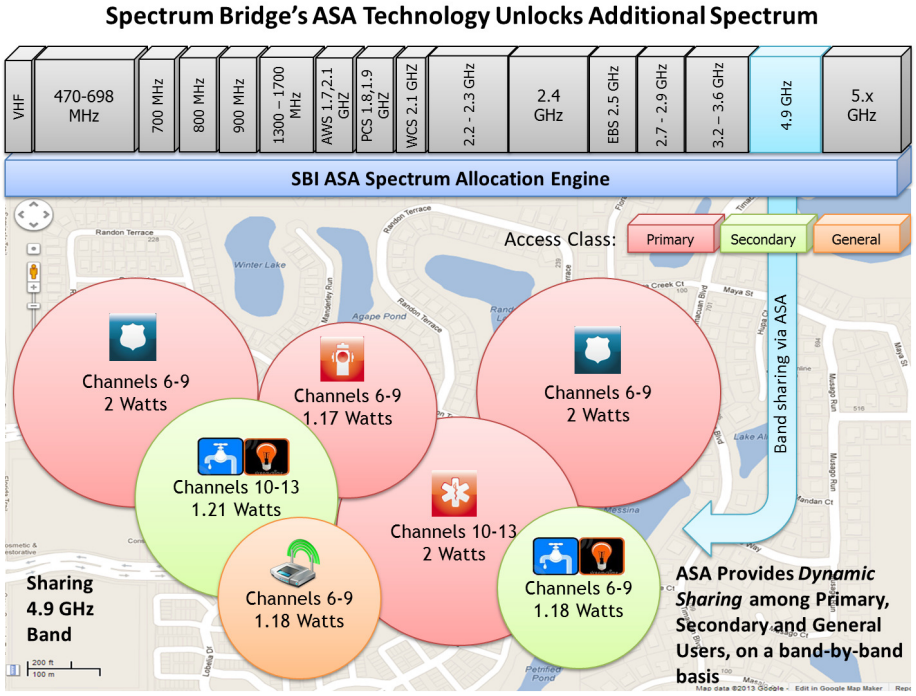

Figure 1.3: Geolocation Database Spectrum Management using Spectrum Bridge Authorized Spectrum Access Technology [82].

1.4 Thesis Contributions

Specific novel contributions of this dissertation are as follows:

1. **Non–Uniform Spectral Sampling (NUSS) for Non–Contiguous Spectral Sampling (NCSS) in wideband sensing scenarios:** A framework is proposed for the use of NUSS techniques. The techniques focus upon reducing data collection complexity for bandwidth occupancy in wideband sensing, which is a key performance requirement in spectrum monitoring. Performance evaluation of stratified spectral sampling techniques for use in NCSS is presented. Implementation algorithms for spectral stratification are presented in support of Random Spectrum Sensing (RSS), which is a special case of NCSS. Finally a case study is presented which: 1) demonstrates one possible way to realize RSS/NCSS using polyphase filter banks; and 2) presents a framework for performance evaluation of RSS/NCSS use in monitoring DSA scenarios.

2. **PHY–based Random Temporal Sampling approach to temporal modeling of spectrum occupancy:** A PHY-layer–based approach for spectrum occupancy estimation is proposed, if user discrimination is not required. In this approach, spectrum occupancy is modelled as an alternating renewal process. Signal measurements are then used to estimate the probability density functions of "ON" and "OFF" times for spectrum occupancy, under various temporal sampling strategies. The scheme is demonstrated on software radio hardware, the Universal Software Defined Radio Platform (USRP) for various scenarios. Performance comparison to CS approaches is then done.

3. **Frame–Based Random Temporal Sampling (FBRTS) approach to temporal modeling of spectrum occupancy:** This novel approach uses sampling inversion techniques for estimating time–based statistical characteristics of the DSA traffic using knowledge of learned information about CR technologies deployed in an area. Considering spectrum occupancy modelled as an alternating renewal process, a point process is constructed using renewals demarcated by frame–based feature semantics common to most current and emerging wireless MAC–layer and PHY–layer specifications. The impact of missed frame detection due to sampling design, or frame errors is then investigated. Finally, the randomly sampled frames from the sampled process are used to recover spectrum occupancy statistics for the full frame sequence using sampling inversion techniques. To the best of the author's knowledge, this aspect of spectrum occupancy estimation has never been explored in the literature. This contribution is presented to address the need to track individual CR behaviour in DSA coexistence scenarios, which remains an open research issue to–date.

4. **Collaborative/Distributed Random Spectral Sampling (CRSS) and Mobile Random Spectral Sampling (MRSS) approaches to collection of spatial spectrum occupancy data:** - This work expands upon the previous contributions. Node collaboration and mobile nodes are incorporated into the previous approaches for collection of spatial diversity to improve estimation performance. The approach is investigated for several spectrum monitoring and compliance enforcement tasks.

Additionally, this contribution adds to the literature on consensus algorithms for low complexity convergence of distributed sensing nodes, through consideration of more realistic mobility models than currently used in the literature on consensus convergence. This is accomplished through the use of bi–directionally coupled simulations for investigation of vehicular networks for spectrum sensing. A distance–based approach is also proposed for consensus convergence in vehicular settings. This specific contribution is has been the basis for work done between the Wireless Innovation Laboratory and Toyota ITC for developing Knowledge–Based Vehicular Communications (KBVC) where sensors randomly sense channels and share estimated transition probabilities to improve channel state prediction in Vehicular Dynamic Spectrum Access (VDSA) networks.

1.4.1 Publications

In support of the above contributions, the following is a list of publications achieved over the course of this PhD.

Journals

1. [86] **S. Rocke** and A. Wyglinski, "Wideband Spectrum Occupancy Estimation using Random Spectral Sampling in Heterogeneous Radio Access Environments" *IEEE Transactions on Vehicular Technology*, Submitted.

2. [87] **S. Rocke** and A. Wyglinski, "Randomized Temporal Spectrum Sensing using Periodic Sampling SDR Platforms", *IEEE Transactions on Vehicular Technology*, Submitted.

Conferences

1. [88] **S.Rocke**, S. Chen, R. Vurruyu, O. Altintas and A. Wyglinski, "Knowledge–based Dynamic Channel Selection in Vehicular Networks", *IEEE VNC*, November, 2012.

2. [89] **S. Rocke** and A. Wyglinski, "Estimation of Spectrum Occupancy in Heterogeneous Radio Access Environments using Random Spectral Sampling", *IEEE SARNOFF*, January, 2012.

3. [90] **S.Rocke** and A. Wyglinski, "Geo–Statistical Analysis of Wireless Spectrum Occupancy using Extreme Value Theory", *IEEE PACRIM*, August, 2011.

In Preparation

1. [91] **S.Rocke** and A. Wyglinski, "Spectrum Monitoring in Dynamic Access Networks: Challenges and Opportunities", *IEEE Communications Magazine*.

2. [92] **S.Rocke** and A. Wyglinski, "Non-Uniform Wideband Spectrum Sensing for Spectrum Monitoring in Dynamic Spectrum Access Networks", *Eurasip JWNC*.

3. [93] **S.Rocke** and A. Wyglinski, "Knowledge-based, Non-Contiguous, Multi-Resolution Wideband Spectrum Sensing in Heterogeneous Radio Access Environments", *IET Signal Processing*.

4. [94] **S.Rocke** and A. Wyglinski, "Frame-based Sampling Inversion Technique for Spectrum Occupancy Estimation for DSA Compliance Verification", *IEEE Transactions on Wireless Communications*.

5. [95] **S.Rocke**, S. Chen, R. Vurruyu, O. Altintas and A. Wyglinski, "Knowledge–based Dynamic Channel Selection for Vehicular Communications", *IEEE Vehicular Technology Magazine*.

6. [96] **S.Rocke**, S. Chen, R. Vurruyu, O. Altintas and A. Wyglinski, "On Vehicular Communications in TVWS: Challenges and Opportunities", *IEEE Communications Magazine*.

1.5 Dissertation Outline

The dissertation is structured as follows. Chapter 2 covers spectrum access methods and the implications for spectrum management, concluding with a review of related work on

spectrum monitoring for DSA networks. Chapter 3 outlines the random spectral sampling framework, and presents results on the non–uniform spectral sampling framework for bandwidth occupancy estimation in heterogeneous wideband scenarios. Chapter 4 presents the PHY–layer based random temporal sensing approach for temporal occupancy estimation. In Chapter 5, details of the frame–based random temporal sampling approach are presented. In Chapter 6, the distributed, mobile sensing framework for compliance monitoring is described. Chapter 7 outlines a future outlook is presented followed by the conclusion.

Chapter 2

Background Knowledge of Spectrum Monitoring in DSA Networks

2.1 Introduction

This chapter provides an overview of various issues surrounding spectrum management for dynamic spectrum access. A brief overview of the challenges of current spectrum management methods, dynamic spectrum access methods and the implications for spectrum management is first presented. The spectrum monitoring problem is then briefly discussed, followed by discussion of several key spectrum monitoring challenges in OSA networks. Several aspects of this work also appear in [91].

2.2 Challenges of Current Spectrum Management Methods

The following section briefly discusses the challenges of current spectrum management methods. The importance of spectrum management for wireless communications is explored, as well as discussion of several shortcomings of the traditional approaches which has led to more market–oriented paradigms to spectrum access. The impact of the ongoing

transition on spectrum management by other stakeholders is then discussed.

2.2.1 The Need for Spectrum Management

Spectrum is an enabler for the delivery of vital services, for both public and private users, such as public safety, national defence, disaster warning, mobile telephony, Internet access, and air and maritime traffic control. As the range of spectrum–facilitated services continues to increase, there has been a tremendous growth in demand for wireless–enabled services in recent years. The most cited example of this phenomenon has been the rapid growth of mobile telephony, mobile broadband, and Internet services (Fig 2.1). There has also been increasing popularity of entirely new applications for example commercial applications using the Global Positioning System (GPS) [1], as well as radio tracking applications using Radio Frequency Identification (RFID) tags, placing increasing burdens on spectrum resources [97].

The increasing demand further emphasizes the need for spectrum management in order to mitigate or entirely avoid excessive interference between different spectrum users. Interference typically arises due to spectrum user transmissions at the same time in close spectral proximity, within some common defined spatial region, potentially resulting in unusable systems. Spectrum management tools provide a means of maximizing the value gained by society through spectrum usage. In fact, a key goal of spectrum management is to facilitate as many efficient and effective spectrum–enabled services as possible while simultaneously minimizing the interference experienced between different spectrum users [35]. Topics highlighting spectrum management and its relevance to society, which have been discussed in the literature, include the following [24]:

1. **Freedom of knowledge and innovation:** Spectrum management should remove constraints to allow new services as well as new company's resulting from related innovations.

2. **Security** - Society expects that wireless communications should be secure (*e.g.*, re-

[1] GPS was originally developed for defense purposes. A comparable example is the transformation of the short messaging service (SMS) in mobile cellular systems, from an engineering system management and trouble–shooting mechanism into its current commercial usage.

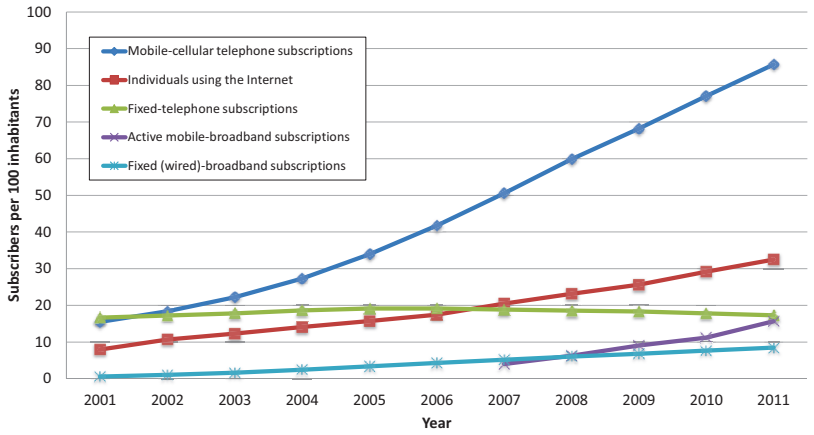

(a) Subscriber penetration rate per 100 inhabitants

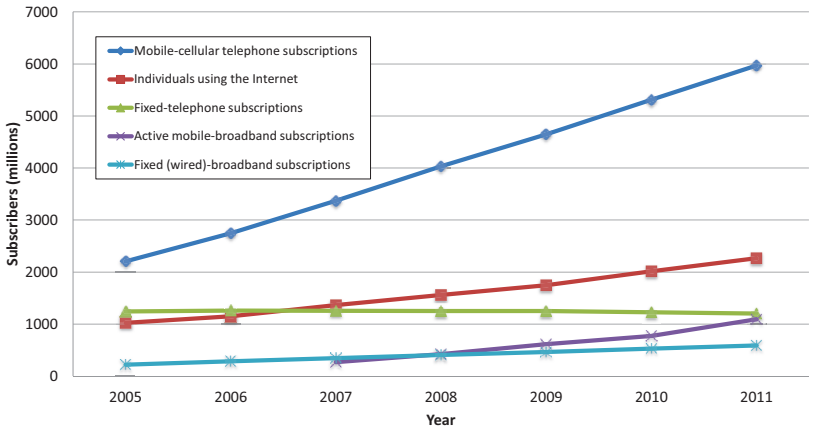

(b) Subscriber penetration rate (millions)

Figure 2.1: Global ICT developments, 2005–2011 [98].

sistant to jamming, eavesdropping and hacking).

3. **Quality of Service (QoS):** Demands for reliable wireless communications, which depends upon electromagnetic compatibility (EMC), is very challenging in emerging wireless environments.

4. **Health and safety:** The rise in wireless technology usage has also raised society's concerns about the safety of electromagnetic waves on the human body.

5. **Building construction:** The selection of building materials without consideration

of RF propagation characteristics, impacts network design, for example in newly developed urban areas.

6. **International harmonization:** Since RF propagation does not distinguish international boundaries, and given the relatively long time scales for harmonizing new applications in spectrum, assessing future spectrum needs in a timely manner is essential.

In addressing these topics, it is imperative that both policy and appropriate technical platforms be used to support decision support for both current and future spectrum needs.

2.2.2 Shortcomings of Traditional Spectrum Management Approaches

Considering the discussion in Section 2.2.1, spectrum management can be viewed as a multi–objective optimization problem, requiring contemplation of both technical and non–technical parameters as bases for optimization, based upon the context of the spectrum users (*e.g.*, technical, functional and economic efficiencies) [1, 99, 100]. *Technical efficiency* principally relates to the above metric as a means of achieving the most intensive spectrum use within interference constraints. *Functional efficiency* relates to the reliability, ease of use, and quality of services provided. *Economic efficiency* relates to the revenue, profit and added value achieved through spectrum policies. These efficiencies collectively form the bases for evaluation of benefits to users, the economy, and to society [99].

However, the regulatory process of ensuring both technical and non–technical efficiency introduces requirements for responsiveness and flexibility for adaptation to the pace of technological development and changing market valuations. In the past, there have been various challenges for achieving this. First, in the spectrum management process the various efficiencies can be competing. For example, public policy goals for safeguarding the provision of services such as defence, safety, and public broadcasting may conflict with technical efficiency objectives. Further, the need for spectrum harmonization for several services (*i.e.*, globally, regionally, nationally) requires considerable efforts in spectrum coordination across jurisdictional boundaries which can further constrain efficiency objectives.

The increasing importance of commercial applications has also encouraged numerous in-

teractions between various regulatory bodies, operators, and manufacturers. This increased interaction is based upon the growing consensus that operators and equipment manufacturers typically posses more knowledge about their spectrum interests and additionally more information, than an administrative body would possess, pertaining to technology selection and deployment as well as consumer preferences.

It is therefore no surprise that spectrum management, even in the simplest of cases, can be a very complex process requiring a multi–faceted approach. While the regulators have in general been able to address spectrum demand during the 20^{th} century via incrementally increasing the spectrum supply, numerous technological advances and telecommunications liberalization have have challenged the regulator's abilities to balance spectrum supply and demand effectively. There is increased pressure on regulators to determine better ways to ration and balance spectrum demand between the numerous diverse competing uses.

Additionally, the regulatory burden of efficiency optimization was not as pronounced as currently required in an environment of rapid technological change and unpredictable markets. This had led to the perception that the predominantly centralized administrations are not as responsive, efficient as required, and that they are biased towards the status quo and incumbent interests [22]. The rigidity of the current regulatory framework was further demonstrated with the onset of telecommunications convergence, which promulgated blurring of the boundaries between traditional service definitions which previously formed the basis of spectrum allocations.

Therefore, from a process–oriented perspective it is almost impossible to predict the value attained through a given service–spectrum allocation. This in turn makes it very difficult to assess how a predominantly "command–and–control" approach to spectrum management can maximize value. Several examples provide evidence in support of this [101]:

1. **Unused allocated spectrum:** Several measurement studies have shown several instances where allocated spectrum is currently being unused, reducing opportunities and possible added value if other services could access the spectrum.

2. **Widely differing spectrum valuations:** The most common example of this is in auctions (*e.g.*, higher 3G valuation versus 3.4GHz) which suggest an imbalance

between different uses.

3. **Barriers to entry of emerging technologies and applications:** Technologies and applications such as mobile TV or vehicular communications have had difficulty in securing sufficient spectrum resources. This is symptomatic of regulatory rigidity.

4. **Insufficient incentives for technology innovation:** Applications such as aviation radar have limited incentives for optimizing their use of spectrum despite the availability of more spectrally efficient technologies.

Also relatively recent management approaches such as spectrum trading and license–exempt spectrum[2] have made management even more challenging. The consequent higher request rates for new spectrum, spectrum reconfiguration, ownership changes, spectrum leasing, and application changes further burden the manager. Dispute resolution also represents another challenge to current spectrum management approaches. Thus management of allocations and assignments either by the regulator, or in some cases the user, may not be achieving the main spectrum management objectives and further are increasingly difficult to administer centrally.

2.2.3 The Shift Towards a More Market–oriented Paradigm

Based upon the previous overview, recognition of increasingly burdened regulatory resources has highlighted the shortcomings of the traditional, centralized approach to spectrum management, spurring research into alternate approaches to spectrum management. In the expanding spectrum marketplace, spectrum is however being valued as any basic commodity. Therefore there has been a long term evolution towards more market–oriented mechanisms [23] ranging from beauty contests to free–market auctions. The intent of market–oriented spectrum management is to facilitate as much decentralized coordination of spectrum use as is reasonably practical and possible.

Regulators worldwide are exploring and incrementally adopting tools and procedures that demonstrate the shift in paradigm. An example of this is the FCC's revision of rules

[2]Such approaches have been deployed in a relatively small proportion of usable spectrum. The majority is still "command–and–control" administered.

governing use of radio spectrum to first allow Frequency Coordinators, and subsequently Guard Band Managers to to lease spectrum according to the spectral and geographic needs of specific classes of private wireless spectrum users [30]. This has provided a means of coordinating the variety of needs both for bandwidth and geographic coverage, and allowed for addressing odd–shaped or small spectrum requirements which if assigned via licenses would typically artificially reduce spectrum opportunities for other spectrum users (*i.e.*, inefficient spectrum use).

Such approaches are however currently limited in application to sub–bands such as the use of Guard Band Managers in the 700MHz band, and most of the spectrum managed by regulatory authorities still is subject to traditional "command–and–control" mechanisms. Recent measurements, (*e.g.*, [2, 3, 102–104]), have demonstrated the artificially induced spectrum shortage resulting from the traditional approach. The artificially–induced spectrum shortage has led many to investigate DSA techniques as a possible solution. DSA represents a more aggressive market–oriented approach to spectrum management which can be seen as a logical evolution based upon the advantages gained through use of Frequency Coordinators and Guard Band Managers for selected sub–bands in the past. There is increasing regulatory interest in DSA, as evidenced by regulatory approval[3] for deployment and experimentation with TV whitespace devices which implement DSA.

2.2.4 Different Domains of Spectrum Management

Although much of the previous discussion focused upon spectrum management from the regulatory perspective, spectrum management in fact exists within various domains. Fig 2.2 illustrates the traditional spectrum management pyramid[4] for basic interactions between key stakeholders for RF spectrum usage. Due to the shift to more market–oriented approaches, the traditional spectrum management role of regulators is increasingly shifted to the service providers and end users. The challenge therefore is to provide mechanisms for ensuring that spectrum management objectives at the highest level are achieved, given

[3]For example USA, Canada, UK, Australia, Singapore, Japan, and South Africa.

[4]This pyramid does not attempt to illustrate the complex interactions between stakeholders. Further, increasing decentralization has blurred the lines between the domains from an organizational perspective. For example, service providers are also service users, and both service providers and end users can impact regulation (*e.g.*, through consultations).

the increased autonomy being granted to the non–regulator stakeholders. From the domain perspective, traditional spectrum management roles are as follows:

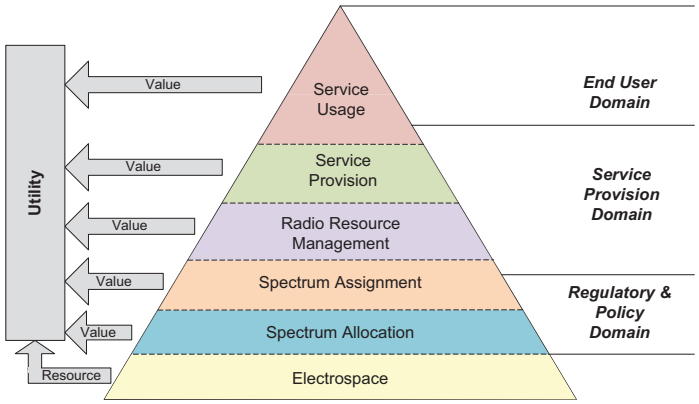

Figure 2.2: Traditional Spectrum Management Pyramid.

1. **The Regulation & Policy Domain:** Traditionally, responsibility for *allocating* particular services/technologies to operate within any given sub–band, and *assigning* these bands to specific users/service providers has been within the domain of regulation and policy. At this level, spectrum management involves allocation, assignment, as well as specification of various operating parameters which should be adhered to, in order to achieve spectrum management objectives. Ensuring regulatory compliance is another aspect of spectrum management in this domain. At this level, value is derived from achieving larger policy objectives which typically stem from human, social and economic considerations.

2. **The Service Provision Domain:** Spectrum management at this level must minimally conform to the requirements of the underlying regulatory regime. Typical spectrum management activities at this level include standards development, network deployment, network operation and management as well as device manufacture, to name a few. Depending upon the network context, (*e.g.*, WLANs, TV Broadcast, Mobile Cellular), spectrum management in terms of allocation of assigned spectrum resources varies by protocol specifications. Such protocols facilitate delivery of services to the end users in line with regulatory requirements. At this level, value is

typically economic in nature.

3. **The End User Domain:** This domain typically has the least spectrum management responsibilities. However, the end user plays an important role in situations where the end user has responsibility for network deployment, operation and management. Examples include home networking, office networking and use of Private Land Mobile Network (PLMN) services. At this level, value is specified in terms of the derived benefits such as access to information services, the Internet, messaging services, financial services, or some information infrastructure for supporting strategic operations.

Each of these domains presents different perspectives on spectrum management as well as value gained through a particular use of the Electrospace. Formally, the *Electrospace* is defined as a theoretical, k–dimensional hyperspace occupied by radio signals, and is composed of various dimensions including time, frequency, spatial location, angle–of–arrival, polarization, code, and possibly others [54]. Within the various domains, resource management principles typically focus upon the sub–space composed of the time, frequency, and spatial location dimensions. Transmitters and their operating parameters can be represented as *Electrospace Volumes* [100]. The problem faced by all spectrum users, independent of domain can thus be stated as follows: *Given N volumes in Electrospace, in the most general sense, disjoint, and given M requests for services, how can the M requests 'best' fit into the N volumes?*

As stated previously, this can be viewed as an optimization problem. In the literature, "efficiency" and "utility" frequently provide the bases for optimization [105–107]. However, there are numerous interpretations of efficiency based upon the context of the users [1, 99]. In many instances, the dimensions used for optimization are based upon spectrum utilization efficiency in which efficiency is viewed as the output to input ratio of the amount of information transferred, (*i.e.*, output), to the spectrum utilization (*i.e.*, input). The input parameter usually involves some representation of the spectrum space required, specified as a function of the product of bandwidth, space and time [100], while the output is dependent on the user/stakeholder perspective. Utility similarly has many interpretations depending

upon the definition of the end user, including both technical and non–technical components, (*e.g.*, economic efficiency and functional efficiency) [99].

Given the implications of opportunistic spectrum usage in the wider community, there needs to be further consideration of the non–technical consumers of spectrum data that may function in roles such as regulators and policy–makers. A suitable metric [100] for this community would provide a tool that can be used to incorporate other non–technical considerations in spectrum management functions at all levels. Spectral occupancy modeling provides a technical basis for the evaluation of spectrum usage, and as a consequence other parameters of interest to the data user [108, 109].

2.3 Harnessing the Electrospace

Achieving higher spectrum utility through opportunistic spectrum access requires new ways of accessing the Electrospace. In this section proposed mechanisms and architectures for accessing the Electrospace are briefly described. This section also briefly discusses the cognitive radio concept, and discusses how this approach can be used to realize the access models and architectures.

2.3.1 Spectrum Access Models

In the traditional "command–and–control" approach, the Electrospace is statically assigned to a spectrum licensee, which as previously discussed, generally results in inefficient utilization of spectrum. This approach limits the flexibility of usage of spectrum according to the time–varying demands of the user [28]. Limitations of this approach include:

- Static assignment to licensees in general cannot be easily changed. In cases where the assigned spectrum is under–utilized, the spectrum cannot be allocated to another user/service provider who can accommodate new potentially more efficient use of the spectrum.

- Even in technology–neutral licensing schemes, the type of wireless service in the licensed spectrum cannot be changed. An example of this is the previous analog TV

allocations which could not be used for other services such as increasing network capacity for mobile cellular communications, even though TV bands were largely unused.

- Spectrum licenses are usually location–invariant. Thus as in the previous point, at various locations the spectrum can remain unused. This was confirmed in several recent spectrum measurement studies. An example of this is the gap between urban and rural service usage.

- Spectrum usage granularity is not dynamic. This limits the ability to allocate the Electrospace in smaller volumes to service demands in scenarios such as in a hotspot scenario.

- In most cases, licensed users are protected from significant interference by unlicensed use. However, if the licensed user is not using the resource (*e.g.*, historic analog TV use) then spectrum utilization can be improved through opportunistic access to the spectrum opportunities provided that unlicensed transmissions do not significantly interfere with or disrupt licensed user operation.

The above reasons summarize many of the compelling arguments which spurred the genesis of open spectrum [27]. Open spectrum encompasses various models and techniques with a more market–oriented shift to spectrum management to facilitate dynamic spectrum management for wireless communications systems. Under this paradigm new spectrum access and licensing models for improving spectrum access efficiency and flexibility are illustrated in Fig. 2.3. These models are now briefly described.

Exclusive Use Model

In the exclusive use model spectrum is licensed for exclusive use, subject to various operating parameters (*e.g.*, maximum transmit power, transmit power mask, operating frequencies, allowable geographic operating range). Thus spectrum is allocated (*e.g.*, perhaps by the regulator) to the licensee with restrictions on geographic and temporal validity. The licensee in turn can grant access rights to unlicensed users, also subject to operating parameters which must in aggregate also satisfy those imposed by the overall assigning body

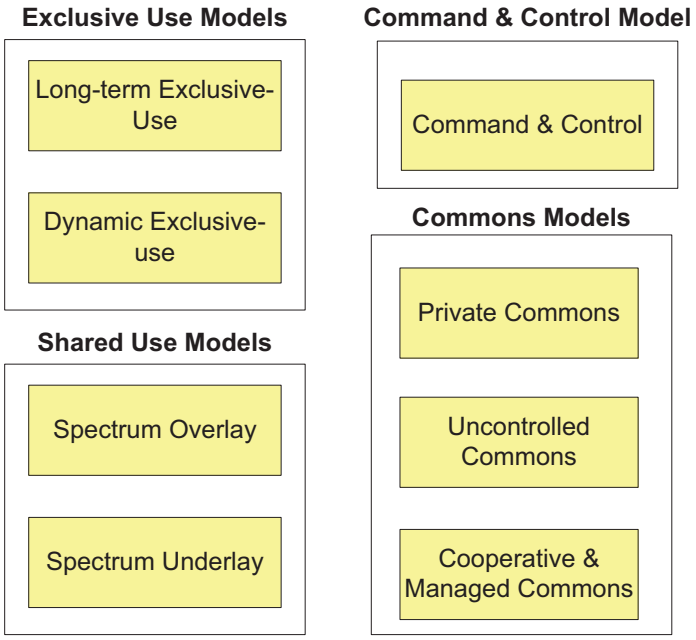

Figure 2.3: Spectrum Access Models.

(*e.g.*, regulator). The exclusive use model can be further classified into *long–term exclusive use* and *dynamic exclusive use*. The main difference between the two approaches is the timescale over which spectrum allocation occurs.

Shared Use Model

In the shared use access model, spectrum can be simultaneously shared between licensed and unlicensed users. Unlicensed users opportunistically use spectrum provided that the spectrum is not currently utilized by licensed users. The operating principle is that unlicensed usage is allowed as long as it does not interfere with licensed usage. Shared use can be further sub–divided into *spectrum overlay* and *spectrum underlay* access methods.

In spectrum overlay operation, while the licensed user maintains the right to exclusive operation within a given band, the unlicensed user opportunistically accesses spectrum at particular times and frequencies with no licensed usage, (*i.e.*, referred to as spectrum holes). Typically this method would be used in FDMA, TDMA, and OFDM systems. In contrast, in spectrum underlay operation, the unlicensed user transmits concurrently with

the licensed user, but does so at a transmit power level that limits the interference levels to the licensed user. Typically this method would be used with CDMA and UWB systems.

Spectrum Commons Model

In the spectrum commons approach, all spectrum users possess the same rights to access the Electrospace, subject to overarching operating parameters typically set through regulations. This access model can be divided into *uncontrolled commons*, *managed commons* and *private commons* sub–models.

In uncontrolled commons access, spectrum is not owned by any user. This is the simplest approach and is already in use in several sub–bands. The most popular examples are the ISM (2.4 GHz) and U–NII (5 GHz) unlicensed bands. While there is no spectrum ownership in this model, there is usually a maximum transmit power constraint. Since there is no control on spectrum access, spectrum users typically suffer from both uncontrolled interference[5] or controlled interference[6] which can reduce spectrum usability. This has been referred to in the literature as the tragedy of the commons [110].

In managed commons access, several of the problems of uncontrolled commons are addressed through mechanisms which allow jointly–controlled spectrum access. Users adhere to the prescribed spectrum etiquette rules for gaining access to the spectrum [26]. This access method requires a management protocol which incorporates reliable and scalable mechanisms for ensuring spectrum etiquette rules are adhered to. This also implies the need for mechanisms to enforce spectrum etiquette rules.

In private commons access, there is an entity who owns rights to the spectrum. The spectrum owner, subject to regulatory operating parameters, is able to specify technologies, protocols, and operating parameters for users to access the owned spectrum. The key features of this model are: 1) Users must receive approval from the spectrum owner prior to opportunistic access of the spectrum 2) Users can access spectrum owned by any user operating under this regime 3) Sensing and coordination protocols must be approved by the spectrum owner, as long as they do not violate overarching regulatory–determined spectrum

[5]From devices outside the network.
[6]From devices within the network.

etiquette rules.

2.3.2 Access Architectures

In addition to the various access models, there are also various access architectures under which these access models can be realized. Each architecture requires different approaches to management. Therefore access architectures for OSA must be contemplated in spectrum management and monitoring approaches. Access architectures can be classified in several ways. For example, [111] presents a very useful approach (Fig. 2.4). [111] classifies access architectures as follows:

- Infrastructure–based versus Infrastructureless Networks
- Centralized versus Distributed Networks
- Single–hop versus Multi–hop Networks

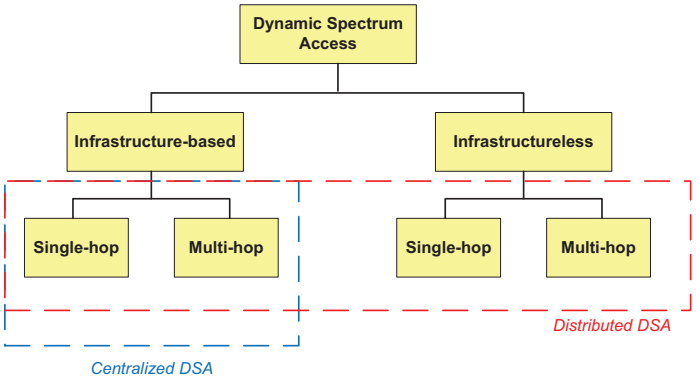

Figure 2.4: Spectrum Access Architectures [111].

2.3.3 Cognitive Radio

Cognitive radio technology, first coined by Mitola and Maguire [112], provides a fundamental enabler for flexible and efficient usage of spectrum through dynamic spectrum access. In the literature, several CR definitions have used based upon the applications and research focus. In some instances emphasis is placed upon "spectrum agility" (*e.g.*, [113, 114]) while

in others the ability to learn and reason is the primary attribute (*e.g.*, [112]). However to–date while there have been many attempts to define cognitive radios, there has not been any globally–adopted formal definition. Examples of the more prevalent definitions include the following:

> "A really smart radio that would be self-, RF- and user aware, and that would include language technology and machine vision along with a lot of high–fidelity knowledge of the RF environment." *Mitola* [112]

> "Cognitive radio is an intelligent wireless communication system that is aware of its surrounding environment (i.e., outside world), and uses the methodology of understanding–by–building to learn from the environment and adapt its internal states to statistical variations in the incoming RF stimuli by making corresponding changes in certain operating parameters (e.g., transmit–power, carrier frequency, and modulation strategy) in real–time, with two primary objectives in mind: highly reliable communication whenever and wherever needed; efficient utilization of the radio spectrum." *Haykin* [115]

> "a) A type of radio in which communications systems are aware of their environment and internal state can make decisions about their radio operating behaviour based on that information and predefined objectives.
>
> b) Cognitive radio...that uses software–defined radio, adaptive radio and other technologies to automatically adjust its behavior or operations to achieve desired objectives." *IEEE 1900* [13]

> "A radio system employing technology that allows the system to obtain knowledge of its operational and geographical environment, established policies and its internal state; to dynamically and autonomously adjust its operational parameters and protocols according to its obtained knowledge in order to achieve predefined objectives; and to learn from the results obtained." *ITU, ETSI* [116, 117]

Of interest for spectrum management is the ability to track both the spectrum agility and learning–based responses of cognitive radios. Regulatory definitions emphasize spectrum agility and awareness aspects of cognitive radios for spectrum monitoring. For example the FCC has specified several features which they believe should be incorporated by cognitive radios including: frequency agility, dynamic frequency selection, adaptive modulation, transmit power control, location awareness, negotiated spectrum use [41].

However, while spectrum agility tracking represents a considerable challenge, the question of how to provide guarantees for cognitive radio behaviour due to the ability to learn

still remains an open issue. The role of learning in cognitive radio adaptation of transmission parameters in changing RF environments according to the changing environment, can be examined with reference to the "cognitive cycle" [112, 118]. Fig 2.5 illustrates the mental processes of a cognitive radio based upon the "cognitive cycle".

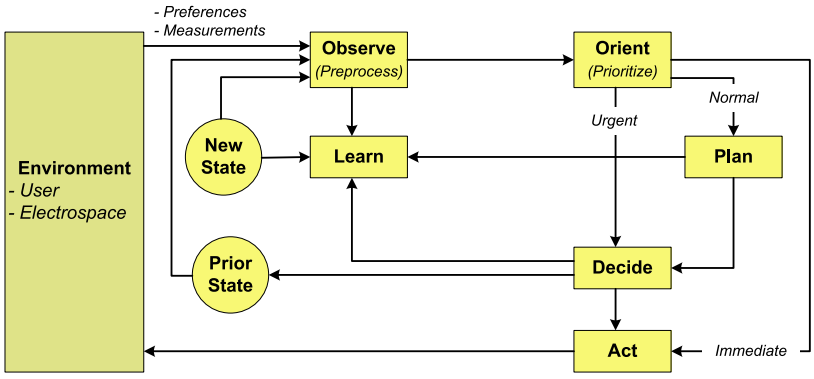

Figure 2.5: Cognitive Cycle based upon Mitola [112].

Drawing on artificial intelligence and machine learning theory [119], cognitive radios learning involves the modification of cognitive radio components to bring the components into closer agreement with available feedback from the operating environment in order to improve the overall cognitive radio performance. This ability to learn implies non–deterministic behaviour in the operating environment, even in response to static inputs to the cognitive radio [25]. This becomes increasingly unwieldy when one considers the multitude of possible optimization objectives as well as the functionality offered cognitive radios through SDR platforms.

2.4 Spectrum Monitoring

While recent technology developments bring OSA closer to realization, it is imperative that spectrum management mechanisms be appropriately developed in support of OSA. Spectrum monitoring, in conjunction with spectrum planning, spectrum engineering and spectrum authorization, represents four essential functions of spectrum management. Monitoring is typically used for planning frequency use, avoidance of incompatible usage, iden-

tification of harmful interference sources and for resolution of spectrum scarcity issues. To support these processes, it is essential that data be collected for study and analysis of spectrum occupancy, Electromagnetic Compatibility (EMC) verification as well as for ensuring user compliance with licence conditions, technical standards and operational standards.

Monitoring provides essential data for understanding and planning channel/band usage, in addition to providing feedback on the effectiveness of current planning and authorization activities. Additionally, through appropriate monitoring processes, statistical information on the technical and operational nature of spectrum occupancy is provided. Essential to promoting spectrum efficiency, objective spectrum management decisions require a means to quantify spectrum usage and to evaluate candidate radio technologies and spectrum access techniques. Furthermore, in highly congested regions, data facilitates essential spectrum engineering activities such as validation of tolerance levels, determining interference probabilities as well as development of band-sharing strategies.

Further, spectrum monitoring facilitates compliance with licence conditions and regulations using processes to determine deviations from authorized parameters, identify interference sources, and locate legal and illegal transmitters. The absence of effective regulations and enforcement procedures, potentially compromises the integrity of the spectrum management process. Consequently, an appropriate framework and process for response and management of complaints, and dispute resolution are crucial.

Further details of spectrum monitoring mechanisms for spectrum management are provided in [35, 120].

2.4.1 Spectrum Monitoring for Cognitive Radio Networks

Given the essential role of spectrum monitoring in spectrum management processes, the increasingly complex mobility and spectrum agility of emerging wireless technologies such as dynamic spectrum access and cognitive radios introduce several challenges to the development of monitoring mechanisms to support spectrum management functions. These include the following:

1. **Generation of large amounts of data:** Even across a limited spectral, tempo-

ral and geographical extent data collection and storage can occur at enormous speeds (*e.g.*, GB/hour) and this is expected to dramatically increase with monitoring requirements for effective management of future DSA deployments. The challenge exists in transforming low–level data (which can usually be extremely voluminous and thus difficult to understand and utilize) into other forms which could be more compact, abstract, and useful in decision–making.

2. **Monitoring for multi–domain decision support:** Effective decision support demands the integration of highly–dimensional, heterogeneous, distributed data as well as a framework for further analysis. There is therefore an urgent need for the application of computational theories and tools to assist Service Providers, Regulators, and Policy–makers in extracting useful knowledge from the rapidly growing volumes of data in spectrum management systems. Additionally, information requirements for spectrum management decision–making varies across the different domains (*i.e.*, Regulatory, Service Provision, Policy, User). This provides further context for decision support, based upon the roles and responsibilities of entities within each of these interacting domains.

3. **Physical node limitations for wideband data collection:** Current wireless emission monitoring and localization techniques employ a mixture of stationary and mobile sensors tuned to a specific narrowband frequency range in order to monitor and possibly triangulate intercepted signals [34–37]. Even using current vector signal analysis techniques to scan larger bands than traditional swept–tuned sensors, such spectrum sensors possess several significant physical limitations that need to be accounted for in any wireless emission monitoring network, namely:

    - The **sweep time** of a spectrum sensor is a finite quantity. Thus, when the sensor is obtaining measurements for one frequency sub–band sample over a finite period of time, it usually cannot sense another spectrally–distant sub–band simultaneously using the same radio frequency (RF) front-end equipment.
    - The **frequency accuracy** of any given spectrum sensing sweep is in part dictated by the frequency resolution of the spectrum sensor which in general in-

creases with monitoring duration. Consequently, a higher resolution spectrum sweep will obtain more accurate results at the expense of a longer sweep time. The converse also holds true (*i.e.*, faster sweep time at the expense of lower resolution) [121].

- The **amplitude accuracy** depends on the frequency resolution as well as the **amplitude variance** of the spectral estimation technique employed. Variance improves with power spectral density estimation, which requires longer monitoring times or for a fixed monitoring time, reduced spectral resolution [121].
- The impact of **mobility** arises when mobile nodes are used for data collection. Mobility introduces several challenges depending upon the monitoring model adopted. At higher mobility rates there can be more stringent timing requirements for measurement and data processing in monitoring networks [35].

Therefore, the technical challenge that exists with these wireless emission monitoring and localization networks is to devise an approach that can accurately intercept most signals of interest within a geographical region of interest, taking account of the physical limitations of current sensor devices. This becomes especially difficult when attempting to sweep a very large frequency range (*e.g.*, $\sim 3\ GHz$) and several of the possible signals that could reside within a specific region possess intermittent transmission behavior (*i.e.*, the signal duty cycle is on the order of a few percent).

2.4.2 Use Cases of Spectrum Monitoring for Cognitive Radio Networks

As previously discussed, the purpose of spectrum monitoring is to support spectrum management processes as well as to resolve interference problems. While the introduction of CRs does not change the basic uses for measurement data, it creates several new scenarios for consideration. Several examples are now discussed.

Assessing Spectrum Occupancy

Assessing spectrum occupancy is important to effective spectrum management. From the CR perspective, it provides data for use in frequency selection for DSA operation. From

the management, planning and policy perspectives, it provides essential data to assess the effectiveness of particular policies, as well as to inform on changing trends in spectrum demands. Typically an assigned band may appear to be crowded, but unless occupancy is measured, there is no way to confirm this. Additionally, knowledge of changing trends provides warning which can be used to prevent the inability to issue new assignments or to prevent quality of service deteriorating below acceptable levels.

Methods for presenting such data varies based upon the purpose. Examples include channel occupancy plots, busy hour plots, occupancy groupings (*e.g.*, by different user classes, services, modulation type or technology, among others), and spatial occupancy variation. The list is as varied as the purposes for the different purposes for the data. In addition to temporal occupancy, which focuses upon the proportion of time for which a spectral resource is occupied, bandwidth occupancy is also used to assess the proportion of a sub–band which may be occupied.

While these approaches to presentation have been traditionally used, the challenges of wideband measurements under possibly more dynamic, stochastic spectrum use presents challenges for collecting the requisite measurements. Further, the spectrum agility and learning ability of cognitive radios also creates the possibility of changing operating parameters including frequencies, power, modulation, and even medium access mechanisms. Emerging vehicular networks, which can potentially transform geographic occupancy behaviour through VDSA, introduce another dimension of complexity. Techniques for accurately measuring wideband occupancy and specifying the measurement accuracy in such DSA environments still remains an open issue.

Verification of Technical and Operational Parameters

Spectrum licenses are generally used as an interference management mechanism, through specification of various transmitter operational parameters. In recent times spectrum masks, such as illustrated in Fig 2.6, have increasingly been used as a means for providing technology–neutral licensing, including use in DSA. The main idea has been to place limits on the co–channel and adjacent–channel power which can be transmitted. This approach has several advantages including increased flexibility in spectrum access and usage, inde-

pendent of technology and applications being used. Furthermore, this approach provides a means for specifying the interference levels to which neighbouring devices may be exposed.

While this approach is the current state–of–the–art in specifying spectrum usage, the non–deterministic behaviour of DSA devices introduces many challenges both on establishing suitable limits as well as evaluating compliance. One approach to address this issue is the introduction of a probabilistic paradigm to licensing, similar to those used in network performance management (*e.g.*, using parameters such as bit/frame error rates, call blocking probability, call drop rate and channel switching probability, to name a few). To–date, while current licensing approaches do not currently deploy such a probabilistic approach to specification of spectrum usage rights, there is increasing realization of the benefits of such a shift in paradigm [25].

For such an approach to be feasible, there needs to be a way to accurately estimate policy compliance and to further indicate the confidence in any measurements made. This is essential for successful DSA deployment. Examples of use cases for such an approach include measuring compliance for providing service level agreements, facilitating public safety guarantees and for providing data for arbitration and dispute resolution.

To the best of the author's knowledge, at the time of writing, there is limited work in the use of a probabilistic approach to technical and operational parameter specification in this manner, for DSA operation. However, based upon related use of such approaches in telecommunications management and network management[7], probabilistic specification of parameters are being contemplated. One example is the use of interference temperature metrics [25]. For this task, the challenges introduced in DSA scenarios again include the requirement for fast accurate wideband measurement. Challenges due to the adaptability and agility of CR's and additionally, high mobility in VDSA scenarios, also increase the difficulty of this task.

[7]Such probabilistic approaches are in mainstream use by service providers and in many private networks, primarily through quality of service and service level agreements.

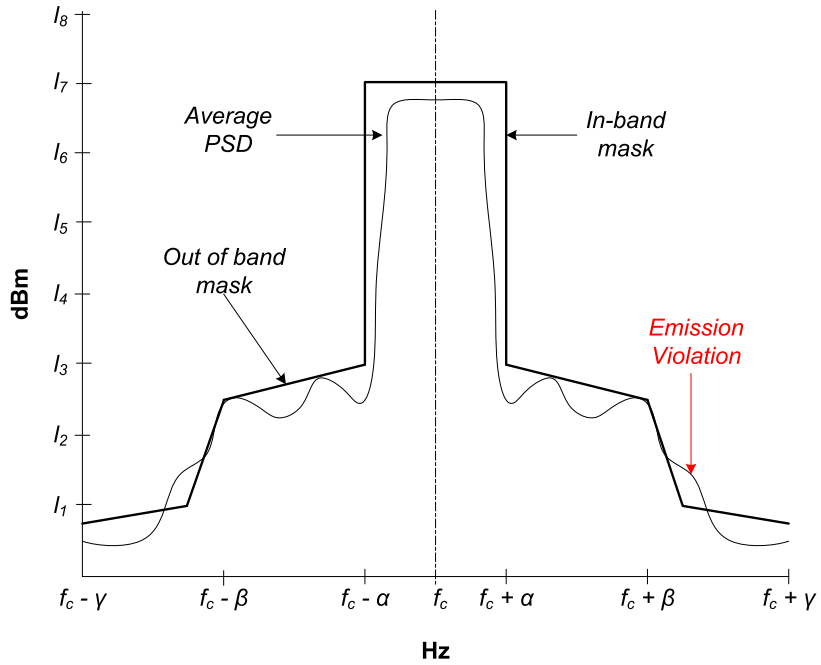

Figure 2.6: Example of a spectrum mask and time–averaged PSD measurement for a channel of interest. Alternatively the Maximum PSD can be used.

Detection, Identification, and Localization of Unauthorized/Misbehaving Transmissions and Interference Sources

This task relates to the previous task of monitoring technical and operational parameters. However, in contrast to assessing the likelihood of non–compliance with specified parameters, in this case misbehaving devices need to be identified and located. Currently there is increasing literature on detection, (*e.g.*, primary user emulation, spectral honeypot, denial of service attacks), which has been seen to be a challenge. Given the time–varying, mobile, possibly intermittent, non–deterministic behaviour of devices in DSA environments envisioned, it would be extremely difficult to detect such behaviour.

Furthermore, location and identification can be even more challenging than detection. Mechanisms for location and identification of authorized but misbehaving transmissions can potentially involve use of the authorizing infrastructure such as the geolocation databases or spectrum brookers which may be used for spectrum access in DSA scenarios. Geolocation databases do not guarantee knowledge of SUs, as database operation depends upon the

regulatory specifications for usage. Spectrum brookers or equivalent devices, may contain details of both SU and PU operations, but mechanisms need to be contemplated for accessing the data in a scalable manner, for compliance monitoring activities. Furthermore, typically use of more data is required for detection, particularly for unauthorized transmissions. Thus location and identification is expected to be equally or more challenging than the case of detection, in general. Again the time–varying, mobile, stochastic characteristics of DSA environments needs to be contemplated in the development of techniques for detection, identification, and location of unauthorized/misbehaving transmissions and interference sources. These are further impacted by the need to clearly articulate spectrum monitoring objectives.

2.4.3 Spectrum Monitoring Infrastructure

Achievement of spectrum monitoring objectives requires the strategic deployment and operation of appropriate measurement infrastructures. Such infrastructure typically can be a network of fixed and mobile monitoring nodes with various capabilities, depending upon management objectives. Consequently many trade–offs exist in development and operation of monitoring infrastructures, such as data accuracy, data currency, accountability, complexity, enforcement requirements, industry needs, infrastructure deployment and operating costs, as well as technology capabilities. An example scenario involving a typical heterogeneous multi–agent wireless spectrum sensing network with fixed and mobile monitoring nodes was illustrated in Fig 1.1. Such a network would provide the required data to facilitate occupancy measurement, spectrum planning, and verification and enforcement of licensing compliance. Traditionally, on the national and regional level, such an infrastructure can be very expensive and complex. Technology innovation has also facilitated increasing use of remote unmanned monitoring approaches taking account of distributed measurements.

In parallel to technological developments, there are also transformations in spectrum monitoring approaches. For example, as opposed to continuous monitoring across all utilized spectrum, there is increasing strategic focus upon monitoring in regions where there is some knowledge of problems and congestion. Another example is the possible outsourcing of some monitoring functionality to government agencies or non–governmental organizations

(NGOs). In such instances the responsibility is shifted to the contracted agency which then shares the monitoring data. Another commonplace arrangement occurs when industry groups assume responsibility for monitoring and spectrum conflict resolution for specific services such as in fixed–link microwave services. Such arrangements allow the regulator to focus upon a smaller subset of public priority bands and services to ensure essential services[8] remain unaffected. This shifting focus to increased third party monitoring is in line with the decentralization of spectrum management functions to facilitate DSA operation. Therefore this shifting trend is expected to continue in years to come.

2.4.4 Performance Metrics for Spectrum Monitoring

In selecting techniques for development of monitoring strategies, both technical and non–technical parameters must be considered. Such deliberation requires considerable context and is therefore not easily addressed at the level of development of monitoring techniques. Therefore, while many possibilities exist for sensing metrics, based upon the literature a few technical evaluation metrics which can be used in assessing the technical performance of monitoring techniques are briefly highlighted as follows:

- **Spectral sweep time:** The spectral sweep time is dependent upon the algorithm used for scanning. For the swept analyzer case, to sweep j disjoint sub–bands the spectral sweep time is given by $T_{sweep} = \sum_{i=1}^{j} \frac{T_{dwell_i} \times FSPAN_i}{RBW_i} + T_{proc_i}$, where T_{dwell_i} is the dwell time at a given center frequency within sub-band i, $FSPAN_i$ is the bandwidth of sub–band i, RBW_i is the resolution bandwidth used in scanning sub–band i, and T_{proc_i} is the processing for that sub-band. This expression becomes more complicated when collaborative sensing is considered, as other factors including information exchange protocols, transmission times and propagation delays must now be considered [122].

- **Measured bandwidth:** Measured bandwidth, or spectral coverage, represents the total bandwidth scanned and in its simplest form is given by $BW = \sum_{i=1}^{j} FSPAN_i$.

[8]Examples of essential services are safety, fire, police, ambulances, and air navigational aids as well as private land mobile networks (PLMNs) for commercial activities.

For probabilistic scanning, such as the random sampling methods proposed in this dissertation, bands are not scanned sequentially as in the swept–tuned analyzer. Thus a probability–weighted summation can be used: $BW = \sum_{i=1}^{j} p_i \times FSPAN_i$, where p_i is the probability of scanning the i^{th} sub–band.

- **Revisit time:** For the swept analyzer the revisit time, $T_{revisit}$, is equivalent to the spectral sweep time. However, for the proposed probabilistic scanning methods, an alternative metric is defined, the expected revisit time: $\bar{T}_{revisit} := E[T_{i,j}|T_{i,j-1}]$, where $T_{i,j}$ and $T_{i,j-1}$ are the j^{th} and $(j-1)^{th}$ times that sub–band i is scanned.

- **Spatial coverage:** The spatial area covered depends upon various parameters such as effective isotropically radiated power (EIRP), path loss, and minimum detectable signal. DSA scenarios in the literature typically assume randomly located emitters, transmitting with different powers. Given the challenges of a deterministic approach to this problem, a probabilistic approach can be used. The total path loss from emitter to sensor, separated by distance, r, is given by, $L(r) = L_{50}(r) + L_s$, where $L_s \sim N(0, \sigma_L^2)$ is the shadowing loss in dB [123], and $L_{50}(r)$ is the median path loss which can be calculated using various existing propagation models, depending upon the specific RF band and environment under consideration [123–125]. σ_L represents the location variability, which is a measure of the shadowing within Ψ [124].

  For a sensor with minimum detectable signal, P_{MDS}, the conditional probability of detecting the emitter given EIRP, P_T,is given by $Prob_{D|P_T}(r) = 1 - Q\left(\frac{P_T - P_{MDS} - L_{50}(r)}{\sigma_L}\right)$, where $Q(x)$ is the complementary cumulative normal distribution. P_{MDS}, represents the device sensitivity which is dependent upon the sensing technique used. It can be shown that for a disc–shaped sensing cell of radius R, the conditional sensing coverage is then given by $Prob_{Cell|P_T}(R) = \frac{1}{2} + \frac{1}{R^2}\int_{r=0}^{R} r \times erf\left(\frac{P_T - P_{MDS} - L_{50}(r)}{\sigma_L\sqrt{2}}\right) dr$. This provides a figure of merit which indicates the ability of the sensor node to detect wireless emissions above a given value within a region.

- K**–coverage:** The sensing network is defined as providing k–coverage, if every point in the region being sensed is within the monitoring range of at least k different sensors [126]. For monitoring performance in DSA scenarios, a modified form of

k–coverage, the conditional k–coverage can be used. It is defined by $C_k\left(P_T\right) = 1 - \prod_{i=1}^{k} Prob_{Cell_i|P_T}(R)$, which is further conditioned on the transmitter EIRP. This can be used to also provide a measure of confidence in the reported measurement results.

While both centralized and decentralized coverage optimization have been studied in the context of dense sensor networks, for example the best and worst coverage problems [127] and the minimum exposure problem [128], monitoring networks can be sparse and coverage is not used as an optimization objective, but rather a means of qualifying the confidence in the sensing results. The rationale for this, is that it is not assumed that the sensor location is deterministic at any given time, (*i.e.*, excluding fixed nodes).

- **Interception probability:** Probability of interception considers temporal, spatial and spectral coverage, and thus combines the coverage metrics. Spatial coverage depends upon the acceptable propagation loss, transmitted power, minimum detectable signal, and location variability which are strictly functions of frequency [124]. Therefore, the cell coverage within a given subband, denoted by $Prob_{Cell|P_T}(R, FSPAN_i)$, can be obtained using the following:
$\left[\frac{1}{2} + \frac{1}{R^2}\int_{r=0}^{R} r \times erf\left(\frac{P_T(FSPAN_i) - P_{MDS}(FSPAN_i) - L_{50}(r,FSPAN_i)}{\sigma_L(FSPAN_i)\sqrt{2}}\right) dr\right] \times \frac{\bar{\tau}_{on}}{\bar{\tau}_{on}+\bar{\tau}_{off}}$,
where $\bar{\tau}_{on}$ and $\bar{\tau}_{off}$ represent the average 'on' and 'off' times for a transmitter operating within the i^{th} sub–band.

  Hence the overall conditional probability of interception for a given power level by a sensor is, $Prob_{Cell|P_T}(R) = \sum_{\Gamma_n} Prob_{Cell|P_T}(R, FSPAN_i)$, where $\Gamma_n \subset \Gamma$ is the set of sub–bands to be monitored within Ψ. From this, k–coverage follows as previously defined.

- **Number of samples collected in a given time:** This is dependent upon the sample rate in space and frequency, as well as the scanning algorithms used, and is given by:
$N = N_{ssweep} \times T_{ssweep} \times N_{fsweep} \times T_{fsweep} \times \pi_s \times \pi_f$,
where π_s and π_f are the average spatial and spectral sample rates, while N_{ssweep} and

N_{fsweep} are the number of spatial and spectral sweeps, respectively and T_{ssweep} and T_{fsweep} are the spatial and spectral sweep times, respectively.

- **Energy consumption:** If focus is placed upon those aspects of node operation that relate to sensing, this objective depends upon computational complexity of the employed sensing techniques. For collaborative sensing, communications functions also consume energy to achieve the sensing objective and must be considered. It must be noted, however, that evaluation of this metric is very implementation dependent.
- **Computational complexity:** The computational complexity is dependent on the computational complexity of the scanning algorithm used, as well as any required data processing. It represents the cost in terms of memory and time resources required for executing a given sensing algorithm.

In most instances the above metrics are more suited to system–level evaluations of monitoring strategies, and are very implementation dependent. Therefore, given the probabilistic nature of the estimation tasks as well as the use of the data for spectrum management and compliance enforcement tasks, in this dissertation primary focus is upon accuracy, with other parameters considered based upon the context. Therefore, for this dissertation, the **bias** and **mean–squared error** (MSE) are primarily used to assess the estimation performance for the proposed techniques.

2.5 Conclusion

In this chapter, several aspects of spectrum monitoring in dynamic spectrum access networks were presented. First, the challenges of current spectrum management approaches were examined and used to motivate the need for management approaches which embrace the shifting paradigm of market–oriented spectrum access methods. Next, an overview of spectrum access models and architectures was presented as well as a discussion of how the cognitive radio functionality facilitates implementation of these models. The main challenges of cognitive radio operation in wireless networks were seen to be the increased

spectrum agility gained through the use of software defined radio platforms, as well as the non–deterministic behaviour that can result from learning algorithms.

Spectrum monitoring was then discussed, motivating its importance in effective spectrum management processes. Key monitoring goals include the collection of strategic collection of data for use in frequency planning, spectrum engineering, EMC validation and for ensuring user compliance with licence conditions, technical standards and operational standards. Representative monitoring use cases for monitoring in DSA scenarios were briefly discussed as well as the need for appropriate monitoring infrastructure for achieving spectrum monitoring objectives. Probabilistic performance metrics were proposed to provide a quantitative technical basis for use in evaluation, designing, and operating infrastructure for spectrum monitoring in future wireless networks, such as DSA scenarios.

The spectrum agility and learning ability of cognitive radios presents various challenges for monitoring for occupancy estimation and compliance verification. Given the non–deterministic behaviour of DSA networks, there is a need for probabilistic approaches to specification of technical and operational parameters for DSA networks. Further, techniques for measurement and specification of accuracy need to be developed which take account of the stochastic specifications. Additional challenges in monitoring networks for DSA operation include wideband monitoring of possibly quicker time–varying, adaptive spectrum usage trends. Such trends include possibly changing operating parameters including frequencies, power, modulation, and even medium access mechanisms. Emerging vehicular networks introduce further complexity in modelling spatial trends in spectrum usage.

To–date, there is limited work in this aspect of monitoring for occupancy measurement and compliance verification in DSA scenarios. Approaches for accurate measurement of wideband spectrum behaviour and specifying the measurement accuracy in such DSA environments still remains an open issue. However the need for such approaches has been viewed as crucial to successful DSA deployment. This motivates the following chapters in this thesis which focus upon temporal and spectral occupancy estimation in DSA scenarios.

Chapter 3

Non–Contiguous Sampling for Spectrum Occupancy Estimation

3.1 Introduction

Measurement of bandwidth occupancy is important for frequency planning, spectrum engineering, interference management and compliance enforcement processes. Through DSA, cognitive radios are currently allowed to dynamically operate over non–contiguous sub–bands within TVWS. Monitoring networks therefore should be capable of monitoring these bands, as well as future spectrum bands allocated for DSA. Such bands may not necessarily be contiguous, may have wide spans, and may be composed of sub–bands with different monitoring requirements. Current swept approaches to monitoring do not allow for simultaneous observation of these bands and typically monitor heterogeneous sub–bands as if they were homogeneous[1]. For example, a licensed TV station operating within a given band may not need to be monitored as often as a band within which a CR network operates. However, current approaches do not allow the flexibility required. Therefore a Non–Contiguous Spectrum Sensing (NCSS) approach to spectrum sensing is proposed, and a probabilistic subset, Random Spectrum Sensing (RSS), is examined as a special case of NCSS. This chapter covers the proposed random spectral sampling approach. Several aspects of this work also

[1]Individual sub–bands may have different monitoring requirements, and are thus not necessarily homogeneous in terms of monitoring requirements.

appear in publications developed for this dissertation: [86, 89, 92, 93].

3.2 Motivation

Opportunistic spectrum access (OSA) networks place new challenges upon existing spectrum monitoring paradigms. A key spectrum monitoring task involves frequency band observations and spectrum occupancy measurements [34, 35]. Currently, limited infrastructure exists for spatio–temporal characterisation of spectrum occupancy across a wide region. Furthermore, although spectrum occupancy modeling forms an important component of effective radio resource management [129–131], there are many obstacles to complete statistics collection even across a limited extent [132]. This is further complicated by emerging OSA networks, where heterogeneous RAT can facilitate either overlay or underlay networks [54]. Additionally, in envisioned OSA environments the Electrospace would be defined by the possibly non–deterministic contributions of various devices using different available RAT.

Another key challenge is wideband characterisation of the Electrospace. Current spectrum monitoring techniques are principally either of two different approaches: 1) Attempting to sense every transmission in the band under observation; or 2) Periodic sensing with statistical estimation of occupancy. Under these two approaches, while the literature illustrates various ways to deal with user detection under different sensing performance requirements, (*e.g.*, energy detection, cyclostationary detection, waveform sensing) [54–57], sensing wide spectrum bands is still a difficult task.

Many techniques have been proposed for wideband sensing such as compressed sensing [58, 59], multi–resolution sensing [60, 61], and collaborative sensing [62, 63], as well as combinations of these [64–66]. However, wideband sensing is still challenged with the interception of intermittent use, particularly in low–occupancy scenarios, and in medium to high–occupancy cases the benefits of using currently proposed techniques can diminish [133][2]. Additionally, current approaches do not account for envisioned intermittent secondary spectrum usage. Furthermore, in many of the approaches, spectrum sensing is

[2]Generally, revisit times must be small enough to scan bands of interest at an acceptable speed to detect individual short transmissions. If, alternatively a statistical approach is used with longer revisit times, then the accuracy of the statistical approach depends on the value of occupancy [134].

channel–oriented and thus ill–suited for modeling the impact of heterogeneous RAT on spectrum occupancy.

One commonality in all proposed sensing techniques is the need for some sort of spectral analysis. In the literature, many spectral estimation methods have been proposed, including classical non–parametric periodogram spectral estimators, as well as parametric methods [121]. In comparison to parametric methods, the nonparametric methods are relatively simpler, well understood, and can be easily computed using existing fast fourier transform algorithms. It is therefore no surprise that non–parametric methods have been a popularly proposed approach for spectrum sensing. However such methods rely upon finite data lengths via windowing, which introduce spectral leakage. In selecting an appropriate windowing function to reduce spectral leakage, a design tradeoff is faced between frequency resolution and spectral dynamic range. The different spectral characteristics of possible signals in a heterogeneous environment introduces further challenges in selecting an appropriate window function for spectral estimation.

To address these challenges a non–contiguous approach to spectrum sensing is proposed. A filter bank approach to implement NCSS for characterisation of wideband spectrum occupancy for spectrum monitoring networks is also presented. While the use of filter banks in spectral estimation is not new, the polyphase formulation naturally fits the proposed multiband, multilevel filter proposed for NCSS techniques. Filter banks also potentially offer various advantages for spectral analysis, for example in multicarrier communications, where spectrum sensing comes at no additional computational cost [135]. For spectrum sensing, filter banks also offer lower complexity alternatives to the near-optimum Thomsons multitaper method [136] achieving almost identical performance [137], and have also been used in estimation of low probability of intercept adaptive frequency hopping signals [138].

In this chapter, a channel–agnostic stratified random spectral sensing approach to statistical characterisation of wideband spectrum occupancy for spectrum monitoring networks is primarily examined. Specifically, a spectral stratification technique is proposed which uses similarity measures for implementation in online RSS. Experimental results obtained during the course of this dissertation suggested that RSS mean–squared error performance depends upon the stratification technique used [89], justifying the proposed stratification technique.

RSS is presented as an alternative to compressed sensing, which in recent literature has been the most frequently investigated alternative for wideband sensing [58, 66, 67].

The significance of the proposed approach partially originates from the fact that the effectiveness of compressed sensing depends upon the choice of a suitable basis matrix and the assumption of sparsity, making it more suited to low–occupancy scenarios. In fact it is under such low–occupancy scenarios that compressed sensing has been motivated as a mechanism for OSA devices. However, from the perspective of spectrum management, there are many instances of interest (*e.g.*, cases of spectral congestion), which negate the sparsity assumption[3]. Also compressed sensing methods are typically used in cases where spectrum reconstruction is a requirement. The spectrum occupancy estimation application does not require spectrum reconstruction, which provides additional motive for the presented RSS approach, since the extra complexity of spectral reconstruction is avoided in RSS.

The rest of this chapter is organised as follows: In Section 3.3 the problem is discussed further, followed by an overview of occupancy modeling, and the proposed NCSS framework in Section 3.4. This is followed by a description of the similarity–based stratification approach and the filter bank implementation description in Section 3.5. Validation of the proposed stratification approach is presented in Section 3.6, followed by results with its use with RSS in Section 3.7. Finally there are concluding remarks in Section 3.8.

3.3 Spectrum Sensing Problem

Consider a heterogeneous radio access scenario without definitions of channels according to specific radio access technologies. Each spectrum sensor is capable of energy detection sensing, and has time and frequency sensing resolutions specified by Δ_t and Δ_f respectively. For a single sensor the sensing objective is to statistically model the spectrum occupancy for spectrum $F = [f_0, f_0 + N_f\Delta_f]$ for time $T = [t_0, t_0 + mN_t\Delta_t]$, where m is the number of time samples per sensing period, $\Delta_f \ll F$ and $\Delta_t \ll T$. In order to model spectrum occupancy, spectral estimation is essential. This can be accomplished using filter bank spectral estimators (FBSEs). FBSEs have been widely used for spectrum analysis applications, with

[3]If a suitable orthonormal basis or alternative transformation can be identified for which there is signal sparsity. However, in general this can be difficult to guarantee using current approaches.

recent application to cognitive radio systems [135].

In the literature, FBSE techniques facilitate signal power measurement at the filter bank outputs. However such methods rely upon finite data lengths via windowing, which introduces challenges. Each sub–band filter determines the frequency resolution of the spectrum analyzer, through the main lobe width of the filter. Resolution is an important parameter in resolving closely spaced signals, even if they have similar energy levels. However, generally higher frequency resolution is associated with more spectral leakage. Side lobe magnitudes introduce spectral leakage from other parts of the spectrum, which introduces bias in spectrum estimates. This reduces the ability of the spectrum sensor to discern signals of dissimilar frequencies and energy levels. This ability is quantified by the dynamic range which is defined as the ratio of the maximum and minimum spectral power levels which can be distinguished by a particular spectral estimation technique.

Several approaches have been proposed to design suitable filter banks which trade off between frequency resolution and dynamic range. To accomplish this, filter parameters such as passband, stopband, ripple, and order can be adjusted. Finite impulse response (FIR) filters are a common choice, particularly when linear phase characteristics are required, even though they typically require higher filter orders to achieve comparable performance to their infinite impulse response (IIR) counterparts. However, increased performance usually comes at the cost of increased implementation complexity.

We consider the above problem, and propose the use of NCSS. The main idea behind NCSS is to separate filters so that at any given time only non–adjacent bands are simultaneously sensed. By sub–band separation, we reduce the constraints imposed by spectral leakage in spectrum sensing applications. The NCSS concept is illustrated in Fig 3.1.

3.4 Non–Contiguous Spectrum Sensing Framework

3.4.1 Bandwidth Occupancy Modeling

In the typical case, the spectrum data set measured by a sensor would consist of power measurements taken across the time and frequency domains at a given location (indexed, n, where n can be a tuple denoting location coordinates), which can be represented by,

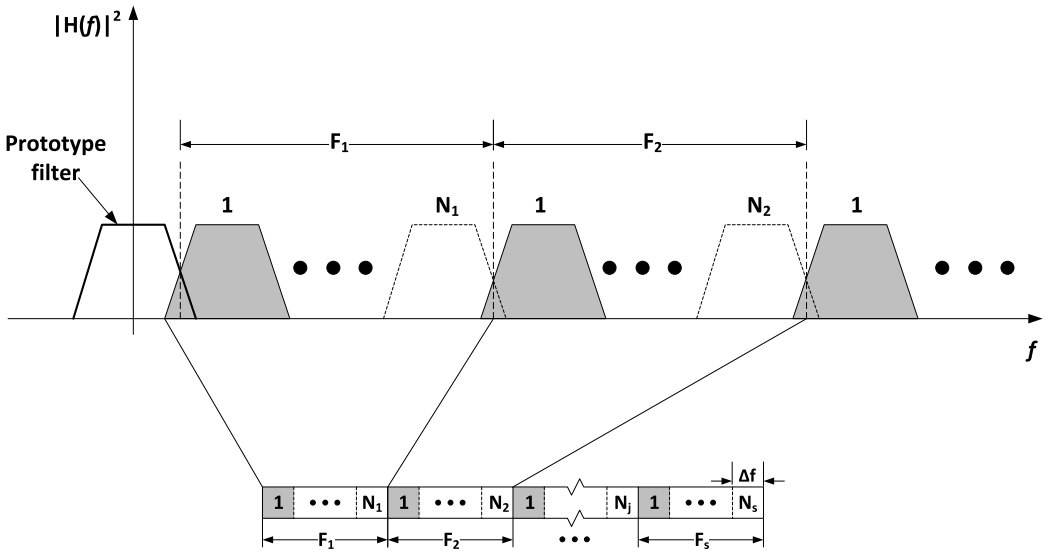

Figure 3.1: Illustration of NCSS. Spacings of F_j separate sensed sub–bands at any instant in time.

$\mathbf{P}_n = [P_n(t,f)]_{t\in T, f\in F, n\in[1,\cdots,N_n]}$. Typically $P_n(t,f)$ is obtained from a function of discrete–time samples $q_n[k], k = Nm+1,\cdots,(N+1)m$. In most cases $P_n(t,f)$ represents the discrete fourier transform of the time samples. However, other transforms (*e.g.*, Wavelet) are possible [121].

Since $\Delta_f \ll F$, each channel would span $l\Delta_f$, where l is not necessarily an integer ($l \in \mathbb{R}$), and may vary for each RAT for heterogeneous access. For channel–agnostic characterisation using energy detection, the occupancy at a given time instant, $t_i \in T$, will be defined as the proportion of spectrum of interest for which the signal exceeds a specified threshold τ:

$$p_f(t_i) = \frac{1}{N_f}\sum_{f\in F} I_{\{P_n(t_i,f)>\tau\}}(f), \tag{3.1}$$

where $I_{\{A\}}(a)$ is the indicator function:

$$I_{\{A\}}(a) = \begin{cases} 0, & a \notin A \\ 1, & a \in A. \end{cases} \tag{3.2}$$

Generally τ can be a function of space, time and frequency. At a given time instant, t_i, denote the measured power for the j^{th} interval $[f_0+(j)\Delta_f, f_0+(j+1)\Delta_f]$ by the random

process, $X_{f_j}(t_i) = P_n(t_i, f_j)$. The corresponding amplitude power distribution cumulative density function is given by $Pr(P_n(t_i, f_j) \leq x)$. For notational brevity $X_{f_j}(t_i)$ and X_{f_j} are used interchangeably in this chapter, and the time of the measurement is implied. Statistically modeling $p_f(t_i)$ across F, strictly requires consideration of the joint density function $Pr\left(\{(X_{f_0}, X_{f_1}, \cdots, X_{fN_f}\right)$. This poses several problems.

In addition to the high dimensionality of this problem, spectral and temporal correlation must be considered. The challenges associated with dependent, heterogeneous random variables are well known [139–141]. When the band under consideration exceeds the coherence bandwidth, for small enough Δ_f there may be dependence between adjacent measurement intervals within the same channel. Also for non–adjacent intervals, such as in non–contiguous orthogonal frequency division multiplexing techniques, there may be some dependence between non–contiguous intervals, even if individual channels were independent. However, through random sampling of the partial sum of dependent random sequences, an asymptotic distribution for $p_f(t_i)$ can be determined [140]. This forms the basis for the methods proposed in this chapter.

3.4.2 Systematic Spectral Sensing

The simplest form of NCSS is based upon periodic temporal sampling (*i.e.*, time interval between sampling instants, $L\Delta_t, L \in \mathbb{N}$, is approximately constant). Consider F is divided into s non–overlapping intervals $\{F_j\}$: $F = \bigcup_{j=1}^{s} F_j$ and $F_j \bigcap F_k = \emptyset, j \neq k; j, k \in \mathbb{N}$ (Fig 3.3). Each of the intervals is of width $N_j \times \Delta_f$. For systematic sampling assume that N_j is constant and without loss of generality, that i^{th} sub–band of each interval is sensed[4]. F_j represents the separation between the j^{th} and $j + 1^{th}$ sensed sub–bands, which would be fixed for systematic spectral sampling, but not necessarily fixed for other sampling strategies. Let $\mathbf{z_j}(t_i) \in \{0, 1\}^{n_j \times 1}$ be the sampling vector for sub–band F_j at time, t_i. Sub–entries of $\mathbf{z_j}(t_i)$ are 1 if the corresponding interval is sampled, and 0 otherwise.

[4]For systematic sampling the value of i is randomly selected from $1, \ldots, N_j$. Note that multiple intervals can be selected in a given sub–band, such that there is a constant spectral separation between consecutively sampled intervals.

3.4.3 Random Spectral Sensing

We will adopt the same notation used for systematic spectral sensing, noting that in this case N_j can vary for each interval. RSS [89] is a special class of NCSS. In RSS the sensed sub–intervals are randomly selected (*i.e.*, $\mathbf{z_j}(t_i)$ is randomly generated according to some probability distribution). By virtue of this definition, sub–bands will not necessarily be sensed periodically in time or frequency. Based upon this, several sensing schemes exist. Fig 3.2 illustrates three possibilities:

1. In static random spectral sensing (SRSS), randomisation is performed at the start of sensing, and remains fixed for the entire duration (or blocks of sufficiently large duration).

2. In block–static random spectral sensing (BRSS), randomisation is performed at the start of contiguous time blocks of length $B_i\Delta_t$ and remains fixed only for each block duration.

3. Dynamic random spectral sensing (DRSS), facilitates frequency randomisation for every sensing interval.

BRSS can be considered to be the most generalised form, with SRSS and DRSS being specific cases with block sizes $B_i \to \infty$ (*i.e.*, $B_i\Delta_t \geq$ measurement time span of interest) and $B_i = 1$ respectively. There would be tradeoffs in each of these schemes when measures of performance such as computational complexity, precision, and sample minimisation are considered. With the exception of SRSS, for each of the above random approaches, sensing coverage of all sub–bands within a bounded interval (*i.e.*, finite revisit time), can be ensured, provided that $P[\mathbf{z}_j[q] = 1] > 0$ [89], where $P[A]$ denotes the probability of event A occurring, and $\mathbf{z}_j[q]$ is the q^{th} element of the vector $\mathbf{z}_j$.

3.4.4 Spectral Sampling

The analysis in this section applies to the previously discussed forms of NCSS: Systematic and Random Spectral Sensing. For this chapter, we simplify our analysis by considering periodic temporal sampling, with randomisation of spectral sampling. Consider F is divided

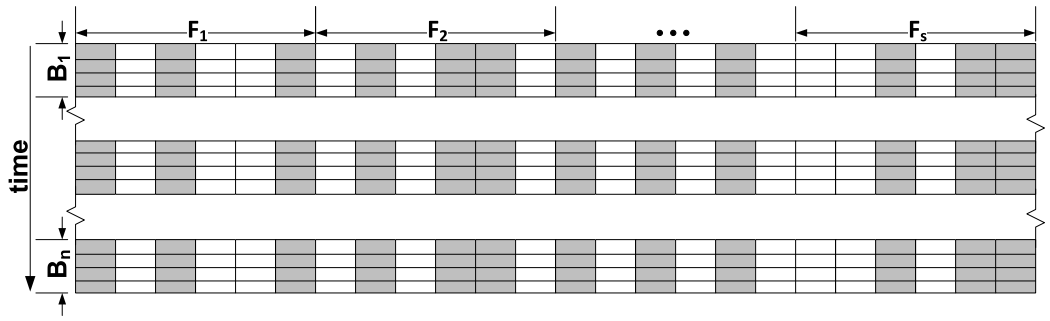

(a) Static random spectral sensing (SRSS)

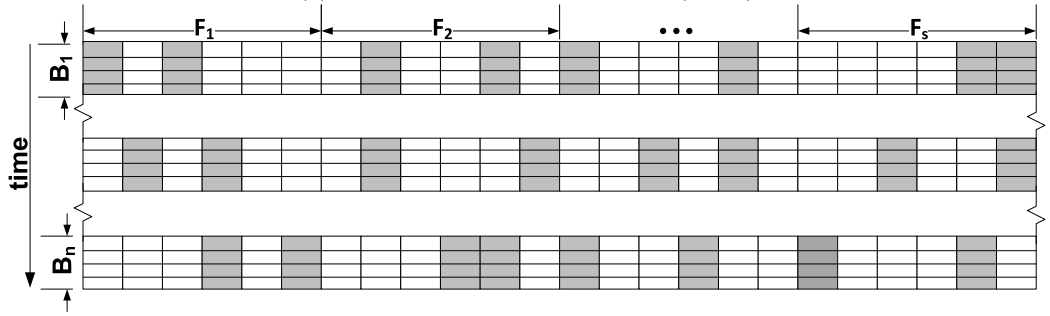

(b) Block-static random spectral sensing (BRSS)

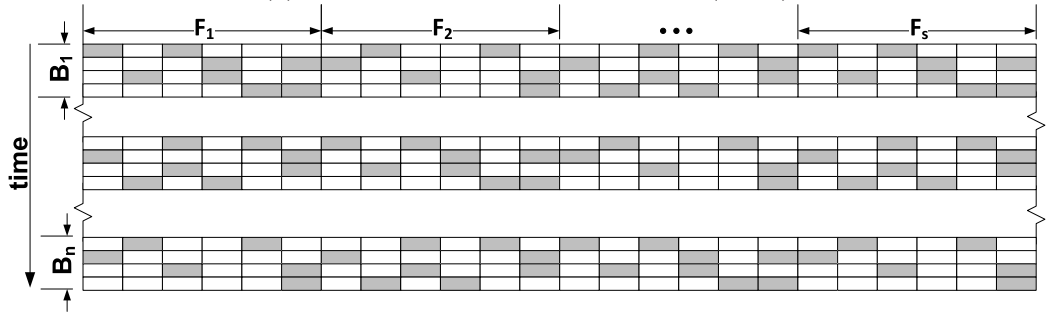

(c) Dynamic random spectral sensing (DRSS)

Figure 3.2: Illustration of random spectral sensing schemes. B_i represent time blocks. F_i represent sub-band groups

into s non–overlapping sub–bands $\{F_j\}$: $F = \bigcup_{j=1}^{s} F_j$ and $F_j \bigcap F_k = \emptyset, j \neq k; j,k \in \mathbb{N}$ (Fig 3.3). Each of the sub–bands is of width $N_j \times \Delta_f$ and a random sample $\mathcal{S}_j$ of size n_j is selected from each. For this study, within each sub–band, each interval is equally likely to be selected[5]. Thus each interval has probability, $\pi_j = \frac{n_j}{N_j}$ of being selected [142]. Let $\mathbf{z_j}(t_i) \in \{0,1\}^{n_j \times 1}$ be the sampling vector for sub–band F_j at time t_i. Sub–entries of $\mathbf{z_j}(t_i)$

[5]For Systematic Spectral Sensing, the sampling vector is fixed and the analysis proceeds similarly.

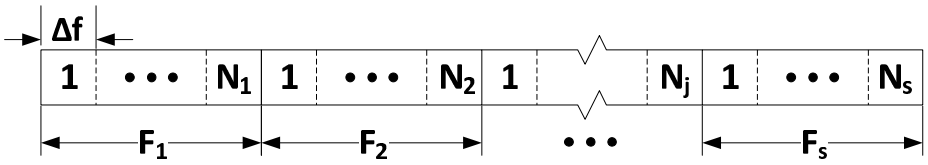

Figure 3.3: Spectrum divided into s sub-bands for random sampling at time t_i.

are 1 if the corresponding interval is sampled, and 0 otherwise. Using (3.2) define $\mathbf{F_j}(t_i)$ as the jth sub-band occupancy vector at time t_i:

$$\mathbf{F_j}(t_i) = \left[I_{\{P_n(t_i,f)>\tau\}}\right]_{f\in F_j, n\in[1,\cdots,N_n]}. \tag{3.3}$$

For a sample $S_j(t_i)$ the bandwidth occupancy of the jth sub–band is then estimated using [142]:

$$\begin{aligned}\hat{p}_{j,t_i} = \hat{p}_j(t_i) &= \frac{1}{n_j}\sum_{k\in S_j(t_i)} F_{j,k}(t_i) \\ &= \frac{1}{n_j}\mathbf{z_j^T}(t_i)\,\mathbf{F_j}(t_i).\end{aligned} \tag{3.4}$$

Using (3.4) the overall bandwidth occupancy can then be estimated as [142]:

$$\begin{aligned}\hat{p}_f(t_i) &= \sum_{j=1}^{s}\frac{N_j}{\sum_{k=1}^{s}N_k}\hat{p}_{j,t_i} \\ &= \sum_{j=1}^{s}\frac{N_j}{n_j\sum_{k=1}^{s}N_k}\mathbf{z_j^T}(t_i)\,\mathbf{F_j}(t_i) \\ &= \sum_{j=1}^{s}\frac{1}{\pi_j N_f}\mathbf{z_j^T}(t_i)\,\mathbf{F_j}(t_i).\end{aligned} \tag{3.5}$$

This represents a stratified sampling approach to occupancy estimation. Alternatives exist, such as cluster–based and complex hybrid sampling approaches [142]. In the heterogeneous RAT scenario, cluster–based and stratified sampling capitalise upon the dependence of adjacent intervals. However, given the larger bound on variance in the cluster–based sampling case [142], in this paper stratified sampling will be the focus. For the stratified

approach it can be shown that an estimate of the occupancy variance is given by [142]:

$$\begin{aligned}\hat{v}_f\left(t_i\right) &= \sum_{j=1}^{s}\left(1-\frac{n_j}{N_j}\right)\left(\frac{N_j}{N_f}\right)^2\frac{\hat{p}_{j,t_i}\left(1-\hat{p}_{j,t_i}\right)}{n_j-1} \\ &= \sum_{j=1}^{s}\left(1-\pi_j\right)\left(\frac{N_j}{N_f}\right)^2\frac{A_j\left(t_i\right)}{n_j^3-n_j^2}\end{aligned} \tag{3.6}$$

where

$$A_j\left(t_i\right)=\mathbf{z_j^T}\left(t_i\right)\mathbf{F_j}\left(t_i\right)\left(n_j-\mathbf{z_j^T}\left(t_i\right)\mathbf{F_j}\left(t_i\right)\right) \tag{3.7}$$

In the heterogeneous RAT context, through random sampling (3.3)-(3.7) provide the basis for interval estimates of sub–band and overall occupancy in terms that do not depend upon specific definitions of channels according to RAT. For this study, proportional allocation will be considered, in which the sampling ratio $\frac{n_j}{N_j}$ is the same for all sub–bands (*i.e.*, $\pi_j=\pi,\forall j$). In spectrum monitoring, a key performance metric is the revisit time. To accommodate the random sampling, the definition is a slightly modified form to that according to [134]. It can be shown that for proportional allocation, the expected revisit time for sensing any given interval is directly proportional to $\frac{1}{\pi}$. It is noted, however, that other allocation schemes exist that take account of strata variances and sampling costs in variance reduction of the estimator (*e.g.*, such as optimal allocation and Neyman allocation) [142], with tradeoffs on the revisit time. For proportional allocation (3.6) becomes:

$$\begin{aligned}\hat{v}_{f_{prop}}\left(t_i\right) &= \frac{\left(1-\pi\right)}{\pi^2}\sum_{j=1}^{s}\left(\frac{1}{N_f}\right)^2\frac{A_j\left(t_i\right)}{n_j-1} \\ &\approx \left(\frac{1}{\pi}-1\right)\sum_{j=1}^{s}\left(\frac{N_j}{{N_f}^2}\right)\hat{p}_{j,t_i}\left(1-\hat{p}_{j,t_i}\right),\end{aligned} \tag{3.8}$$

where the approximation is valid for $\pi N_j \gg 1$. Using (3.5) and (3.8) and assuming normality the $100(1-\alpha)\%$ confidence interval for the proportional allocation occupancy estimate is therefore given by:

$$\hat{p}_f(t_i) \pm z_{\frac{\alpha}{2}}\sqrt{\hat{v}_{f_{prop}}(t_i)}, \tag{3.9}$$

where $z_{\frac{\alpha}{2}}$ is the $(1-\frac{\alpha}{2})^{th}$ percentile of the standard normal distribution. For smaller values of π, $t_{\frac{\alpha}{2}}$, the $(1-\frac{\alpha}{2})^{th}$ percentile of the t–distribution with $\pi N_f - s$ degrees of freedom is used instead of $z_{\frac{\alpha}{2}}$.

3.5 RSS Implementation

3.5.1 Spectral Stratification

The effectiveness of stratified sampling, measured by the variance estimator of the occupancy given in (3.6), depends upon the ability to determine appropriate strata for grouping similar sub-bands together [142]. As typically done in stratified sampling, this can be accomplished by first collecting preliminary data for coarse characterisation of similar sub–bands. In [89] RSS was investigated experimentally for two simple stratification schemes: stratification according to available licensing information and equal spectral width stratification.

In the former approach, it was assumed that stratification according to available licensing information would group the spectrum into bands with sufficiently similar occupancy characteristics. This assumption appears reasonable when current static primary user licensing strategies are considered. Further, although over the wider spectrum covering multiple strata the technologies are heterogeneous, within each individual stratum the RAT are generally similar. Based upon this premise, the case where licensing information is available for a given area was then considered. This information can be obtained for example through coarse knowledge of licensing information for the spectrum band of interest or national allocation plans. The spectral boundaries are then used for determining suitable strata (*e.g.*, stratification into cellular, paging or WCS sub–bands).

However, this approach assumes that sensors can be programmed or have access to licensing data for online adaptation of sensing as necessary. Problems with this approach are:

1. The assumption of intra–stratum homogeneity may not be valid for all sub–bands,
2. Considerable configuration of devices may be required during measurement, and
3. This approach lacks the flexibility required for envisioned dynamic and stochastic OSA environments, compared to current static spectral assignments.

As opposed to the above licensing approach to stratification and monitoring, it is still possible to use equal stratification in which the spectrum is divided into equally–sized sub–bands without consideration of which services or technologies exist in each case. For this

scheme, sub–bands are of equal width (*i.e.*, $N_j = N, \forall j$). While this approach is relatively simple, the assumption of intra–stratum homogeneity may not be met depending on the size of stratum chosen. Additionally, experimental results show that for this method of stratification the variance of occupancy estimates generally exceeds that of the licensing approach, resulting in less precise estimates for spectrum occupancy because of correlation between sampled intervals decreasing the effective sample size [89].

From the experiments, for both approaches, within some sub–bands there can still be considerable heterogeneity if a stratum included several channels and if the channels exhibited different occupancy characteristics. An example was when cellular band occupancy was divided into smaller bands. The mean–squared error (MSE) performance was worse compared to overall wide band occupancy estimation, if the sampled intervals were not representative of the entire cellular band being sensed [89]. In practice, both spectral correlation and intra–stratum heterogeneity adversely impact RSS performance using the above stratification approaches, and therefore the use of similarity metrics is proposed to aid in spectrum stratification.

3.5.2 Spectral Similarity

The proposed approach is based upon the similarity between intervals decreasing with their separation. Similarity is assessed through the use of distance–based metrics. A larger distance between intervals means less similarity between the intervals. Initially the entire band is monitored for duration $N_0\Delta_t$ time units. Each column of the resulting $\mathbf{P}_n$ represents a time series of measurements for a single interval of width Δ_f. The k^{th} interval represents the time series, $P_n(t, f_k)$, where f_k, n are frequency and location indices, respectively.

Because of possibly different characteristics at different measurement locations, at each location, $\mathbf{P}_n$ can be converted to $\mathbf{G}_n$ using the gray–scale (*i.e.*, scaled to the interval [0,1]) linear transformation:

$$\mathbf{G}_n = \frac{\mathbf{P}_n - \min \mathbf{P}_n}{\max \mathbf{P}_n - \min \mathbf{P}_n}, \tag{3.10}$$

where $\max \mathbf{P}_n$ and $\min \mathbf{P}_n$ are the maximum and minimum values of $\mathbf{P}_n$, respectively. This approach is not necessary in online implementation, but facilitates a simple way to define

ϵ–similarity for multiple locations. Intervals are considered similar if the gray–scale distance between them does not exceed $\epsilon \in [0, 1]$. This allows a fixed gray–scale similarity threshold to be used at different locations. However this value would be scaled depending upon the signal strength parameters at a given location.

Alternatively $\mathbf{P}_n$ can be converted into an occupancy matrix, $\mathbf{O}_n$, which contains binary elements. Each matrix element in $\mathbf{O}_n$ is 1 if a signal is present, and 0 if no signal is present. If energy detection is used to convert $\mathbf{P}_n$ to $\mathbf{O}_n$ at each site, a threshold, $\tau_n(t_i, f_j)$, can be determined for each element in $\mathbf{P}_n$. This formulation of the threshold as a function of time, frequency, and space allows for possible scenarios in which OSA occurs within bands using different technologies. The formulation also allows for use of global thresholds, or band–specific thresholds.

In practice, thresholds can be set across the entire spectrum of interest, based upon equipment sensitivity and specified regulatory limits. For example, for initial TV White Space applications, the FCC set incumbent sensing level requirements at -114 dBm for protection of wireless microphones [143]. Other approaches have also been suggested in the literature such as automatic thresholding (*e.g.*, automatic thresholding using Otsu's threshold selection method for gray–level histograms [144]). For a given threshold $P_n(t_i, f_j) \leq \tau_n(t_i, f_j)$ are classified as noise, while all others are classified as signals. A classification matrix, $\mathbf{O}_n$, can then be constructed where:

$$O_n(t_i, f_j) = \begin{cases} 0, & P_n(t_i, f_j) \leq \tau_n(t_i, f_j) \\ 1, & P_n(t_i, f_j) > \tau_n(t_i, f_j) \end{cases}. \tag{3.11}$$

For the initial measurement duration, processes are assumed to be stationary, which can be realised in practice by appropriate choice of the duration. Pairwise distances between measured spectral intervals are calculated. Although several distance metrics are possible, in general the Minkowski distance metrics have the lowest complexity, and includes the Hamming, Manhattan, Euclidean, and Chebyshev distances as special cases [145]. It is also noted that in addition to those metrics indicated, measures of statistical correlation, such as Pearson's Correlation coefficient can also be used. While each distance metric has its advantages for different data types, for non–binary data the Manhattan distance has the

lowest complexity [145]. For binary data, such as the occupancy matrix, $\mathbf{O}_n$, the Hamming distance is a more appropriate metric.

Using the selected distance metric, the distance matrix can be calculated using the following procedure, for $i \in [1, N_0], j \in [1, N_f], n \in [1, \cdots, N_n]$:

1: **function** DISTMAT($\epsilon, [P_n(t_i, f_j)]$)
2: $\mathbf{D} := \mathbf{0}$; ▷ $N_f \times N_f$ matrix of zeros
3: $\mathbf{I} := \mathbf{1}$; ▷ $N_f \times N_f$ matrix of ones
4: **for** $k \leftarrow 2, N_f$ **do**
5: $\mathbf{v}_k = [P_n(t_1, f_k), \ldots, P_n(t_{N_0}, f_k)]^T$;
6: **for** $l \leftarrow 1, k-1$ **do**
7: $\mathbf{v}_l = [P_n(t_1, f_l), \ldots, P_n(t_{N_0}, f_l)]^T$;
8: $\mathbf{D}[k,l], \mathbf{D}[l,k] \leftarrow \mathbf{dist}(\mathbf{v}_k, \mathbf{v}_l)$;
9: **if** $\mathbf{D}[k,l] > \epsilon$ **then**
10: $\mathbf{I}[k,l], \mathbf{I}[k,l] \leftarrow 0$;
11: **end if**
12: **end for**
13: **end for**
14: **end function**

The notation $\mathbf{A}[i,j]$ is used to denote the entry in the i^{th} row and j^{th} column of the matrix $\mathbf{A}$. For vectors the notation $a[i]$ denotes the i^{th} entry in the array or vector a. $\mathbf{D}$ represents the $N_f \times N_f$ distance matrix and $\mathbf{I}$ is a similar dimensioned matrix where if the i^{th} and j^{th} sub–bands are ϵ–similar, then the $\mathbf{I}[i,j]$ and $\mathbf{I}[j,i]$ matrix entries are set to 1. Non–similar pairs are conversely set to 0. $\mathbf{P}_n$ can be substituted by its gray–scale equivalent, $\mathbf{G}_n$, or by the occupancy matrix, $\mathbf{O}_n$, in the above procedure.

Figs 3.5–3.8 illustrate examples of calculated distance matrices for captured spectrum data. Time series of correlated interval pairs exhibit smaller distances than dis–similar interval pairs. In Figs 3.5–3.8 these manifest as ϵ–squares, which are sub–matrices in which all the terms are less than ϵ. Thus ϵ–squares would produce a block diagonal matrix. Even in cases where disjoint bands have distances less than ϵ, in this study, focus is on stratification of contiguous intervals. Therefore this becomes a search along the diagonal for ϵ–squares:

```
1: function MatSearch(I)
2:     s ← 0;                                   ▷ s : number of strata identified
3:     starts[1], ends[1] ← 1;
4:     k, l ← 1;
5:     repeat
6:         repeat
7:             l ← l + 1;
8:         until I[k, l] = 0 or l > N_f
9:         if l ≤ N_f then
10:            s ← s + 1;
11:            starts[s] ← k;
12:            ends[s] ← l − 1;
13:            k ← l;
14:        end if
15:    until k = N_f
16: end function
```

Therefore, using the distance matrix, contiguous intervals with similar characteristics can be identified and treated as separate strata. However, it is noted that stratification of non–contiguous intervals are an extension of the search routine. The tradeoff would be increased complexity, in also keeping track of non–contiguous spectral intervals in a given stratum. At this time non–contiguous intervals are not considered, and thus it is assumed that intervals which would be classed as similar are close together. For low occupancy as well as high occupancy bands this prevents the stratification approach from grouping bands together which may not be correlated (*e.g.*, non–contiguous broadcasting TV channels or non–contiguous unoccupied bands).

3.5.3 Randomised Time-Frequency Sampling Algorithm

In sub–section 3.4.3 the RSS schemes were presented. As previously stated, DRSS and SRSS are special cases of BRSS. Therefore in this sub–section the BRSS algorithm is presented, from which the other algorithms can be derived by setting the block size

accordingly. A key output of the procedures in sub–section 3.5.2 is the identification of strata for RSS. $starts[j]$ and $ends[j], j = 1, \ldots, s$ respectively provide start and end points for each stratum. Using identified strata, BRSS then follows:

1: **function** BRSS($B_i, numBlks, N_0, \pi, \epsilon$)
2: $\quad\mathbf{P}_n \leftarrow Scan(F, \hat{1}, N_0)$; ▷ $\hat{1} : N_f \times 1$ vector of ones
3: $\quad$DistMat($\epsilon, \mathbf{P}_n$);
4: $\quad$MatSearch($\mathbf{I}$);
5: $\quad$**for** $l_1 \leftarrow 1, numBlks$ **do**
6: $\quad\quad\mathbf{z} \leftarrow \hat{0}$; ▷ $\hat{0} : N_f \times 1$ vector of zeros
7: $\quad\quad$**for** $j \leftarrow 1, s$ **do**
8: $\quad\quad\quad N_j \leftarrow ends[j] - starts[j] + 1$;
9: $\quad\quad\quad n_j \leftarrow \pi \times N_j$;
10: $\quad\quad\quad ind[] \leftarrow RndChoose(n_j, starts[j], ends[j])$;
11: $\quad\quad\quad$**for** $k \leftarrow 1, n_j$ **do**
12: $\quad\quad\quad\quad\mathbf{z}\,[ind[k]] \leftarrow 1$;
13: $\quad\quad\quad$**end for**
14: $\quad\quad$**end for**
15: $\quad\quad$**for** $l_2 \leftarrow 1, B_i$ **do**
16: $\quad\quad\quad\mathbf{P}_n \leftarrow Scan(F, \mathbf{z}, 1)$;
17: $\quad\quad\quad\hat{p}_f[l_1 \times B_i + l_2] \leftarrow OccEstimate(\mathbf{P}_n)$
18: $\quad\quad$**end for**
19: $\quad$**end for**
20: **end function**

Thus the overall process consists of an initial period $N_0\Delta_t$ in which the entire band of interest is sensed, followed by stratification, followed by BRSS for some amount of time. The stratification process does not need to be performed after every single BRSS period due to the sensing overhead. However, in dynamic situations it should be performed frequently enough so that the strata can be adapted based upon the changing sub–band groupings across the sensed wide band. This behaviour is controlled via lines 2–4, and the outermost for loop in line 5. There is thus a tradeoff between stratification adaptability and the sensing

overhead, which can be tuned using $numBlks$ to determine how many blocks should be scanned before another stratification is performed.

Line 2 scans the entire band of interest, F, for N_0 sweeps. The function $Scan(a, \mathbf{b}, c)$ scans band a for c sweeps. $\mathbf{b}$ is the binary sampling vector which determines which sub–intervals are to be sampled in the function call. Lines 3–4 perform spectral stratification, as described in sub–section 3.5.2. The outer for loop starting in line 5 controls how many blocks are scanned using the stratification obtained. Line 6 initialises the sampling vector to all zeros at the start of each block. The dimensionality of the sampling vector is determined by the width of the band being scanned simultaneously, and the resolution bandwidth.

Lines 7–14 create the sampling vector for the entire band of interest. In line 10 the function $RndChoose$ is used to randomly select n_j sub–intervals within the j^{th} stratum. The function $RndChoose(a, b, c)$ randomly selects a numbers within the interval $[b, c]$. The for loop in lines 11–13 sets the corresponding locations in the sampling vector to 1 to indicate that these randomly selected intervals will be sampled within the stratum. Finally, lines 15–18 implement RSS for B_i sweeps and for each sweep uses the $OccEstimate$ routine to implement the occupancy estimation discussed in sub–section 3.4.4.

3.5.4 Filter Bank Implementation

The previous sub–sections illustrate procedures for stratification and BRSS implementation. However, an important issue to be resolved is the provision of a means of actually performing the RSS in the spectrum sensor. Typical FFT spectrum sensors based on sensing contiguous intervals in general would not be able to perform RSS without dropping some sensed sub–bands, which is inefficient. Swept–tuned sensors can be used with some mechanism for randomly selecting intervals to visit. However, in general the sweep time is much longer than the more recent FFT–based counterparts, and swept–tuned sensors do not facilitate simultaneous sensing of wide bands as do the FFT–based counterparts.

In this sub–section a discussion is now presented on how RSS can be accomplished using filter–banks, which is relatively more suited to RSS implementation than the other options listed above. FBSEs have been widely used for spectrum analysis applications, with recent application to cognitive radio systems [135]. To implement RSS the framework of adjustable

multilevel filters [146] is employed. Consider the multilevel filter, $G(z)$, which has M sub–bands each of equal width, $\Delta_f = \frac{2\pi}{M}$. Clearly $M = \sum_{j=1}^{s} N_j$. $G(z)$ can be formulated in terms of a prototype filter, $H(z)$, which is a low–pass filter, for the zeroth band. $H(z)$ is given by:

$$H(z) = \sum_{n=0}^{N-1} h[n] z^{-n}, \tag{3.12}$$

where $h[k]$ is the filter impulse response for $H(z)$. $H(z)$ can be expressed in the M–component polyphase form:

$$H(z) = \sum_{l=0}^{M-1} z^{-l} E_l(z^M), \tag{3.13}$$

where we let $N = MK$, and the polyphase components are given by:

$$E_l(z) = \sum_{n=0}^{K} h[l + nM] z^{-n}. \tag{3.14}$$

The k^{th} band is centered at $\frac{2k\pi}{M}$, and the corresponding filter is given by:

$$H_k(z) = H(zW_M^k) = \sum_{l=0}^{M-1} (z^{-1} W_M^{-k})^l E_l(z^M), \tag{3.15}$$

where $W_M = e^{-i\frac{2\pi}{M}}$. The multilevel filter $G(z)$ can then be obtained using:

$$G(z) = \sum_{k=0}^{M-1} G_k(z) = \sum_{k=0}^{M-1} \beta_k H_k(z). \tag{3.16}$$

This means that the multilevel filter can be implemented via the polyphase structure shown in Fig 3.4. In designing the multilevel filter it is sufficient that the unsampled sub–bands are attenuated below τ used for occupancy determination. In practice, the sub–band levels can therefore be adjusted depending on the value of τ for a given sub–band (*e.g.*, using adaptive thresholding). However, for simplicity such variable thresholding is not considered here. Therefore only 2 gains, γ_0 and γ_1, are considered in this study. The former is the gain for an unsampled sub–band and the latter is the gain for a sampled sub–band. Ideally, these are set to 0 and 1 respectively, but in filter design this is not necessary. Using the above multilevel filter framework, the implementation of the *Scan* function in the RSS implementation naturally follows: the set of gains, β_i, are determined from the sampling vector, $\mathbf{z}$.

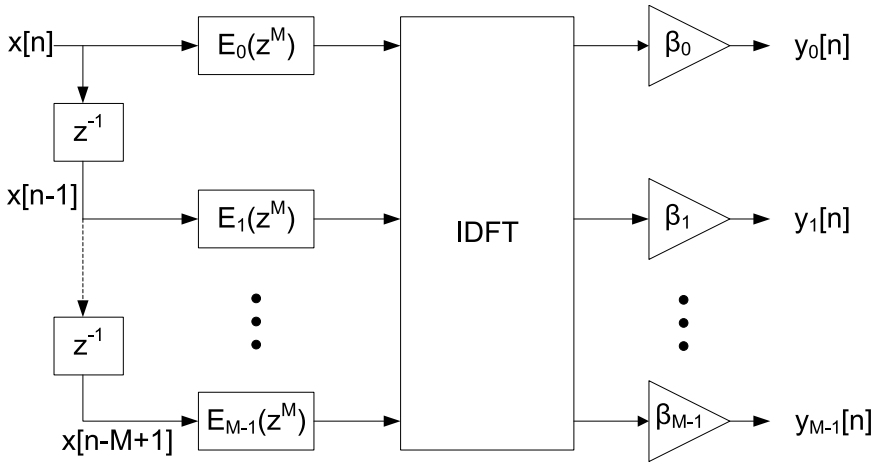

Figure 3.4: Polyphase implementation of an M–band multilevel filter.

3.6 Validation of Stratification Technique for RSS

Before using the proposed stratification technique with the RSS algorithm to provide occupancy estimates, the similarity–based stratification was validated experimentally. Validation involved assessment of:

1. Whether the correct number of strata can be identified
2. If the edges of the sub–bands could be correctly identified

3.6.1 Experimental Setup

In order to address the above validation criteria, several USRPs were configured to transmit signals within the 2.44–2.48 GHz band. The objective was to produce a heterogeneous RAT scenario for which another USRP could be used to sense the spectrum and execute the stratification technique. The use of USRPs was further justified in validation since this approach was also used to simulate dynamic spectrum environments which may not be realised in current static allocation approaches, but may be encountered in future OSA networking scenarios.

Details of the scenario are shown in Table 3.1. Ten different sub–bands (*i.e.*, strata)

Table 3.1: Spectrum Scenario. Details for channels within each sub–band.

Parameter	**Band 1**	**Band 2**	**Band 3**	**Band 4**	**Band 5**
Sub–band Bandwidths	2 MHz	2 MHz	4 MHz	2 MHz	6 MHz
Channel Bandwidths	200 kHz	400 kHz	400 kHz	200 kHz	300 kHz
Channel in Sub–band	10	5	10	10	20
$\frac{\lambda_{OFF}}{\lambda_{ON}}$	0.25	0.43	1	0.33	1.22
Average Channel Occupancy, u	0.2	0.3	0.5	0.25	0.55
Parameter	**Band 6**	**Band 7**	**Band 8**	**Band 9**	**Band 10**
Sub–band Bandwidths	4 MHz	4 MHz	6 MHz	2 MHz	4 MHz
Channel Bandwidths	200 kHz	400 kHz	200 kHz	100 kHz	400 kHz
Channel in Sub–band	20	10	30	20	10
$\frac{\lambda_{OFF}}{\lambda_{ON}}$	1.5	3	9	0.11	0.25
Average Channel Occupancy, u	0.6	0.75	0.9	0.1	0.2

of different bandwidths were created. Guard bands of width 200 kHz were allocated between adjacent strata, to accommodate leakage between the adjacent bands, due to USRP transmissions. Each sub–band contained several channels, which had different temporal characteristics. For simplicity in each channel the spectral occupancy was modeled using a Poisson process [147] with parameter λ as shown in Table 3.1.

The receiving USRP was configured with resolution bandwidth, $\Delta_f = 5$ kHz, to scan the spectrum of interest, $F \in [2.44, 2.48]$ GHz. The measurement duration, N_0, was varied from 1 minute to 20 minutes. The sensed data was stored to compare our proposed approach to existing techniques. These comparisons were done offline so that the approaches would use the same data set.

3.6.2 Spectral Stratification Validation

In each case, to evaluate out proposed approach spectral similarity was determined using distance matrices calculated from the measurement data, using various distance metrics. Figs 3.5–3.8 illustrate several examples using the hamming metric with the occupancy matrix (*i.e.*,$\mathbf{O}_n$), and Pearson's correlation metric with the measurement matrix (*i.e.*,$\mathbf{P}_n$), for $N_0 = 5$ minutes. In each figure, darker areas represent higher similarity spectral regions.

Results show that excluding the guard bands, 10 spectral regions were found corresponding to the strata allocations in Table 3.1. These were the darker regions in the figures.

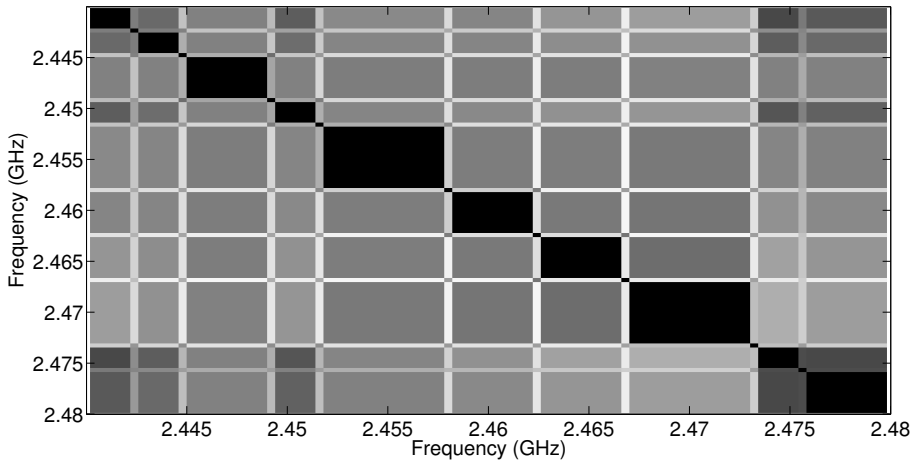

Figure 3.5: Occupancy matrix, $\mathbf{O}_n$, with Hamming metric. USRP Transmissions.

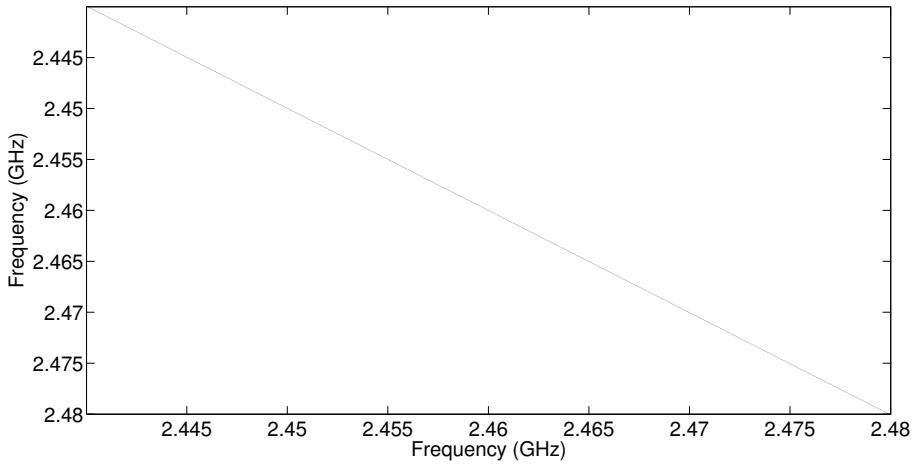

Figure 3.6: Occupancy matrix, $\mathbf{O}_n$, with Hamming metric. No USRP Transmissions.

Between the darker regions were lighter regions roughly corresponding to the guard band regions. Lighter colors indicated areas with less similarity. However, the number of strata identified, depended upon the ϵ value chosen for the similarity threshold (Fig 3.9).

In determining strata, distances in the range $[0, \epsilon)$ are considered similar. Therefore, lower values of ϵ cause the stratification procedure to divide the band into more strata. Conversely, higher ϵ values would aggregate contiguous regions together as being similar,

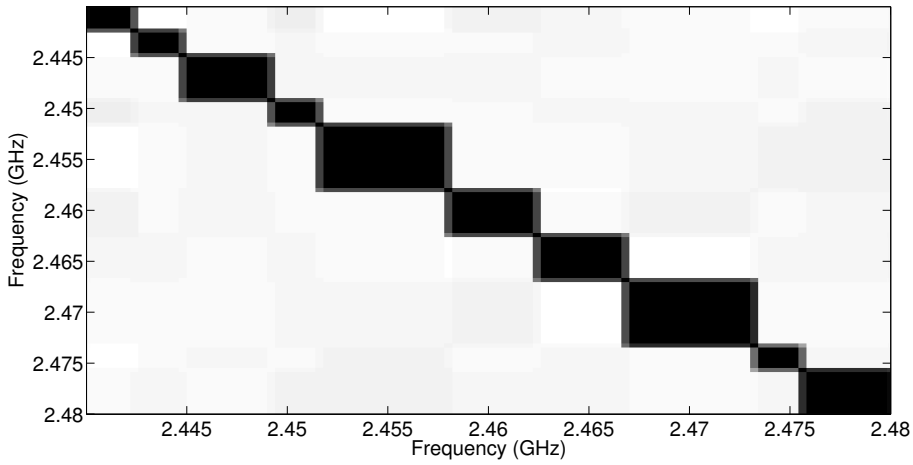

Figure 3.7: Measurement matrix, $\mathbf{P}_n$, with Pearson's metric. USRP Transmissions.

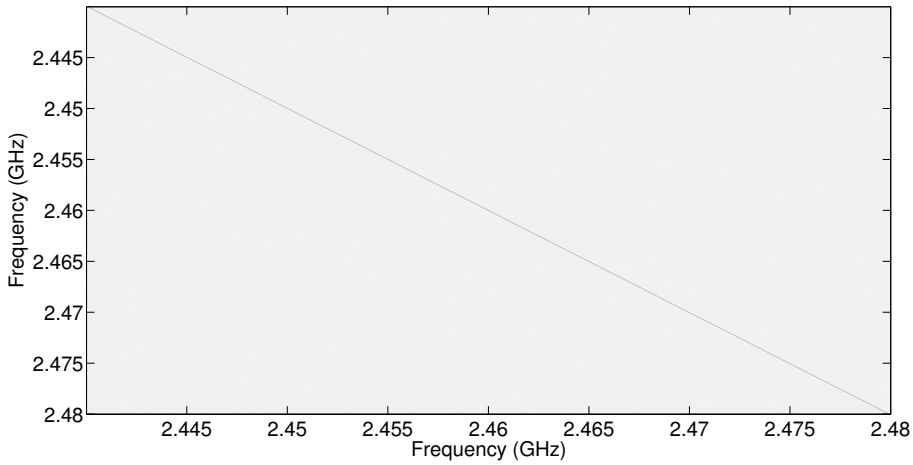

Figure 3.8: Measurement matrix, $\mathbf{P}_n$, with Pearson's metric. No USRP Transmissions.

thus resulting in fewer strata. However in this case there would be more intra–stratum homogeneity, as increasingly dis–similar regions can be grouped together. Entropy was used to measure strata homogeneity (Fig 3.10). Lower values for entropy indicate increased strata homogeneity. The results of Fig 3.9 and Fig 3.10 illustrate that as the number of clusters identified by the technique increased the strata homogeneity also increased.

Figs 3.5–3.8 also illustrate comparison calculations within unoccupied bands, when the

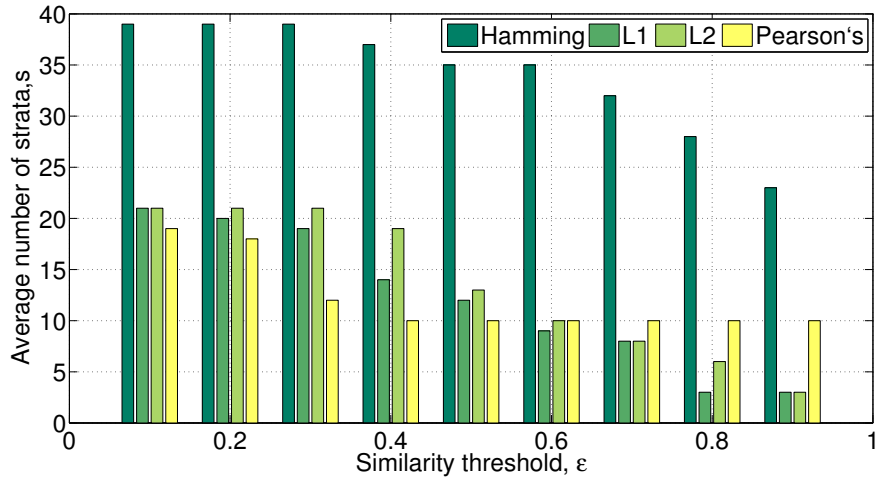

Figure 3.9: Comparison of average number of strata found for different initialisation values for proposed stratification technique using different distance metrics.

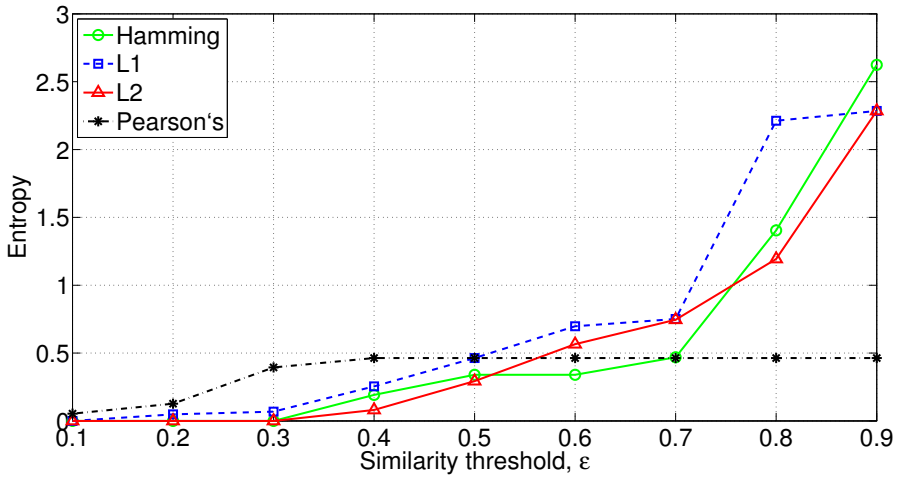

Figure 3.10: Comparison of strata homogeneity for proposed stratification technique using different distance metrics.

USRPs did not transmit. In scenarios where no USRP signals were transmitted, the number of strata identified was approximately, N_f (*i.e.*, the number of non–overlapping intervals in the entire scanned bandwidth, $|F| = 40$ MHz). This supported the lack of significant correlation between contiguous scanned intervals. The diagonal lines in the example plots with no USRP transmissions in Fig 3.6 and Fig 3.8 illustrate that in general, intervals were significantly similar to themselves, but not to other intervals. Similar results were obtained

using the Manhattan and Euclidean distances.

Because there was spectral leakage in the guard bands, the similarity was higher in guard bands than in a sub–band in which no USRP was transmitting. These were the gray areas of the figures. However the similarity was not as high as within each identified sub–band, but was higher than between dis–similar sub–bands. Depending on the ϵ value, guard bands thus aggregated with adjacent sub–bands allocated for USRP transmissions.

3.6.3 Comparison to K–means Clustering

The proposed stratification technique aims to group together bands with similar temporal occupancy chacteristics. It was therefore compared to existing techniques used to group similar objects together. Initially, k–means, expectation maximisation and agglomerative hierarchical clustering techniques were selected as they are popular approaches used in the literature [145]. However it was quickly realised that the latter 2 were more suited for offline analysis and did not scale as well as k–means did to larger data sets. Since our focus is on adapting techniques for online use, in this study only k–means is presented for comparison.

The basic k–means algorithm requires user specification of the number of clusters, k, for grouping of data. It then iterates through assigning objects to the closest centroids and then recomputing cluster centroids. The algorithm loops until cluster centroids do not change significantly in subsequent iterations. Adaptations such as agglomerating nearby clusters, random initialisation, and bisecting k–means improve on the basic algorithm. With these adaptations, k–means attempts to minimise an objective function based upon the selected distance metric. For example, the Euclidean metric used the sum of squares errors, while the Manhattan metric used the sum of absolute errors. This objective function therefore provides one means of assessing cluster quality.

Because the data was high–dimensional (*i.e.*, N_0–dimensional) and it was expected that there should be 10 natural clusters excluding the guard–bands, in our experiments, k was varied between 10 and 40 and the k–means algorithm was executed using the same distance metrics which were used for the proposed stratification technique. Since the basic k–means technique did not allow for variation of ϵ, the k variations provided a way to assess cluster quality for comparison to our technique: *determine k–values that minimise the expected*

value of the objective function.

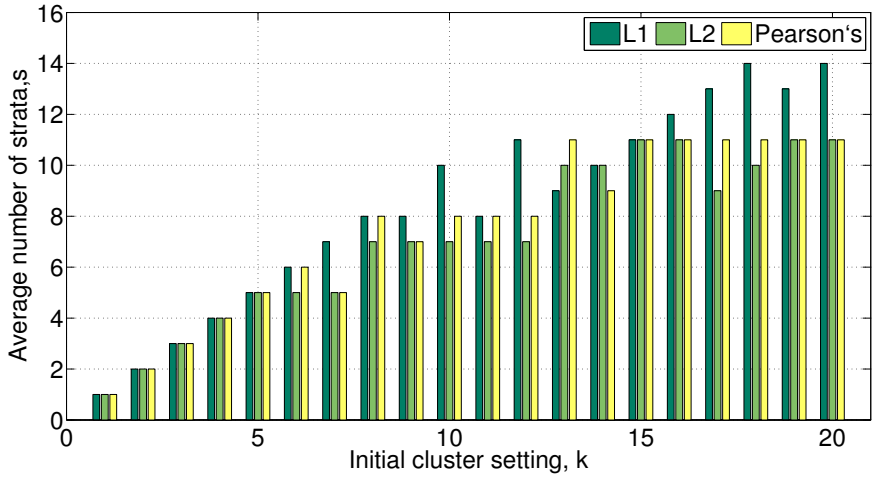

Figure 3.11: Comparison of average number of strata found for different initialisation values for k–means clustering using different distance metrics.

For each value of k, the clustering technique was repeated 50 times with random initialisation of centroids, and the iteration which produced the minimum objective function was chosen as the best. The performance was also statistically evaluated based upon the expected value of the objective function as well as its variance. Experiments showed that even with increasing k the average number of clusters obtained did not exceed 15 (Fig 3.11). This was interesting to note because it was expected that there should be 21 natural clusters based upon the experimental setup (*i.e.*, 10 sub–bands plus 11 guard bands). The two main reasons for the smaller number of clusters were:

1. Some unoccupied guard bands or guard bands with leakage were grouped into similar clusters in some instances

2. Some guard bands and also actual sub–bands with transmissions were sufficiently similar to be grouped together

Small values of k (*i.e.*, $k < 10$), capped the number of strata which could be found, thus limiting the k–means algorithm performance, in terms of strata homogeneity. Also, based upon the objective function, $k \in [15, 21]$ produced the best performance on average.

Fig 3.12 illustrates results for various values of k using different distance metrics for the objective function.

Comparison of the proposed technique to the k–means algorithm highlighted one important issue: *While the proposed technique always produced the same strata for every run, for a specific run of the k–means algorithm the number of clusters obtained was dependent upon initial cluster centroids selected.* The initialisation also affected which of the guard bands would be aggregated with the 10 sub–bands.

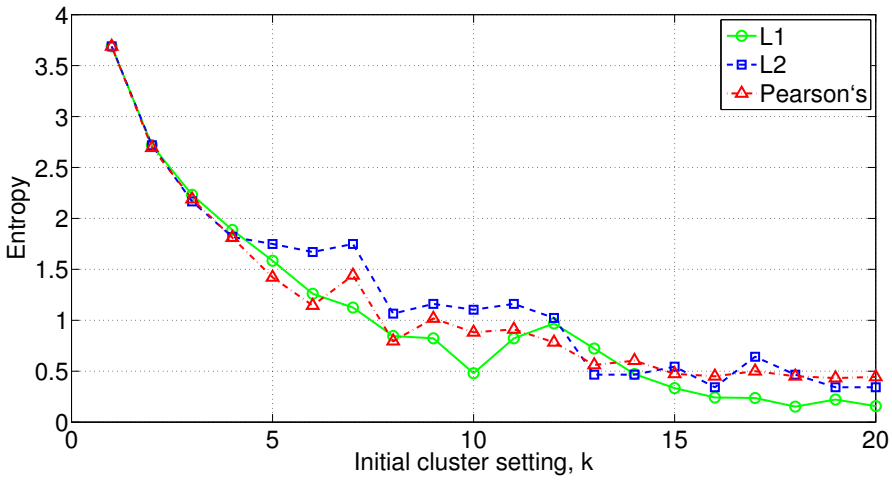

Figure 3.12: Comparison of strata homogeneity for k–means clustering using different distance metrics.

To further validate the method, it was necessary to determine correct identification of the sub–bands allocated to the USRPs. This is essentially a clustering evaluation problem where the true spectral groupings are known. In the cluster validation literature, entropy is commonly used for cluster validation [145]. Therefore this was used to assess the purity of the identified strata through comparison of the proportions of misclassified intervals within a given sub–band.

Fig 3.10 and Fig 3.12 illustrate that better performance were obtained for decreasing ϵ and increasing k, respectively. Specifically, for the proposed technique the number of strata identified was dependent upon ϵ: *as ϵ was increased more dissimilar bands were aggregated, and there were less strata identified. Lower values of ϵ increase the number of*

strata identified, and the strata were also more homogeneous as required.

A key requirement of the stratification approach is to limit complexity so that it can be used in online occupancy measurement and estimation. It is noted that performance of the algorithms in terms of complexity is highly dependent upon specific implementations, and which enhancements are used. However, several qualitative statements can be made with respect to online use in spectrum occupancy estimation using RSS.

First, for online use since k–means requires an initial guess of the number of clusters, it requires iterations to determine a suitable clustering (*i.e.*, unless a large value for k is used at initialisation). However, the proposed technique requires a single iteration for identifying spectral strata. Second, k–means identifies strata even with non–contiguous bands, while the MatSearch algorithm assumes contiguous bands. However the MatSearch algorithm can be enhanced for non–contiguous bands, but as previously stated, for this paper the focus is on contiguous cases.

3.7 Evaluation of RSS with Stratification Technique

Following validation of the proposed technique, the next step was to estimate spectrum occupancy for spectrum measurements.

3.7.1 Measurement Data

To evaluate RSS usage for spectrum occupancy estimation, data used in this paper were from spectrum measurements taken at the Wireless Innovation Laboratory, at Worcester Polytechnic Institute. Measurements were made using in–house developed software, SQUIRREL (Spectrum Query Utility Interface for Real-time Radio Electromagnetics), to control an Agilent CSA series N1996a Spectrum analyzer in order to collect the data. Table 3.2 describes the measurement parameters used for collecting spectrum data.

A global threshold, τ, was determined using Otsu's threshold selection method for gray–level histograms [144]. Otsu's algorithm is a nonparametric, unsupervised threshold selection method which can utilise the zeroth–order and first–order cumulative moments of the gray–level histogram for $\mathbf{P}_n$ to maximise the separability between the signal and noise

classes. This provided the occupancy "ground truth" which was used for comparison to the sampling schemes presented in this paper.

A random group method using stratified sampling was then used to estimate the sampling distributions for each of the sampling schemes considered. The random group method is commonly used in estimating sampling distributions by creating independent samples for which parameters of interest can be estimated [142]. For each case investigated, the random group approach was used to obtain 1000 independent sample realisations, which were then used to evaluate the occupancy in each case. These were then used to statistically characterise the sample distributions of interest.

Table 3.2: Spectrum Measurement Setup.

Parameter	**Value**
Measurement Start Time, t_0	16:52 April 4, 2011
Measurement Stop Time, t_{N_t}	20:44 April 5, 2011
Fstart, f_0	800 MHz
Fstop, f_{N_f}	1 GHz
Δt	2 seconds
Δf	20 kHz
N_t	50,184
N_f	11,000

For the licensing approach, the spectrum range considered was divided into 15 strata according to US spectrum allocation information [85]. Table 3.3 summarises the strata allocation scheme used along with the main services of interest within. Although the allocation served as the basis for spectral division, as seen in Table 3.3 the boundaries may not be exactly aligned with specific service boundaries.

3.7.2 Sub–band Occupancy

To investigate the behavior of the stratification techniques with RSS occupancy estimation, several of the 15 sub–bands were selected based upon observed service and occupancy characteristics. For example, the Cellular down and Unlicensed sub–bands were chosen based upon the observed relatively dynamic nature of the services, while SMR up/SMR down and Paging were chosen because there was the possibility of heterogeneous RAT within these bands. In contrast, the Aviation sub–band was selected as there was not ex-

Table 3.3: Service–based Spectrum Allocations.

Range (MHz)	**General Service Description**
800-806	Low Power (LP) TV / LP Aux. / Pub. Safety
806-824	SMR Up / Pub. Safety
824-849	Cellular Up
849-851	Commercial Air-Ground (CAGR)
851-869	SMR Down / Pub. Safety
869-894	Cellular Down
894-901	CAGR / SMR
901-902	Narrowband PCS (N-PCS)
902-928	ISM / Amateur Radio / LMS
928-935	Paging / N-PCS / Multiple Address Service
935-941	SMS / Narrowband PCS
941-944	Fixed Microwave Service (FMS)
944-952	Broadcast Aux. / FMS / LP Aux.
952-960	FMS
960-1000	Aviation

pected to be any occupancy within the measurement area based upon the service allocation. Bandwidth occupancy within the sub–bands investigated ranged from low to medium occupancy (*i.e.*, $\sim$ 0%–50%). Figs 3.13– 3.16 provide a comparison of the proposed distance–based stratification technique to equal stratification using the time–averaged MSE for these sub–bands.

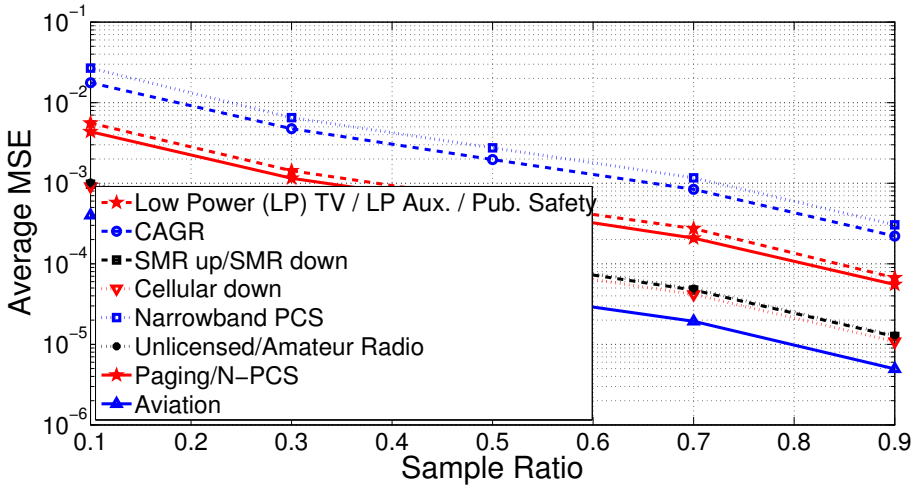

Figure 3.13: Time-averaged MSE for equal stratification, across several service bands. N_0 = 5 minutes, BRSS Block size = 10 mins.

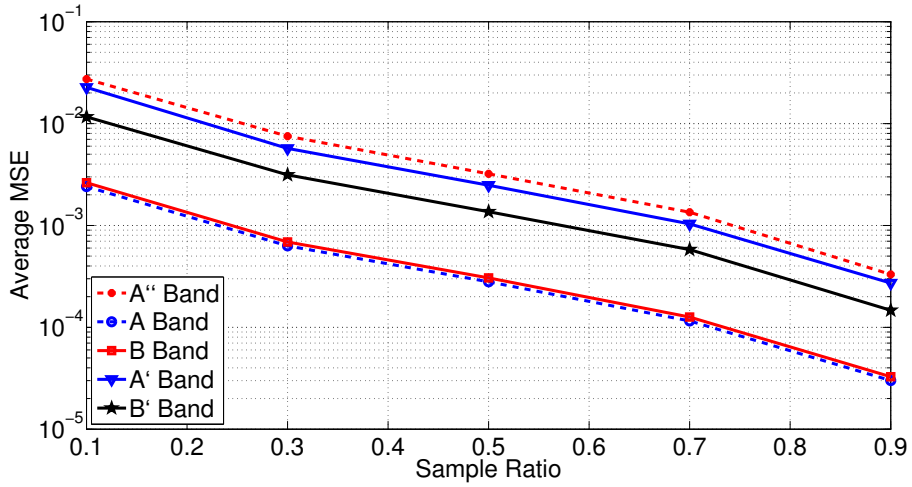

Figure 3.14: Time-averaged MSE for equal stratification, across Cellular sub–bands. $N_0 =$ 5 minutes, BRSS Block size = 10 mins.

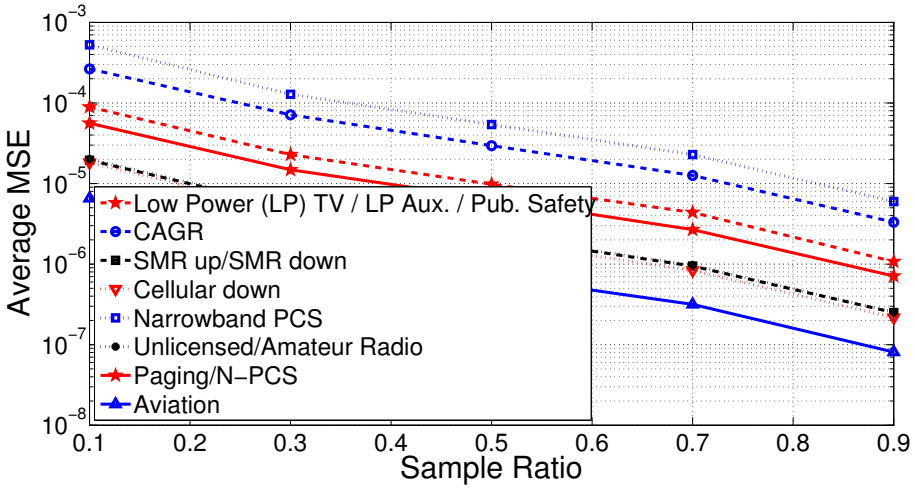

Figure 3.15: Time-averaged MSE for distance–based stratification technique, across several service bands. $N_0 = 5$ minutes, BRSS Block size = 10 mins.

For each sub–band, the MSE decreases with increasing sampling ratio as expected, based upon (3.8). No significant signals were observed in the Aviation sub–band so adjacent samples did not form channels. Thus there was no channel–related correlation between closely spaced spectral samples (i.e. assuming independent noise), hence the lower MSE. This was further supported in other sub–bands which contained occupied channels and had increased correlation resulting in increased MSE under the assumption of inter–strata

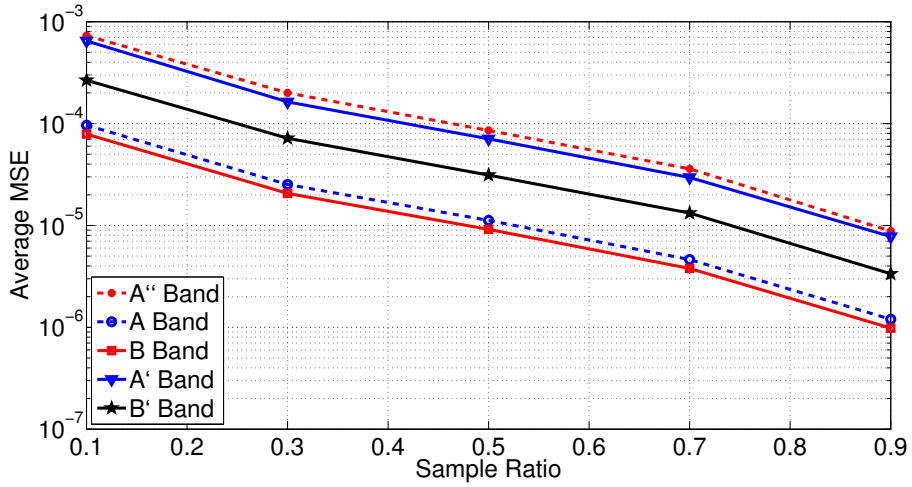

Figure 3.16: Time-averaged MSE for distance–based stratification technique, across Cellular sub–band. $N_0 = 5$ minutes, BRSS Block size = 10 mins.

homogeneity for random sampling. Additionally, although the SMR up and SMR down sub–bands were separate, the MSE of the estimate under random sampling was similar for both cases. This may be due to the symmetry of the assignments for the uplink and downlink bands, given the nature of the service. For a given sample ratio, the MSE for bands which contained multiple service allocations were higher.

Fig 3.14 and Fig 3.16 illustrate time–averaged MSE for bands A”, A, B, A’, and B’ in the cellular 850 MHz downlink sub–band. Only results for equal–sized stratification and the proposed stratification technique are shown for brevity. However, k–means performance was slightly worse than the latter approach, while license–based stratification was between the performance of equal–sized stratification and the proposed technique. The results clearly illustrate the improved performance using the proposed technique. Although A and B bands contained GSM and CDMA signals, (and hence different channel specifications), the MSE was improved using proposed technique compared to just use of equal–sized or license–based techniques.

Table 3.4 provides further example results for the SMR up/SMR down bands. The results demonstrate that while similar performance is obtained for both assignment–based and equal–sized stratification of sub-bands, the proposed stratification technique was better

Table 3.4: Comparison of time-averaged MSE for different stratification approaches for the SMR up/ SMR down sub–bands. $N_0 = 20$ minutes, BRSS Block size = 20 minutes. Each value must be multiplied by 0.001 to get actual MSE value.

Stratification	**Sampling Ratio, π**				
	0.1	**0.3**	**0.5**	**0.7**	**0.9**
No Stratification	1.82377	0.45827	0.19554	0.08336	0.02162
10 Equal–sized Strata	1.76713	0.45347	0.20077	0.08411	0.02180
Assignment–based Strata	1.70715	0.41368	0.19064	0.08317	0.02134
Proposed Stratification Technique	0.81672	0.16290	0.04972	0.02687	0.005922
K–means	0.92456	0.17833	0.053917	0.02409	0.005176

in terms of the time–averaged MSE. Performance using k–means and the proposed technique was similar. This was also observed for the other sub–bands investigated, where the proposed stratification technique gave the best performance in terms of sampling bias and MSE.

3.8 Conclusion

In this chapter, the NCSS concept was introduced as an alternative way of simultaneously sensing non–contiguous sub–bands. Such scenarios may result from the need to monitor channels which may not be contiguous. Using NCSS, a framework for bandwidth occupancy estimation using stratified sampling techniques and random spectral sampling was proposed. Further, one means of implementing NCSS/RCSS using a multiband polyphase filterbank approach was presented. Experimental results suggested that bandwidth occupancy estimation using RSS techniques was dependent upon appropriate stratification of similar sub–bands.

To achieve online stratification, a distance–based approach to automatic stratification was proposed for use with random spectral sampling for characterisation of bandwidth occupancy in spectrum monitoring networks. The proposed approach was validated via simulations and through use of spectrum measurements taken at WPI for about 24 hours, spanning 800 MHz – 1 GHz. The results illustrated that the technique improved on the previous non–adaptive stratification techniques proposed for random spectral sampling. Results further suggest that random spectral sampling can be used in wideband occupancy characterisation, with increasing accuracy as the sampling ratio increases to 1.

Based on the above results, without specific details of operator frequency planning, assignment–based stratification was seen to introduce higher sampling bias and MSE when used for bandwidth estimation via RSS compared to the proposed stratification approach. Also, it may not be practical to use such an approach at a very granular level. While equal–sized stratification can be used in cases where simplicity is warranted, it does not take account of strata heterogeneity for stratification. Consequently, it does not perform as well as well as when automatic stratification is used. In contrast, k–means provides one way to automatically stratify the sensed spectrum. However, the proposed technique provides a relatively simpler way to achieve similar performance in an online setting. Both k–means and the proposed approaches give similar performance in the heterogeneous RAT case, for comparable sampling ratios.

Furthermore, unlike typical compressed sensing schemes for low signal occupancy scenarios, in the proposed RSS approach the spectrum reconstruction objective is relaxed to improve performance in medium to high occupancy settings. This method thus facilitates statistical occupancy characterisation for various occupancy levels, which is a key spectrum monitoring objective, without requiring the sparsity assumptions of compressed sensing.

Chapter 4

PHY–based Temporal Occupancy Estimation

4.1 Introduction

In the previous chapter, several aspects of estimating bandwidth occupancy were contemplated, and a random sampling approach for wideband spectrum sensing and occupancy estimation was proposed. Another common spectrum monitoring output for spectrum management is the estimation of temporal occupancy statistics for channels. In emerging DSA networks, this is even more crucial for spectrum management as well as for compliance enforcement, since operational parameters for DSA additionally can include temporal validity constraints. In this chapter and the next chapter, two aspects of temporal occupancy estimation are examined.

Specifically, this chapter deals with temporal occupancy estimation of selected spectrum bands when there is no need to discriminate between specific users. This is particularly useful for frequency planning and spectrum engineering activities [35, 120]. Traditionally, to support such spectrum management activities, current approaches for temporal occupancy estimation typically determine the proportion of time during the measurement interval, for which spectrum is occupied (*e.g.*, [5, 35, 134]). In envisioned OSA scenarios, this estimation task may be more difficult, given the dynamics of proposed OSA techniques.

In this chapter, *random temporal sampling* is explored, for sampling of signal characteristics for estimation of overall channel occupancy. A PHY–based approach for spectrum occupancy estimation is proposed, if user discrimination is not required. In this approach, signal measurements are used to estimate temporal characteristics for spectrum occupancy, under various temporal sampling strategies.

Several aspects of this work also appear in publications developed for this dissertation: [87, 148].

4.2 Motivation

Opportunistic spectrum access (OSA) networks [149] place new challenges upon existing spectrum monitoring paradigms [54, 56]. In response to increasing demand for radiocommunications services, regulatory developments in many jurisdictions have created new opportunities for more flexible allocation and assignment of, as well as operation within previously unavailable spectrum bands (*e.g.*, [41, 42]). However, measurement and modelling of spectrum usage trends by primary and secondary users is an essential element for effective spectrum management within the various increasingly market–based spectrum allocation and access models in future OSA–based deployments [54, 56, 134]. Such models provide invaluable data for use in various spectrum management processes such as spectrum planning, spectrum engineering, channel blocking complaint verification and evaluation of spectrum usage efficiency.

However, hardware limitations and energy constraints restrict complete knowledge of spectrum opportunities which would be gained through continuous sensing of the entire spectrum of interest. Thus sampling has been investigated for estimation and temporal characterisation of spectrum occupancy. In the literature to–date, several approaches have been presented (*e.g.*, [16, 150–155]), with the majority of research to–date focussed upon periodic sampling approaches. In many of the proposed approaches, dense sampling is generally assumed, which is typically expensive in terms of computational costs and energy consumption, which may make it impractical for deployment scenarios involving wireless devices with limited power. This has promoted investigation of sparse sampling approaches

such as compressed sensing (CS) [156–158]. As shown in [159], randomisation of sensing intervals can outperform periodic sensing, in sparse sampling scenarios.

However, while CS offers advantages for scenarios requiring signal reconstruction from sparse samples, related recent work using CS techniques in OSA [160] highlight crucial CS challenges [58, 159, 160]:

1. Effective use of CS requires the determination of suitable basis matrices to introduce the required signal sparsity

2. CS effectiveness is also based upon adequate incoherence of the sparse signal with the measurement matrix

3. CS trades sample size for the computational cost of signal reconstruction. Maintaining sufficiently low computational cost is crucial to real–time performance.

In particular, for occupancy estimation there may be instances where signal sparsity may not be guaranteed, (*e.g.*, in congested areas such as in urban scenarios [5]). In such instances, unless some sparse representation can be devised, the sparsity assumption required for CS would not be satisfied. Also, in such cases the sampling must be at least at the Landau rate to prevent aliasing effects from occurring (*i.e.*, which would negate the benefit of sparse sampling in the first place). Determination of suitable sparse bases is still an open area of research.

One promising approach involved extraction of cyclostationary features of wideband signals, in which signals were shown to be sparse, and therefore CS was applied [161]. However, through the signal transformation, the signal dimensionality was increased to obtain the required sparsity. In effect, the signals of interest would require a similar sample size for reconstruction in a higher dimensional space. [162] proposed an improvement to reduce the complexity of the approach by only reconstructing signals of interest. However, the assumption in this approach was that the technique would be used by SUs for OSA, and therefore the bands of interest would be sufficiently sparse for OSA to be feasible. Similarly to bandwidth occupancy estimation, the computational cost of signal reconstruction for temporal occupancy estimation is not necessary [35, 120, 134]. Therefore, alternate (sparse)

random sampling approaches to estimate the temporal spectrum occupancy are suggested for accomplishing the required monitoring tasks.

In this chapter, models for randomised temporal sensing deployment on periodic sensing platforms in OSA networks and their performance in spectral occupancy estimation are examined. To the best of the author's knowledge, little work has been done on the proposed randomised temporal sensing approach. Unlike typical compressed sensing schemes for low signal occupancy scenarios, in the proposed approach the spectrum reconstruction objective is relaxed to improve performance in medium to high occupancy settings. This method thus facilitates statistical occupancy characterisation for various occupancy levels. Furthermore, the approach also facilitates inclusion of periodic sensing scenarios. The performance of various sampling designs in estimating channel occupancy for channels modelled as alternating renewal processes is investigated. Specific contributions are as follows:

1. A framework is presented for performance analysis of various temporal sampling strategies, and a lower bound is derived for random temporal sensing variance

2. A low–computational–cost model for online randomised temporal sensing deployment on periodic sensing platforms for characterisation of spectrum occupancy is proposed

3. The randomised sensing approach is demonstrated using USRPs, for which several performance studies are carried out

4. The approach is compared to several CS–based techniques for occupancy estimation.

The proposed method is proposed for cases where there is more spectrum agility than deployed non–OSA technologies currently allow, in particular where there may be intelligently changing transmission parameters in response to the sensed state of the spectrum, such as enabled by cognitive radio devices. The resulting occupancy models can then be used to make appropriate decisions for spectrum management or for spectrum accounting.

The rest of this chapter is organised as follows: In Section 4.3 the spectrum occupancy model is presented, followed by an overview of temporal occupancy estimation using various temporal sensing strategies in Section 4.4. This is followed by an overview of performance analysis of sensing strategies in Section 4.5 and the online randomisation algorithm in

Section 4.6. Experimental results are presented in Section 4.7. Finally there are concluding remarks in Section 4.8.

4.3 Spectral Occupancy Model

Current wireless networks support a multitude of voice and data services with different characteristics, making multi–service traffic modelling very challenging. The literature illustrates many approaches based upon analytical and empirically–fitted representations for various single–service and multi–service scenarios, (*e.g.*, [163, 164].) For this dissertation, temporal spectral occupancy is modelled using a continuous–time alternating renewal process [165]. This model has been frequently used in the literature particularly due to its simplicity.

Spectrum occupancy is modelled as a binary random variable, $X(t)$, alternating between *occupied* (*i.e.*, $X(t) = 1$) and *free* (*i.e.*, $X(t) = 0$) states (Fig. 4.1). The j^{th} occupied event occurs between α_j and ω_j, and is of duration $\tau_{occ,j} = \omega_j - \alpha_j$. Similarly, the j^{th} white–space event occurs between ω_j and α_{j+1}, and is of duration $\tau_{free,j} = \alpha_{j+1} - \omega_j$. At $t = 0$ the channel is assumed to be occupied (*i.e.*, $X(0) = 1$). By definition of an alternating renewal process, $\tau_{occ,j}$ and $\tau_{free,j}$ are defined by probability density functions $g(t)$ and $h(t)$ (where $t > 0$), respectively. Although in general $\tau_{occ,j}$ and $\tau_{free,j}$ can be dependent within the j^{th} cycle, for this dissertation it is assumed that occupied and free interval durations are independent. Further, the sequences $\{\tau_{occ,j}\}$ and $\{\tau_{free,j}\}$ are independent and identically distributed.

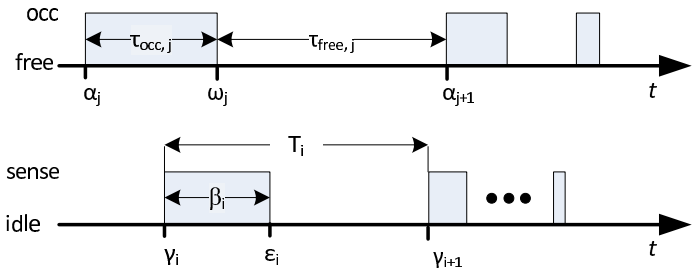

Figure 4.1: Spectrum occupancy model (top figure) and spectrum sampling model (bottom figure).

4.4 Estimating Temporal Occupancy using Random Temporal Sampling

Assume that each spectrum sensor has physical layer temporal sensing resolution specified by Δ_t. For a sensor network, the sensing objective is typically to statistically model the channel occupancy for time $T = [t_0, t_0 + N_t\eta\Delta_t]$, where t_0 is the start of the sensing interval of interest, N_t is the number of sampling opportunities in T, η indicates the average number of Δ_t increments for a single detection processing cycle within any sensing period, and $\Delta_t \ll T$. For the interval duration $\eta\Delta_t$, any detection technique such as energy detection or cyclostationary detection can be used.

Each temporal sampling strategy would have its own sensing interval and sensing duration based upon the physical–layer sensing parameters identified above. Sensing can be placed into one of four types of sensing schemes (Fig. 4.2). T and T_i (i = 1, 2,$\cdots$, n) are respectively the fixed and random time intervals between the starts of successive scans. β and β_i represent the fixed and random sensing durations respectively. In periodic sensing, the sensing intervals, T, and the sensing durations, β, are approximately constant[1] ($T_{min} < \beta < T$). In contrast, in random sensing as illustrated in Fig. 4.2 it is possible to randomise either β_i, or T_i, or both ($T_{min} < \beta_i < T_i$).

Sensors are either in the *sensing* or *idle* states, depending on whether a sensing event is occurring or not. It is additionally assumed that the temporal sampling parameters are integer multiples of the PHY–layer resolution, Δ_t, (*i.e.*, with consideration of the previously–mentioned jitter). Therefore, the sensing process also can be modelled as a discrete–time binary variable, $Y[k]$ alternating between *sensing*, (*i.e.*, $Y[k] = 1$), and *idle*, (*i.e.*, $Y[k] = 0$), states. Note that while for periodic sensing $Y[k]$ would be approximately deterministic, this may not be the case for the random sampling schemes. Other activities not related to sensing are ignored during the idle state. As a consequence of the temporal sensing parameter assumption, denote γ_i and ϵ_i as the discrete start and end times of the ith sensing event, where $0 \leq \gamma_i < \epsilon_i$ (Fig. 4.1). Thus $\beta_i = \epsilon_i - \gamma_i = m_i\Delta_t$ and $T_i = \gamma_{i+1} - \gamma_i = l_i\Delta_t$,

[1]There is expected to be some jitter for signal processing, but this is assumed to be negligible, compared to the average durations of T and β.

$(m_i, l_i) \in \mathbb{N}^+$.

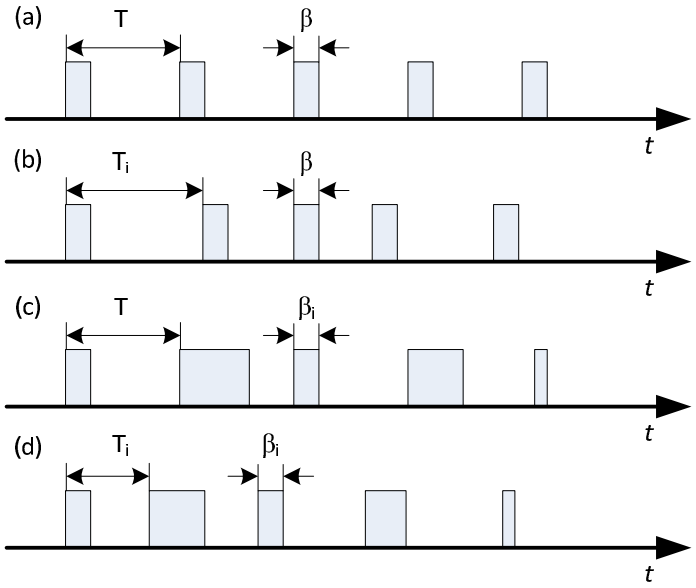

Figure 4.2: Taxonomy of temporal sampling schemes. (a) Periodic sampling. (b)-(d) Random sampling. Subscripted variables denote randomised sensing parameters. All other variables are non–random. Blocks represent sensing event.

4.4.1 Temporal Sensing Framework

While there exist many sampling approaches, in this section the following approaches are examined: systematic sampling, simple random sampling, stratified sampling and cluster sampling [142]. Each approach is briefly discussed below. However, it is noted that other more complex approaches exist, which may combine these simpler approaches.

Systematic Sampling

Systematic sampling is equivalent to periodic sampling in which the increments between successive sampling points are approximately constant [166]. However, systematic sampling involves selecting some random starting point to sample, after which the time between successive samples is constant. By definition, including the initial randomly selected and subsequent sampling points, the sequence of consecutive sampling points $\{t_k\} \in T$ are spaced $l\Delta_t$ apart, where $l \in \mathbb{N}^+$. Let $\mathbf{z} \in \{0,1\}^{N_t \times 1}$ be the sampling vector for interval T.

Entries of $\mathbf{z}$ are 1 if the corresponding sampling opportunity is selected, and 0 otherwise. Also define $X(t)_{\{t\in T\}}$ as vector $\mathbf{X_T}$. $\mathbf{X_T} \in \{0,1\}^{N_t\times 1}$ represents the $N_t \times 1$ occupancy vector with entries of 0 or 1 representing free or occupied instants, respectively. Detection can be done using any of the techniques presented in the literature, such as energy detection or cyclostationary detection. For a sample $\mathcal{S}_P$ of size n_P the occupancy of T is estimated using:

$$\hat{\mu}_P = \frac{1}{n_P}\sum_{t_k\in\mathcal{S}_P} X_{t_k} = \frac{1}{n_P}\mathbf{z}\cdot\mathbf{X_T} \tag{4.1}$$

where '$\cdot$' is the vector scalar product operator.

Simple Random Sampling

In simple random sampling (SRS) a sample $\mathcal{S}_{SRS}$ of size n_{SRS} is randomly selected from the N_t possible sampling opportunities. Each opportunity is equally–likely to be selected. Thus sensing is a Bernoulli process [147], where each possible sampling instant $t_k \in T$ has probability, $\pi = \frac{n_{SRS}}{N_t}$ of being selected [142]. The vectors $\mathbf{z} \in \{0,1\}^{N_t\times 1}$ and $\mathbf{X_T}$ are defined similarly as for systematic sampling. The occupancy of T is estimated using:

$$\hat{\mu}_{SRS} = \frac{1}{n_{SRS}}\sum_{t_k\in S_{SRS}} X_{t_k} = \frac{1}{n_{SRS}}\mathbf{z}\cdot\mathbf{X_T} = \frac{1}{\pi N_t}\mathbf{z}\cdot\mathbf{X_T} \tag{4.2}$$

Stratified Sampling

In stratified sampling, T is divided into s non–overlapping sub–intervals $\{T_j\} \in \{0,1\}^{N_j\times 1}$: $T = \bigcup_{j=1}^{s} T_j$ and $T_j \bigcap T_k = \emptyset, j \neq k; j,k \in \mathbb{N}$. SRS is done for each sub–interval T_j. Each T_j is of duration $N_j \times \eta\Delta_t$ and a random sample $\mathcal{S}_j$ of size n_j is selected from each. Within each T_j each sampling opportunity is equally–likely to be selected. Thus within T_j, each possible sampling instant $t_j \in T_j$ has probability, $\pi_j = \frac{n_j}{N_j}$ of being selected [142]. Let $\mathbf{z_j} \in \{0,1\}^{N_j\times 1}$ be the sampling vector for sub–interval T_j. Sub–entries of $\mathbf{z_j}$ are 1 if the corresponding sampling opportunity is selected, and 0 otherwise. Also, define $X_{\{t\in T_j\}}$ as vector $\mathbf{X_{T_j}} \in \{0,1\}^{N_j\times 1}$. For a sample $\mathcal{S}_j$ the occupancy of T_j is estimated using:

$$\hat{\mu}_j = \frac{1}{n_j} \sum_{t \in \mathcal{S}_j} X_t = \frac{1}{n_j} \mathbf{z_j} \cdot \mathbf{X_{T_j}} \tag{4.3}$$

From (4.3) the overall occupancy can then be estimated as [142]:

$$\begin{aligned} \hat{\mu}_{St} &= \sum_{j=1}^{s} \frac{N_j}{\sum_{k=1}^{s} N_k} \hat{u}_j = \sum_{j=1}^{s} \frac{N_j}{n_j \sum_{k=1}^{s} N_k} \mathbf{z_j} \cdot \mathbf{X_{T_j}} \\ &= \sum_{j=1}^{s} \frac{1}{\pi_j N_t} \mathbf{z_j} \cdot \mathbf{X_{T_j}}, \end{aligned} \tag{4.4}$$

Cluster Sampling

In cluster sampling, T is divided into M_c non–overlapping sub–intervals $\{T_j\}$ in a similar manner to that for stratified sampling. In one–stage cluster sampling a subset of sub–intervals from $\{T_j\}$ are randomly selected. Only this subset is sampled (usually periodically), ignoring the rest. In multi–stage sampling, the sampled clusters can themselves be sampled using another scheme, resulting in more complex sampling designs. In this chapter, focus will be upon one–stage sampling.

A random sample $\mathcal{S}_c$ of size m_c sub–intervals is randomly selected, each with equal probability, $\pi_c = \frac{m_c}{M_c}$ of being chosen. Each T_j is of duration $N_j \times \eta\Delta_t$ and is sampled at every sampling opportunity within. There are thus N_j opportunities to be sampled in each cluster. Vector $\mathbf{X_{T_j}}$ is defined as in previous cases, while $\mathbf{1}$ defines a $N_j \times 1$ vector with all elements = 1. For a sampled sub–interval, the occupancy of T_j can be estimated using (4.3), while the overall occupancy is estimated using similar procedures to those used for the previous sampling approaches:

$$\begin{aligned} \hat{\mu}_C &= \sum_{j \in \mathcal{S}_c} \frac{M_c}{m_c \sum_{k=1}^{M_c} N_k} \mathbf{1} \cdot \mathbf{X_{T_j}} \\ &= \sum_{j \in \mathcal{S}_c} \frac{1}{\pi_c N_t} \mathbf{1} \cdot \mathbf{X_{T_j}}, \end{aligned} \tag{4.5}$$

4.5 Performance of Random Temporal Sampling Strategies

The theoretical performance of the temporal sampling strategies and resulting estimators can be evaluated in terms of the bias and variance introduced. Theoretical expressions for

these performance metrics are now derived for the sampling strategies presented in the previous section.

Denote the Laplace transforms of the probability density functions by $\mathcal{L}\{g(t)\} = \hat{g}(s)$ and $\mathcal{L}\{h(t)\} = \hat{h}(s)$. Under the assumption of equilibrium, define the transition probabilities for $X(t)$, $\pi_{qr}(k\Delta_t)$, as the probabilities of observing state r at time, $t + k\Delta_t$, given that state q was observed at time, t, *i.e.*, $q, r \in \{0, 1\}$ [166]:

$$\begin{aligned}
\pi_{00}(k\Delta_t) &= \frac{\mu_0}{(\mu_0 + \mu_1)} + \frac{\psi(k\Delta_t)}{\mu_0}, \\
\pi_{01}(k\Delta_t) &= \frac{\mu_1}{(\mu_0 + \mu_1)} - \frac{\psi(k\Delta_t)}{\mu_0}, \\
\pi_{10}(k\Delta_t) &= \frac{\mu_0}{(\mu_0 + \mu_1)} - \frac{\psi(k\Delta_t)}{\mu_1}, \\
\pi_{11}(k\Delta_t) &= \frac{\mu_1}{(\mu_0 + \mu_1)} + \frac{\psi(k\Delta_t)}{\mu_1}.
\end{aligned} \tag{4.6}$$

where $\mu_0 = E[\tau_{free,j}]$ and $\mu_1 = E[\tau_{occ,j}]$ are the mean off–time and on–time and $\psi(k\Delta_t) = (\mu_0 + \mu_1) cov(X(t), X(t + k\Delta_t))$. It can be shown that [166]:

$$\hat{\psi}(s) = \frac{\mu_0 \mu_1}{(\mu_0 + \mu_1)\, s} - \frac{\{1 - \hat{g}(s)\}\{1 - \hat{h}(s)\}}{s^2\{1 - \hat{g}(s)\,\hat{h}(s)\}}. \tag{4.7}$$

Based upon Eqn (4.6), it can be seen that the equilibrium probabilities can be further expressed as:

$$\begin{aligned}
\pi_{00}(k\Delta_t) &= (1 - \mu) + \frac{cov(X(t), X(t + k\Delta_t))}{(1 - \mu)}, \\
\pi_{01}(k\Delta_t) &= \mu - \frac{cov(X(t), X(t + k\Delta_t))}{(1 - \mu)}, \\
\pi_{10}(k\Delta_t) &= (1 - \mu) - \frac{cov(X(t), X(t + k\Delta_t))}{\mu}, \\
\pi_{11}(k\Delta_t) &= \mu + \frac{cov(X(t), X(t + k\Delta_t))}{\mu},
\end{aligned} \tag{4.8}$$

where $\mu = \frac{\mu_1}{(\mu_0 + \mu_1)}$ is the true temporal occupancy. Now assuming equilibrium and considering the i^{th} and $(i + 1)^{th}$ sampling instants spaced $k\Delta_t$ apart, let y_i be 1 if the channel is

occupied at the i^{th} sampling instant and 0 if it is not. It is easily shown that [147, 166]:

$$\begin{aligned} E[y_i] &= \frac{\mu_1}{(\mu_0+\mu_1)} = \mu, \\ var\,(y_i) &= \frac{\mu_0\mu_1}{(\mu_0+\mu_1)^2} = \mu(1-\mu), \\ cov\,(y_i, y_{i+k}) &= \frac{\psi\,(k\Delta_t)}{(\mu_0+\mu_1)}. \end{aligned} \tag{4.9}$$

4.5.1 Bias

The bias for an estimator based upon a selected temporal sampling approach, $\hat{\mu}$, is given by $Bias(\hat{\mu}) = E[\hat{\mu}] - \mu$, where μ is the true value for the temporal occupancy.

For periodic sampling, assuming equilibrium the bias is 0 since,

$$E[\hat{\mu}_P] = E\left[\frac{1}{n_P}\sum_{t_k\in\mathcal{S}_P} y_{t_k}\right] = \frac{1}{n_P}\sum_{t_k\in\mathcal{S}_P} E[y_{t_k}] = \mu. \tag{4.10}$$

For simple random sampling,

$$E[\hat{\mu}_{SRS}] = E\left[\frac{1}{n_{SRS}}\sum_{t_k\in\mathcal{S}_{SRS}} y_{t_k}\right] = \frac{1}{n_{SRS}}\sum_{t_k\in\mathcal{S}_{SRS}} E[y_{t_k}]. \tag{4.11}$$

Now,

$$\begin{aligned} E[y_{t_k}] &= P[\{\mathbf{z}[t_k]=1\}\cap\{X(t_k)=1\}] \\ &= P[\{\mathbf{z}[t_k]=1\}]P[\{X(t_k)=1\}] \\ &= \pi\mu, \end{aligned} \tag{4.12}$$

where the second line follows from the fact that sampling instants are independent of $X(t)$ for simple random sampling. Combining Eqns (4.11)–(4.12), it therefore follows that:

$$E[\hat{\mu}_{SRS}] = \pi\mu. \tag{4.13}$$

Hence the bias for simple random sampling is given by:

$$Bias(\hat{\mu}_{SRS}) = \mu - \pi\mu = (1-\pi)\mu. \tag{4.14}$$

Stratified sampling uses simple random sampling for each strata. Therefore the results from Eqn (4.14) can be used for each strata. Therefore for the j^{th} stratum:

$$E[\hat{\mu}_j] = \pi_j \mu. \tag{4.15}$$

The expected value of the estimator for stratified sampling is therefore given by:

$$\begin{aligned} E[\hat{\mu}_{St}] &= E\left[\sum_{j=1}^{S} \frac{1}{N_t \pi_j} \sum_{t_k \in \mathcal{S}_j} y_{t_k}\right], \\ &= \sum_{j=1}^{S} \frac{1}{N_t \pi_j} \sum_{t_k \in \mathcal{S}_j} E[y_{t_k}], \\ &= \sum_{j=1}^{S} \frac{1}{N_t \pi_j} \sum_{t_k \in \mathcal{S}_j} \pi_j \mu, \\ &= \sum_{j=1}^{S} \frac{\pi_j N_j}{N_t} \mu, \\ &= \pi\mu \sum_{j=1}^{S} \frac{N_j}{N_t} = \pi\mu. \end{aligned} \tag{4.16}$$

Hence, $Bias(\hat{\mu}_{SRS}) = Bias(\hat{\mu}_{St}) = (1-\pi)\mu$.

Cluster sampling uses periodic sampling for each strata selected, where strata are selected using simple random sampling. Therefore it can be easily seen that for the j^{th} selected cluster, $E[\hat{\mu}_j] = E[\hat{\mu}_P] = \mu$. Now it can therefore be seen that the estimator from cluster sampling is unbiased:

$$E[\hat{\mu}_C] = \sum_{j \in \mathcal{S}_c} \frac{M_c}{m_c N_t} N_j \mu = \sum_{j \in \mathcal{S}_c} \frac{\mu}{m_c} = \mu. \tag{4.17}$$

The relative error can then be used to normalise the performance based upon the temporal occupancy. Since the bias is a random variable due to the random sampling design, the expected relative error will be used. The expected value of the relative error can be derived from the bias using, $\epsilon_{\hat{\mu}} = \frac{|Bias(\hat{\mu})|}{\mu}$. Thus, from Eqns (4.10)–(4.17):

$$\epsilon_{\hat{\mu}_P} = \epsilon_{\hat{\mu}_C} = 0. \tag{4.18}$$

$$\epsilon_{\hat{\mu}_{SRS}} = \epsilon_{\hat{\mu}_{St}} = (1-\pi). \tag{4.19}$$

4.5.2 Precision

For each sampling design, the precision can be evaluated by the variance of the estimator. This can be derived using Eqns (4.6)–(4.9). Using these equations, it is easily shown for systematic sampling that the variance of the estimator is given by [147, 166]:

$$var\left(\hat{\mu}_P\right) = \frac{\mu(1-\mu)}{n_P} + \frac{2}{n_P^2\left(\mu_0+\mu_1\right)}\sum_{j=1}^{n_P}\left(n_P - j\right)\psi\left(j\eta\Delta_t\right). \tag{4.20}$$

As opposed to systematic sampling, for random sampling the increments between successive samples becomes a random variable, η_j, and from (4.20) the conditional variance, given sampling vector $\mathbf{z}$, is therefore:

$$var\left(\hat{u}|\mathbf{m}\right) = \frac{\mu(1-\mu)}{n} + \frac{2}{n^2\left(\mu_0+\mu_1\right)}\sum_{j=1}^{n}\sum_{l>j}^{n}\psi\left((m_l - m_j)\eta\Delta_t\right), \tag{4.21}$$

where $\mathbf{m} = [m_1, m_2, \cdots, m_n]$, and $\{m_1, \ldots, m_n\}$ is the ordered sequence representing the n sampling instants within the sampling vector. Therefore, the variance is given by:

$$\begin{aligned} var\left(\hat{\mu}\right) &= \sum_{\mathcal{M}} var\left(\hat{u}|\mathbf{m}\right)P(\mathbf{m}), \\ &= \sum_{\mathcal{M}} \frac{1}{|\mathcal{M}|} var\left(\hat{u}|\mathbf{m}\right), \\ &= \frac{\mu(1-\mu)}{n} + \frac{2}{n^2\left(\mu_0+\mu_1\right)|\mathcal{M}|}\sum_{\mathcal{M}}\sum_{j=1}^{n}\sum_{l>j}^{n}\psi\left((m_l - m_j)\eta\Delta_t\right), \end{aligned} \tag{4.22}$$

where $\mathcal{M}$ is the set of all possible sampling vectors of sample size n, for the given sampling design. Note that this is typically a subset of all possible vectors of size n, since the sampling design defines the possible realisations of $\mathbf{m}$. $|\mathcal{M}|$ denotes the size of the set. For the sampling designs presented, it can be easily shown that $P(\mathbf{m}) = \frac{1}{|\mathcal{M}|}$, as each realisation of $\mathbf{m}$ is equally–likely from the subset based upon the sampling designs [142]. For example, for simple random sampling, the probability of choosing any n sampling instants from the possible N_t is given by $P(\mathbf{m}) = \frac{1}{\binom{N_t}{n}}$ [142]. The final line of Eqn (4.22) is obtained through substitution of Eqn (4.21) into the expression on the second line of of Eqn (4.22).

For large sample sizes, n, or for quickly decaying functions, $\psi\left(k\Delta_t\right)$, the summation term in Eqn (4.22) approximates to zero. In fact, under the assumption of independence

between sampled values, $cov\left(X\left(t\right), X\left(t+k\Delta_t\right)\right) = 0$, and therefore the summation term vanishes. This gives the lower bound for the variance achievable by random sampling as:

$$var\left(\hat{u}\right) \geq \frac{\mu(1-\mu)}{n} = \frac{\mu(1-\mu)}{\pi N_t} \tag{4.23}$$

Eqn (4.22) also gives several key insights into the performance of the sampling designs, which can be used in practical scenarios. First, the independence assumption may not hold for short measurement intervals. In such instances there is likely to be some correlation between $X(t)$ at sampling instants. Alternatively, for arbitrary $h(t)$ and $g(t)$, $\psi\left(k\Delta_t\right)$ may not decay rapidly. Clearly, denser sampling increases $|\mathcal{M}|$ which in the limit as $n \rightarrow \infty$, approximates to continuous sampling, which can decrease the variance under certain conditions.

However, for DSA scenarios, sparse sampling is of particular interest. In such scenarios performance depends upon the rate of decay of $\psi\left(k\Delta_t\right)$. For example, for Poisson and Erlang processes, $\psi\left(k\Delta_t\right)$ decays exponentially, and increasing $\eta\Delta_t$ brings the variance closer to the lower bound in Eqn (4.23) [166]. For arbitrary functions, $g(t)$, $h(t)$, it may not be numerically tractable to evaluate $\psi\left(k\Delta_t\right)$, and thus analysis in such cases would require use of computer-aided techniques.

4.5.3 Temporal Occupancy Model

In addition to the temporal occupancy, the channel can be further characterised in terms of several other parameters which may be of interest in spectrum management and compliance enforcement. Examples include:

1. **Time to the r^{th} occupancy event:** For some fixed value of r, the random variable defining the time at which the r^{th} occupancy interval occurs may be required.

2. **Number of occupied intervals occurring in time interval, N_T:** For some fixed measurement time, T, the number of occupied events, N_T occurring may be required.

3. **The renewal function, $H(T)$:** Based upon the last parameter, this is the mean value of N_T. The renewal function is defined as $H(T) = E[N_T]$.

4. **Renewal density, $h(t)$:** This defines the mean number of occupancy events expected to occur in a narrow interval near the time of interest. It is defined as $h(t) = \lim_{\Delta t \to 0^+} \frac{E[N_{t+\Delta t} - N_t]}{\Delta t}$.

5. **Hgher moments of N_T:** Higher moments of N_T may be required for temporal occupancy characterisation.

6. **Backward recurrence time, U_t:** This gives the random variable for the length of time measured backwards from a time, t, to the last renewal at or before t. This therefore can be used to estimate how long a transmitter has been transmitting.

7. **Forward recurrence time, V_t:** This gives the random variable for the length of time measured forwards from time, t, to the next occupancy event. This can be similarly used to estimate how long the current "ON" or "OFF' period will last for.

8. **Survivor function, $\mathcal{F}(\tau)$:** This defines the probability that a given "ON" or "OFF" period will exceed some value, τ. It can be used in a similar manner to U_t and V_t for estimating the duration of an "OFF" or "ON" interval.

Estimators for these parameters can be derived using standard renewal theory. However, the performance of such estimators depends upon the occupancy model used (*i.e.* the functions $h(t)$ and $g(t)$). However these PDF's have unknown parameters. The estimation problem is thus the parameter estimation using samples, $\{\mathcal{S}_j\}$, and random sampling vectors, $\{\mathbf{z_j}\}$. In the literature while there has been work in estimation of these parameters from a theoretical perspective, there has been limited work in the extension to estimation of temporal spectrum occupancy. Since in general, many of the parameters are functions of $\hat{\mu}$ [159, 166], in this chapter focus will be on the temporal occupancy estimation of $\hat{\mu}$, where $\hat{\mu}$ denotes any of the previous estimators of occupancy. Several of the above parameters will be considered in the next chapter.

4.6 Random Temporal Sampling Implementation

Each of the above sampling approaches depends upon the selection of a subset n of the N sampling opportunities. In typical applications, the sample design is carried out in

advance to select the sampling opportunities. However, this is not suited for online sampling of spectrum occupancy. Thus a windowing approach is proposed to obtain windows of duration T within which sequential sampling is carried out using the algorithm presented in Fig 4.3. Sampling is done on the primary sampled unit, (*i.e.*, cluster or time instant), according to the previous sampling designs. *skip* is periodic or randomly generated (based upon the sampling design) as a function of n and N so that $skip \in [0, N-1]$.

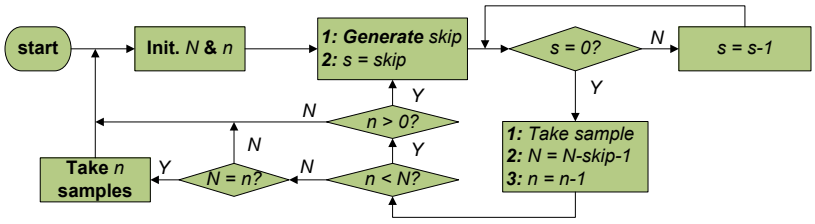

Figure 4.3: Algorithm for online random sampling.

4.7 Experimental Results

This section summarises results obtained from investigating the various sampling techniques, using the proposed online random temporal sampling algorithm. First, bias and precision of the sampling designs were compared. Following this, the impact of sampling interval duration and sampling sparsity was investigated. Next, the impact of detector performance on occupancy estimation was studied. Finally, the performance of the approach to CS–based occupancy estimation was done. Because computational performance is very implementation–specific, qualitative comparisons of randomised sensing to CS are presented.

4.7.1 Experiment 1: Comparison of Bias and Precision for Sampling Designs

Experiments were conducted using the Universal Software-Defined Radio Peripheral 2 (USRP2) platform. The performance of the sampling design implementations was investigated by generating known artificial spectrum occupancy profiles, (*i.e.*, modelled as alter-

nating processes) representing different occupancy levels. Poisson processes[2] of minimum duration 5000 time units were generated with various occupancy levels $\hat{\mu}$. The sampling ratio was varied for a window size, $T = 1000\eta\Delta_t$, while the minimum sensor resolution, $\eta\Delta_t = 10^k : k \in \{-3, -2, -1, 0\}\ s$.

For each artificially generated process, a random group method [142] was then used to create 1000 independent sample realisations of each sampling design. Random group methods are very useful in situations where it is numerically intractable to compare performance of sampling techniques [142]. Sampling designs investigated were systematic, simple random sampling, stratified sampling and simple cluster–based sampling. More complex techniques, (*e.g.*, hybrid approaches) were not investigated.

For each realisation of a sampling design, the occupancy was calculated using the respective equation from Eqns (4.1)–(4.5). These were used to estimate the relative error and variance for the realisations. For the experiments, designs were then compared based upon the estimated average relative error and variance introduced through the sampling techniques used.

Relative Error: Fig 4.4 illustrates the expected relative error introduced using each sample design implemented using the online randomisation algorithm presented in Fig 4.3. The results demonstrated that 1–stage cluster sampling and systematic sampling designs had lower relative errors compared to simple random sampling and stratified sampling approaches. Relative error performance improved as the sampling ratio was increased. The results further demonstrate that as sampling density increased, sampling tended to continuous sampling, and the errors decreased for all sampling approaches. Stratified sampling and simple random sampling had similar performances. As discussed in Chapter 3, this would be due to the use of equal–sized strata without taking account of strata homogeneity. Also, as expected, cluster sampling and systematic sampling performance appeared to be independent of the sampling ratio used. The relative errors, however, were not constant, and in fact were slightly biased. This was due in part to the effect of misclassification of

[2]Other PDF's for the "ON" and "OFF" time could be used, but this model is popularly used in the literature to represent OSA behaviour, (*e.g.*, [109, 167–170]), particularly due to its simplicity [159].

the renewal process at selected sampling instants, for the transmitter SNR. This effect was investigated further in Experiment 3.

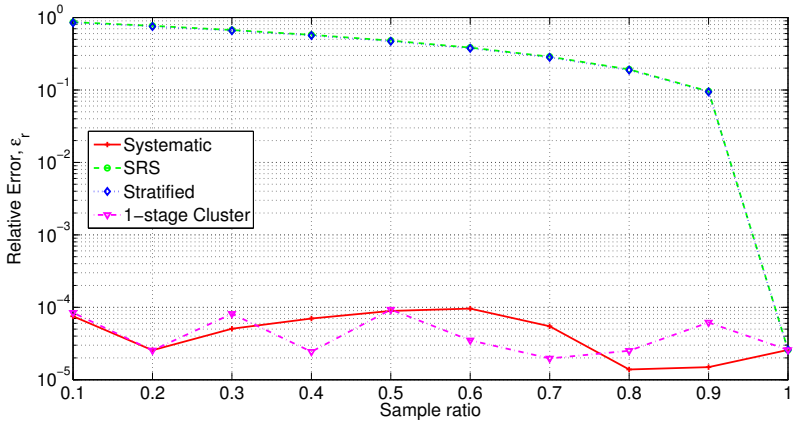

Figure 4.4: Comparison of relative errors for sampling designs.

Variance: Figs 4.5–4.9 compare the theoretical lower bound to the variance introduced using each sampling design, based upon Fig. 4.3. The results demonstrate that the experimental variances obtained were higher than the theoretical case. This indicated that there was some correlation between samples. Variance may also have been introduced through other experimental factors such as the detector used for occupancy classification. In all cases, the general trend indicated that variance peaked for 50% occupancy. Further, for a given occupancy level, the variance increased as the sampling ratio decreased to 0. The order of increasing performance of in terms of variance was: periodic, SRS, 1–stage cluster, stratified. However for low sample ratios stratified sampling performed the worst despite having the lowest variance values for all other occupancy levels investigated.

4.7.2 Experiment 2: Impact of Sampling Duration and Sparsity

Spectrum occupancy profiles were artificially generated using the USRP2 platform. Other USRP2 devices were configured to perform periodic and random sensing in integer multiples of the sensor resolution. To investigate the impact the measurement duration on performance, the window size was varied between $T = [100, 10000]\eta\Delta_t$, for $\eta\Delta_t = 0.01$ s. To investigate the impact of the sampling sparsity on performance, for the same sample

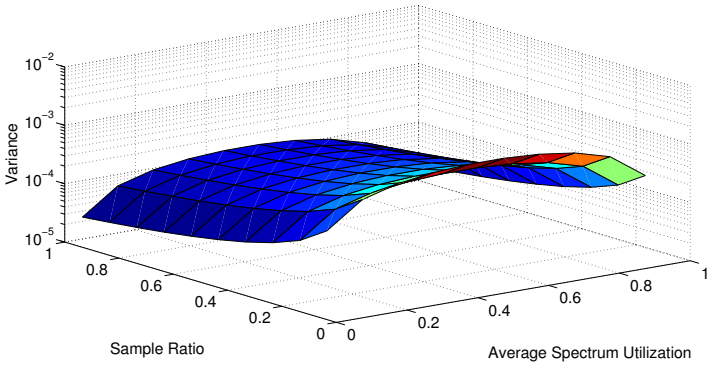

Figure 4.5: Theoretical bound on the variance for sampling designs.

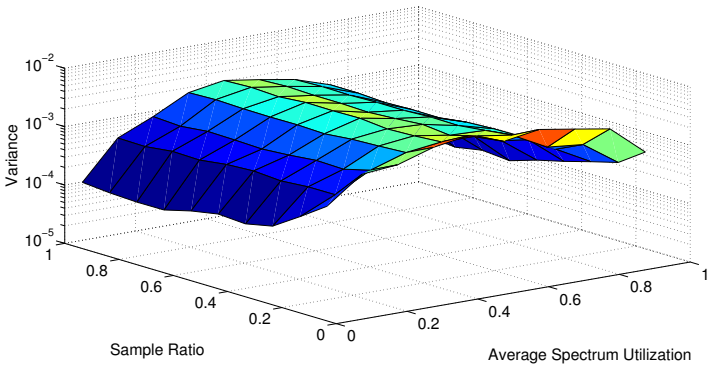

Figure 4.6: Estimator variance for a Poisson Process using periodic (systematic) sampling.

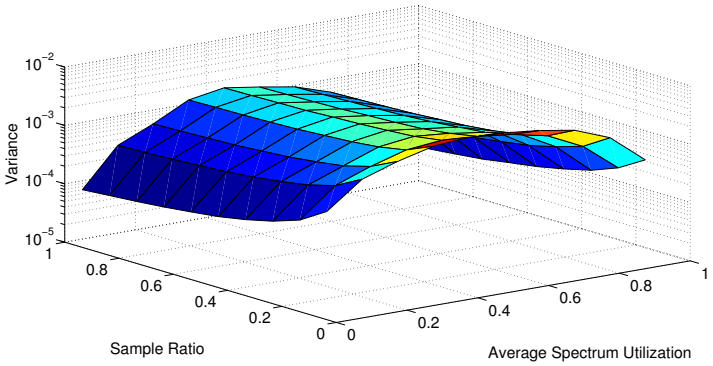

Figure 4.7: Estimator variance for a Poisson Process using SRS sampling.

size, $\eta\Delta_t$ was varied between $(0.001, 1)$ s. The collected data was then used to determine occupancy levels using energy detection with a threshold determined through noise level measurements before the actual USRP2 transmissions occurred. The random group method

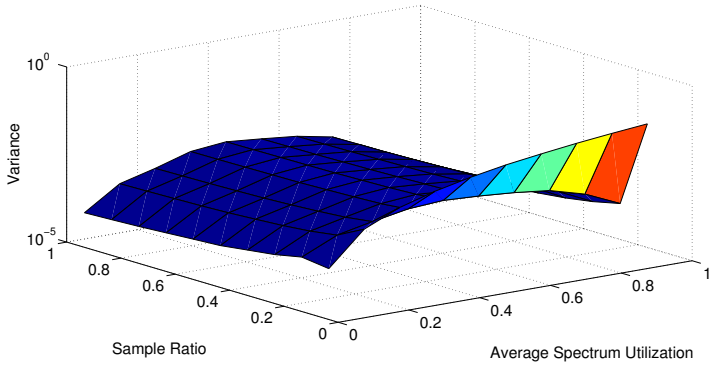

Figure 4.8: Estimator variance for a Poisson Process using stratified sampling.

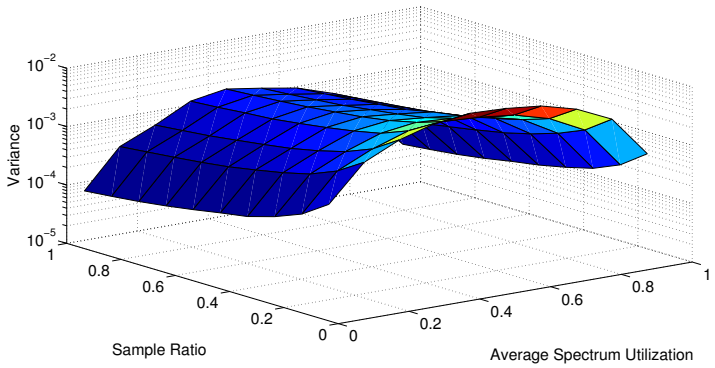

Figure 4.9: Estimator variance for a Poisson Process using 1-stage cluster sampling.

was then used to determine the relative error and variance of the estimators, based upon the known traffic profiles generated. Examples of this are presented in Figs 4.10–Fig 4.12, for a Poisson process.

The figures demonstrate that randomised sensing can outperform periodic sensing. Fig 4.10 demonstrated that the bias was independent of the duration of measurement for the sampling designs investigated. However, as shown in Fig 4.11, the precision increased as the measurement duration increased. Fig 4.12 illustrated the effect of sparser sampling. As the sensor resolution was increased the correlation between samples was reduced. This could be explained by the fact that the correlation for samples from a Poisson process has exponential decay [166]. Therefore, by increasing the sampling sparsity, for the same number of samples, the estimators produced samples that tended to be approximately independent.

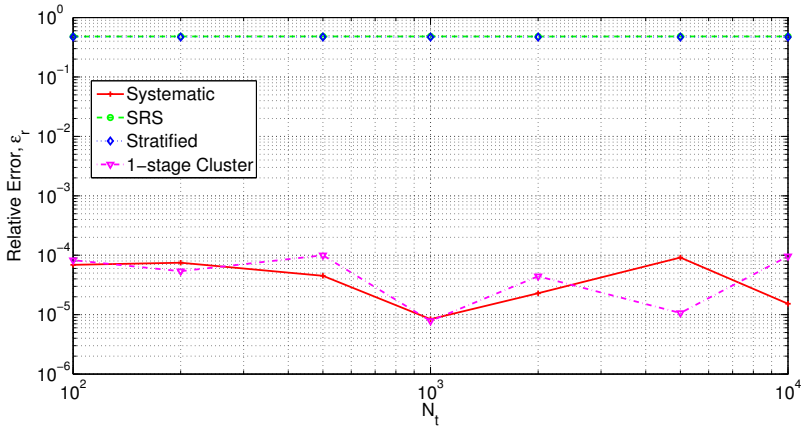

Figure 4.10: Comparison of estimator relative error versus measurement duration for a Poisson Process using different temporal sampling strategies, ($\mu = 0.5, \pi = 0.5$).

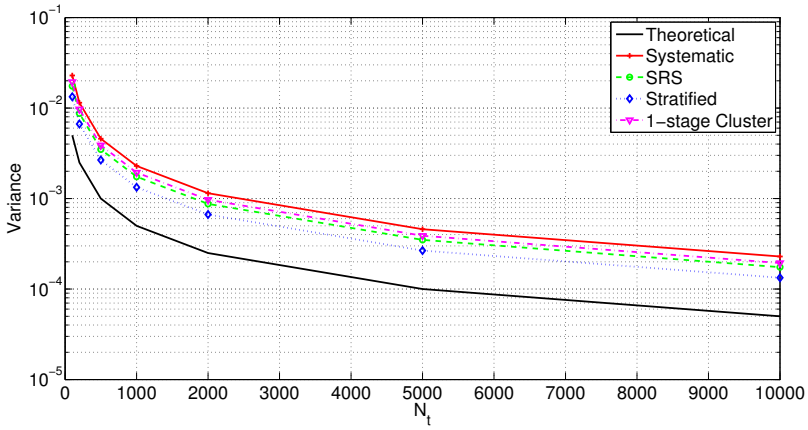

Figure 4.11: Comparison of estimator variance versus measurement duration for a Poisson Process using different temporal sampling strategies, ($\mu = 0.5, \pi = 0.5$).

As the sample dependence decreased, the variance tended to the theoretical bound for independent samples. The slightly higher variance observed could be explained by considering practical factors such as mis–classification errors due to false alarm and missed detection events, for example.

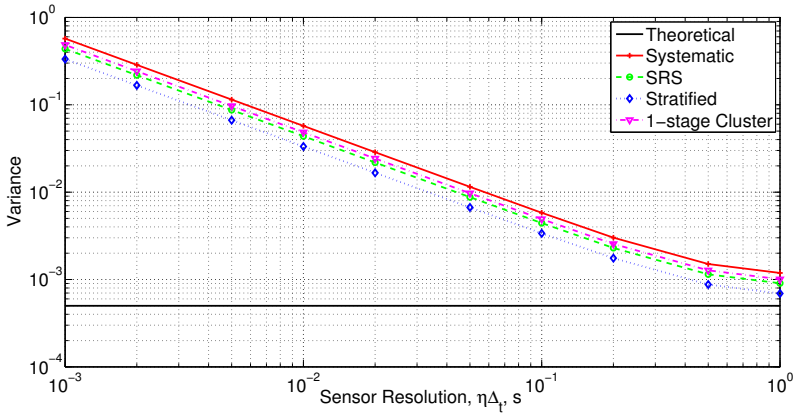

Figure 4.12: Comparison of estimator variance versus sensor resolution for a Poisson Process using different temporal sampling strategies, ($\mu = 0.5, \pi = 0.5$, sample size = 500).

4.7.3 Experiment 3: Impact of Detector Performance

The SNR for the experiments was also observed to impact performance. Experiment 2 was repeated for different SNRs. The SNR was varied by varying the USRP transmit power. The use of high transmit power levels for a high SNR, separated the signal strengths for occupied and unoccupied signals, allowing for a threshold which clearly demarcated the two states. However the impact of low SNRs, as observed through reduced signal and noise separation leading to increased false–alarm and missed–detection events was also studied. The impact of detector performance on the estimation was examined by comparison of two detectors, energy detection and cyclostationary detection, for different SNR levels. Figs 4.13–4.14 illustrate the results of the experiments. The results suggest that occupancy misclassification impacts performance. Higher SNR, due to higher transmit powers, decreases the misclassification errors and improves performance. A similar effect is observed when cyclostationary detection is used at low SNRs. This can be explained by noting that cyclostationary detection typically exhibits better classification performance at lower SNRs.

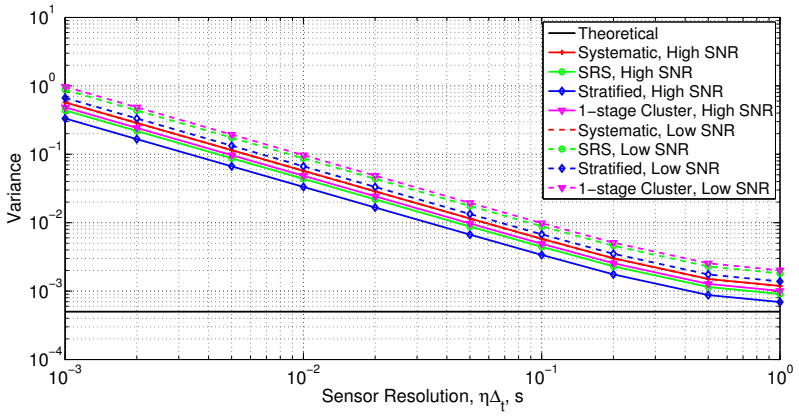

Figure 4.13: Effect of SNR on estimator variance, ($\mu = 0.5, \pi = 0.5$, sample size = 500).

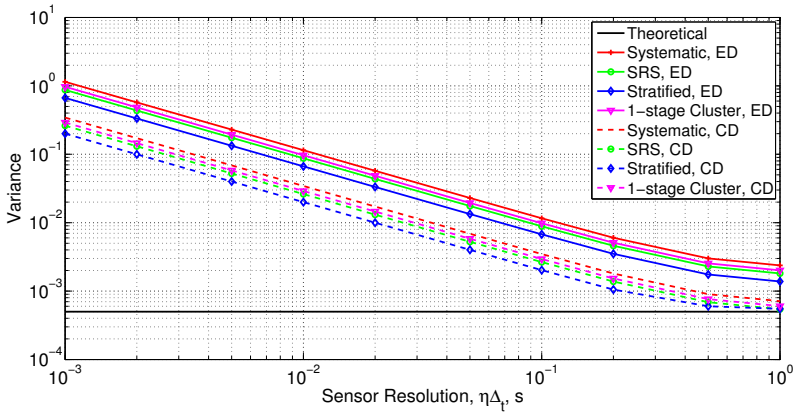

Figure 4.14: Comparison of estimator variance for Energy detection (ED) and Cyclostationary detection (CD) at low SNR, for a Poisson Process using different temporal sampling strategies, ($\mu = 0.5, \pi = 0.5$, sample size = 500).

4.7.4 Experiment 4: Comparison to CS–based Occupancy Estimation

The data collected from the previous experiments were then used to compare the random approaches to a CS–based approach. Specifically, signal reconstruction was done on sparse, randomly selected samples of the collected data, then Eqn (4.1) was used to estimate the occupancy. Prior to reconstruction, signal measurements, $\mathbf{Y}$, were converted using the

gray–scale (*i.e.*, scaled to the interval [0,1]) linear transformation:

$$\mathbf{G} = \frac{\mathbf{Y} - \min \mathbf{Y}}{\max \mathbf{Y} - \min \mathbf{Y}}, \tag{4.24}$$

where $\max \mathbf{Y}$ and $\min \mathbf{Y}$ are the maximum and minimum values of $\mathbf{Y}$, respectively. The reconstructed data was then classified into occupied or unoccupied based upon a fixed threshold, ϵ, and then used to determine occupancy levels.

The CS–based technique was used on 1000 random realisations of the sampling process, from which the variance of the occupancy estimate was determined. Since the CS–based technique used Eqn (4.1) for estimating the occupancy, the bias was not determined as it was expected to be unbiased for the reconstructed signal. Figs 4.15–4.16 illustrate the comparison to the previous random sampling approaches. At low sampling ratios, the signal was not perfectly reconstructed using the CS–based approach. However, at higher sampling ratios reconstruction was accomplished in most cases, and the occupancy estimates had lower variance. However, as seen in Fig 4.16, as the utilisation increased, perfect reconstruction could only be accomplished for higher sampling ratios, which further limits the effectiveness of the CS technique for higher occupancy scenarios. This could be explained by noting that CS requires that sufficient signal samples be provided to account for signal sparsity.

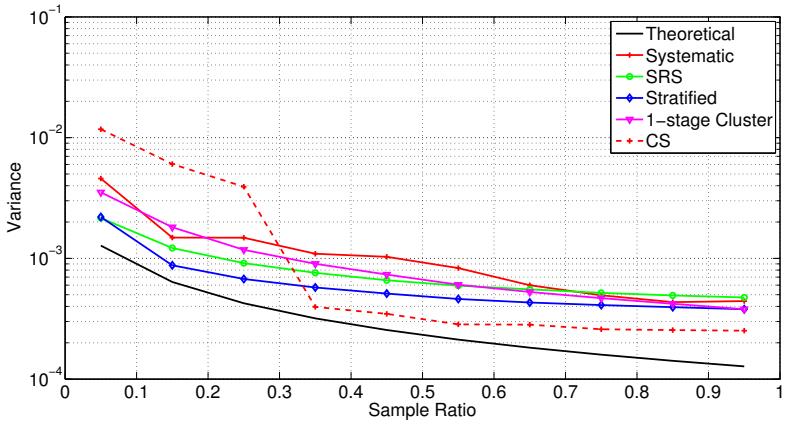

Figure 4.15: Comparison of estimator variance for CS–based approach, at low utilisation, for a Poisson Process, ($\mu = 0.1$).

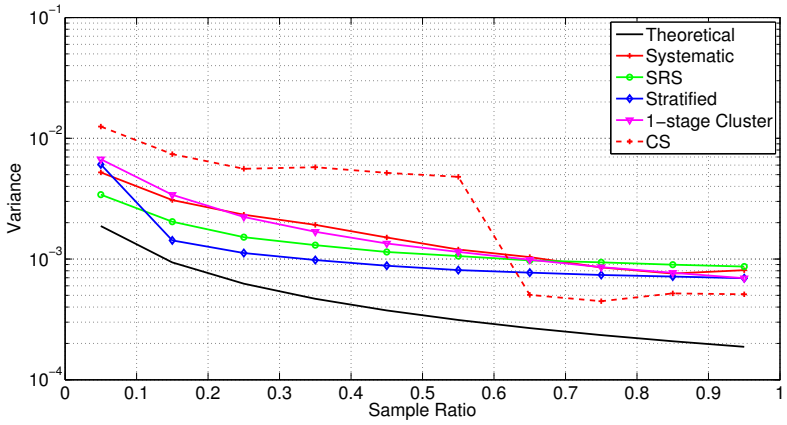

Figure 4.16: Comparison of estimator variance for CS–based approach, at medium utilisation, for a Poisson Process, ($\mu = 0.25$).

4.8 Conclusion

In this chapter, the use of randomised temporal sensing was investigated for temporal occupancy characterisation. A framework for performance analysis of random temporal sensing was presented, and a lower bound on sensing performance in terms of estimator precision was derived for spectrum occupancy modelled as an alternating renewal process. The lower bound was seen to be independent of the probability density functions which define the alternating renewal process model for temporal spectrum occupancy. An implementation of randomised sensing on periodic sensing platforms was presented using an online randomisation algorithm, and this was used to carry out several experiments relating to the performance of random temporal sensing using USRP hardware.

The results show that randomised temporal sensing can outperform periodic sensing using the algorithm presented in this chapter. Performance of random sampling in terms of precision was seen to approach the theoretical lower bound using larger sample sizes, or through sparser sampling, for processes with decaying autocorrelation functions. The latter approach introduced more independence between samples.

The results also demonstrated the impact of detector performance on the estimator variance. For low SNR scenarios, the use of cyclostationary detection, which gives better signal

detection than energy detection, exhibited better performance for temporal occupancy estimation. While user discrimination was not considered in this chapter, cyclostationary feature detection additionally presented one way of coarse discrimination between users with different cyclostationary features, (*e.g.*, modulation type, transmission bandwidth).

Finally, comparison was made between the proposed random sampling approach and a CS–based approach. For low occupancy scenarios, the CS–based approach performed better than the proposed random approach, at lower sampling ratios due to signal reconstruction. However, in medium and high utilisation scenarios, the CS–based approach performed worse, and required higher sampling ratios to achieve comparable performance to the random sampling approach proposed. Therefore, the CS–based approach was seen to be less suited for use in temporal occupancy estimation in scenarios where spectrum congestion may occur. Further, the CS–based approach first reconstructs the signal prior to occupancy estimation. The reconstruction stage is avoided entirely in the random sampling approaches presented. Therefore, although specific comparisons of computational cost would be implementation specific, it can be said that the random approaches would be lower cost compared to CS–based techniques, all things being equal, since they do not have to reconstruct the signal for temporal occupancy estimation.

While the investigations focussed upon estimation of temporal utilisation, extending the approach to estimation of other temporal occupancy parameters was also discussed. The random sampling approach was therefore seen to offer a low complexity alternative to existing techniques for characterisation of temporal spectrum occupancy. Furthermore, unlike typical compressed sensing schemes for low signal occupancy scenarios, in the proposed random temporal sensing approach the reconstruction objective is relaxed to improve performance in medium to high occupancy settings. This method thus facilitates statistical occupancy characterisation for various occupancy levels, which is a key spectrum monitoring objective, without requiring the sparsity assumptions of compressed sensing.

Chapter 5

Frame–based Temporal Occupancy Estimation in OSA Networks

5.1 Introduction

Cognitive radios are currently allowed to opportunistically operate within specified sub–bands, (*i.e.*, TVWS bands at the time of this writing). Monitoring networks therefore should be capable of monitoring across these bands. In the previous chapter, temporal occupancy estimation within spectrum bands was examined, when there is no requirement to track individual user or network behaviours. This followed from current approaches for temporal occupancy estimation which typically are used to determine the proportion of time during the measurement interval, for which a spectrum band of interest is occupied (*e.g.*, [5, 35, 134]). This approach was in line with the predominantly licensed–based access models where individual users/networks did not need to be tracked.

However, depending upon the specific measurement objectives, discrimination between different users/networks may be required. Typically, this involves emitter localization and direction–finding and can be done using characteristics such as call signs or particular signal characteristics, (*e.g.*, signal strength) [35, 134]. In envisioned OSA scenarios, such tracking may be more difficult, given the dynamics of proposed OSA techniques. An example scenario involving multi–channel access and spectrum agility, (*e.g.*, dynamic frequency se-

lection (DFS)), across several bands is illustrated in Fig 5.1. Multi–channel access and spectrum agility represent significant challenges to temporal occupancy modelling for individual users/networks in OSA scenarios.

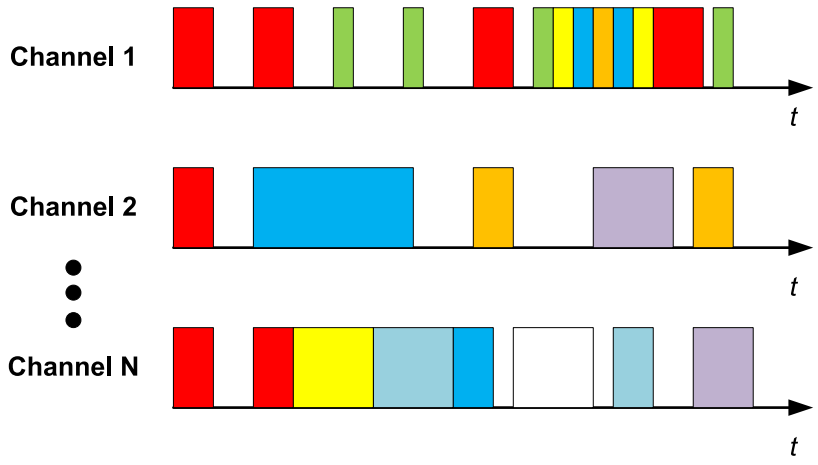

Figure 5.1: N–channel OSA scenario for user/network tracking. Each colored rectangle represents a sequence of consecutive frame transmissions, resulting in spectrum occupancy by a given user/network on the channel of interest. Simultaneous transmission across channels by a single user represents multi–channel operation, while changing channels at different times represents the dynamic frequency selection aspect of spectrum agility.

In this chapter, the random temporal sampling approach for estimation of temporal spectrum occupancy parameters is expanded. A frame–based sampling inversion technique for spectrum occupancy estimation is proposed, which can be used for estimating temporal parameters for a given user/network of interest. In this approach, parameters from randomly sampled PLCP frames are used to characterise temporal occupancy, using statistics such as the probability density functions of "ON" and "OFF" times for spectrum occupancy. The performance of the proposed approach is examined for temporal occupancy characterization in circumstances where the monitoring node misses frames due to the sampling design, sensor limitations or through error conditions on a given channel. This approach is investigated for use in OSA coexistence scenarios which involve multiple standards operating in TVWS.

Several aspects of this work also appear in publications developed for this thesis: [87, 94].

5.2 Motivation

Spectrum monitoring for user discrimination in heterogeneous OSA scenarios, (*e.g.*, TV whitespace (TVWS) coexistence scenarios) remains a widely under–studied issue. In traditional spectrum management approaches, this is accomplished using a combination of location/direction–finding techniques and use of signal strength to isolate a particular user signal [35, 134]. However this approach may not be well suited to the dynamic behaviour of OSA devices, particularly those with quickly–varying behaviours. While there has been recent work on coexistence scenarios in TVWS [171–173], with the exception of IEEE 802.19[1], in most proposed monitoring approaches the emphasis is on networks involving a single technology, (*e.g.*, IEEE 802.22 networks [16, 150, 153]). Such approaches are therefore limited in scope.

Other approaches focus upon discrimination between primary and secondary users (*i.e.*, user detection. For example, [69–71].) but not on discrimination of users for compliance verification. In the literature, there is related work which can facilitate discrimination both between and within groups of primary and secondary users. Examples include source separation techniques, automatic modulation classification techniques and waveform and feature–based detection techniques. However to–date, while such techniques have been used for classification of user groups based on specific traits, these techniques have not been used for more detailed user accounting, (*e.g.*, in temporal occupancy classification of individual users). As discussed in the previous chapter, user discrimination using such features is based upon the assumption that individual users/networks of interest can be uniquely identified by their features, which may not always hold in practice.

An alternative approach found in the literature uses active monitoring techniques, which employ enabling service infrastructure, such as geolocation databases, network management entities, access points or even ad hoc cluster formations, to also collect useful data which may be sufficiently detailed for user accounting. However, access to such data requires data exchange mechanisms for acquisition and conversion of heterogeneous data to a suitable

[1]IEEE 802.19 is still at the early stages of development at the time of writing.

format[2]. Furthermore, the accuracy and currency of such data[3] as well as the scalability (*i.e.*, when there are many network deployments) are issues with such active approaches. The accuracy of such approaches is also based upon the assumption that data on all users is accessible. This may not be the case particularly when spectrum usage does not conform to specified operational parameters for spectrum access (*e.g.*, unauthorised spectrum access and operation, such as primary user emulation). Through direct measurements, passive monitoring networks can aid in addressing various aspects of these issues.

Using the passive monitoring paradigm, in this chapter a novel frame–based sampling inversion technique is proposed for temporal occupancy characterization in OSA networks. Specific contributions are as follows:

1. Considering spectrum occupancy modelled as an alternating renewal process, marked point processes are constructed using renewals demarcated by frame–based feature semantics common to most current and emerging wireless MAC and PHY layer specifications;

2. Each marked point process can be associated with a given user or frame–based characteristic such as source–destination address pairs, facilitating specific monitoring of wireless emissions for each user/network of interest;

3. A frame sampling strategy used to construct sampled marked finite point processes, and recover spectrum occupancy statistics for the full frame sequence using sampling inversion techniques;

4. The analysis presented expands upon the literature on sampling inversion by considering the effect of missed detection of renewals in the sampling inversion process. This accounts for missed frames due to practical considerations in DSA networks;

5. A probabilistic model for variable data transmission rates due to MAC/PHY layer protocol mechanisms is also proposed to relate nominal frame lengths and data rates,

[2]Successfully merging data from possibly heterogeneous sources is dependent upon the data format as well as on the technical/environmental conditions during data collection.

[3]As an example, FCC–mandated geolocation databases focus upon primary users and therefore do not account for secondary users.

obtained from frame headers, to actual frame reception time for spectrum occupancy estimation;

The proposed method facilitates probabilistic characterisation of individual users, and is proposed for cases where there is more spectrum agility than deployed non–OSA technologies currently allow, in particular where there may be intelligently changing transmission parameters in response to the sensed state of the spectrum, such as enabled by cognitive radio devices. The resulting occupancy models can then be used to make appropriate decisions for spectrum management or for spectrum accounting.

The rest of this chapter is organised as follows: In Section 5.3 an overview of frame–based random temporal sensing concepts is presented, followed by a review of related work to which this chapter contributes. Next, Section 5.5 describes the proposed approach and demonstrates the application to characterisation of various temporal occupancy parameters. Experimental results are presented in Section 5.6. Finally there are concluding remarks in Section 5.7.

5.3 Frame–based Random Temporal Sensing Overview

In the previous chapter, the PHY–based random temporal sensing results indicated that while random sensing can outperform periodic sensing, the question of per user/network tracking in multi–channel OSA scenarios still remained. Given the real–time operation requirements for DSA monitoring approach, frame–based temporal sensing is proposed.

The approach is partly based upon [174, 175] for sample inversion of packets and flows. However, several differences must be noted:

1. In the literature on protocol data unit (PDU) arrival point process definitions, typically PDU arrivals are specified as the instants at which each entire PDU is received by the layer of interest (*i.e.*, where the duration of PDU reception is implicitly assumed negligible). In contrast, the frame arrival event (*i.e.*, which corresponds to the start of spectrum occupancy) is defined as the instant that the frame preamble is being received.

2. The duration of actual frame reception is used to estimate the spectrum occupancy.

3. Unless there are multi–channel interfaces, and based upon the traditional point process definition, multiple packets are typically not received at the same time. However due to interference, there may be possible overlap in frame receptions. this work considers such situations.

4. Missed detection of PDUs have not been considered in the literature on sampling inversion. In the proposed frame–based approach, the missed detection events are considered.

Another characteristic of frame–based sampling is the use of a shared wireless medium allowing for distributed sensing and estimation approaches. To the best of the author's knowledge, distributed estimation has not been explored in the sampling inversion literature. However, in this chapter, focus is on single sensor application of the proposed techniques, and distributed sensing is treated in Chapter 6.

5.3.1 Assumptions

This approach applies to PLCP formats, in which start–of–frame and end–of–frame delimiters are used for framing. Most wireless protocols in operation use this approach. However, there are other framing formats which would not work for this sensing scheme. In such instances, the PHY–based technique in the previous chapter is suggested, assuming that uniquely identifiable features can be determined. For the frame–based approach, several assumptions are made:

1. Sensing devices are able to detect frames and identify specific PLCP standards through their characteristic frame delimiters.

2. Sensing devices know the PLCP frame format, and are able to decode it.

3. The frame length and data rate do not change during individual frame transmission/reception, and can be determined from frame data.

4. Frames contain information (*e.g.*, source and destination addresses or upper layer protocol field) which can be used to associate sampled frames which are related.

5. Although multiple PLCPs exist, only one is being used during each individual frame reception.

6. The temporal characteristics are stationary for the measurement and estimation interval, and the measurement interval is sufficiently long to obtain sufficient samples of the process of interest.

A consequence of these assumptions is that the model relating the frame length to the transmission time is relatively simple and requires minimal processing time for decoding the relevant parts of the frame header. This is advantageous for real time implementations. More complex models can potentially increase estimation accuracy but this requires a tradeoff with increased processing time. The assumption of prior knowledge of the frame format follows from the fact that standards for OSA operation must be certified and thus would be known in advance. Further, all currently proposed and approved standards for the MAC/PHY layer (*e.g.*, IEEE 802.11af, IEEE 802.22, ECMA-392) also satisfy the assumptions on the frame containing length and association information.

5.3.2 Frame Reception

Intervals of spectrum occupancy occur as a result of one or more PHY–layer frame transmissions being received by the spectrum sensing device. At the PHY layer, protocol data units (PDUs) may be fragmented and/or directly encapsulated for wireless transmission (and consequent reception). Whether transmissions are point–to–point, multicast or broadcast in nature, the wireless medium is occupied for any detected frame transmission, whether or not it is intended for the sensing device.

Of interest in this chapter are PLCP (or equivalent) frames (*e.g.*, Fig 5.2) as opposed to other PDUs, since the PLCP lengths are in general more directly related to spectrum occupancy, compared to higher layer PDUs. Higher–layer PDUs incorporate more complex protocol mechanisms (*e.g.*, flow/error control, fragmentation and reassembly) which can obscure the relationship between spectrum occupancy and PDU length. An example of this

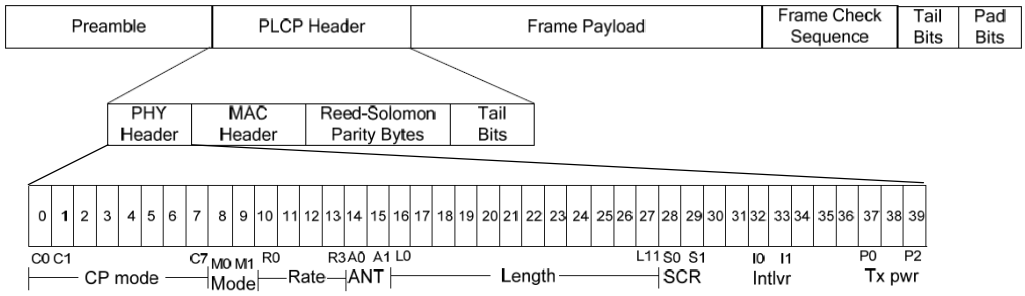

Figure 5.2: Example of PLCP Frame Structure Semantics for ECMA-392 [44].

is given in Figs 5.3–5.6. Data were collected both at WPI and UWI for approximately 8 hours, and appropriately sanitised for anonymity using available software tools. As seen in the figures, although some of the variance may be accounted for due to the measurement procedure as well as various delays, the correlation between PDU length and spectrum occupancy duration is more evident for the lower layers. There is an observable linear relationship between the PDU lengths and reception times. Further, the sum of all random components can be approximated by uniform distributions in many instances or is Gaussian distributed in some instances (*i.e.*, particularly for TCP PDUs)[4]. In general, the span increases for higher layer PDUs.

While it is possible to develop models relating spectrum occupancy to PDU length for higher layer protocols, in general these are more complex, have higher computational costs to decode PDUs and develop models, may not be applicable for spectrum access network semantics [5]. Further, higher–layer PDUs can be encrypted thus restricting access to required PDU header information for occupancy modelling. Therefore the concept of PDU sample inversion is demonstrated using PLCP where the least information is required, (*i.e.*, compared to higher layers), and possibly more precise, simpler models can be used to relate frame reception to spectrum occupancy.

As seen in Fig 5.2, it is possible to determine both the nominal data rate and the nominal

[4]In reality the PDF of the total delay will be the m–fold convolution of the PDFs of the m delays [147]. However, assuming that a few delays are dominant, then the total delay can be suitably approximated based upon the dominant delays. The limit for the summation of several terms is approximately Gaussian distributed by the Central Limit Theorem [147].

[5]For example, transport layer protocols focus on end–to–end semantics which would obscure lower–layer network semantics, such as the use of spectrum access at the PHY layer.

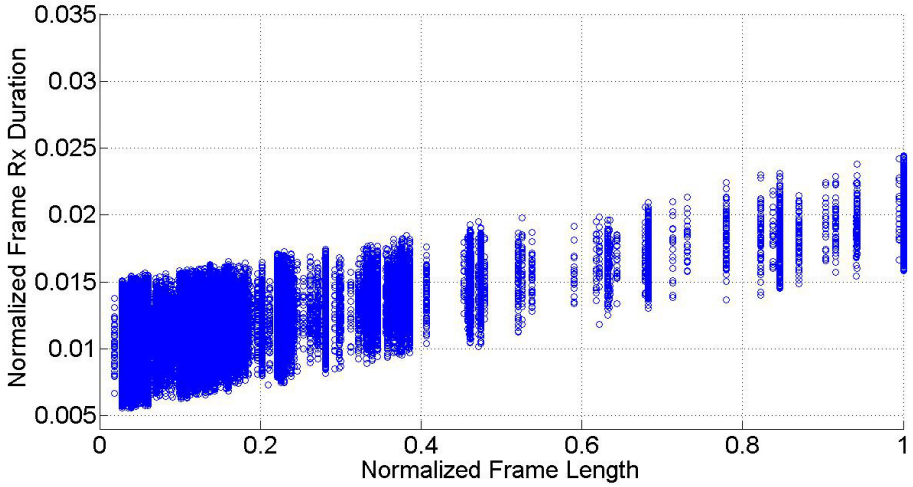

Figure 5.3: Scatter plot of frame size to frame reception time for UWI data.

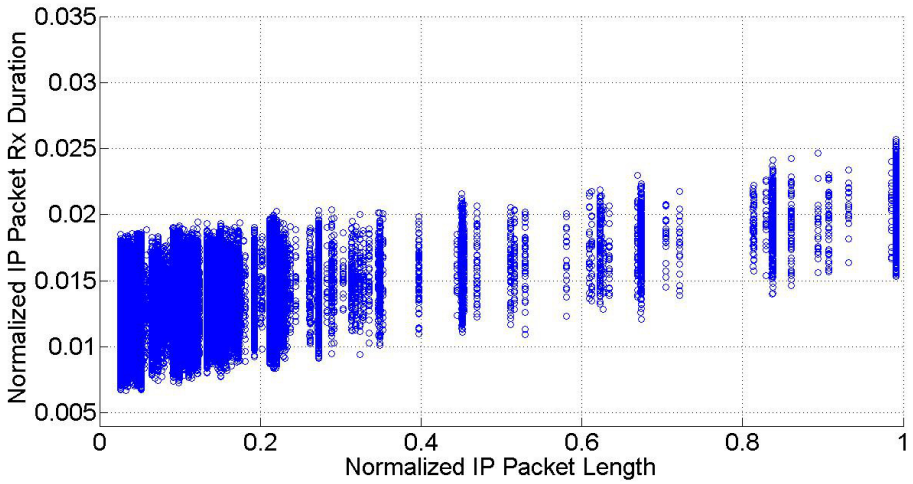

Figure 5.4: Scatter plot of IP packet size to packet reception time for UWI data.

frame length from the PLCP header provided that the standard definition is known. For authorised transmissions, this can be reasonably assumed. In cases where such information is unavailable, occupancy time durations can still be determined by detection of frame starts and ends, using any of the available techniques in the literature, such as energy detection, cyclostationary detection or waveform detection techniques [54]. This was the approach used in the previous chapter. Fig 4.10 and Fig 4.11 illustrate examples of occupancy esti-

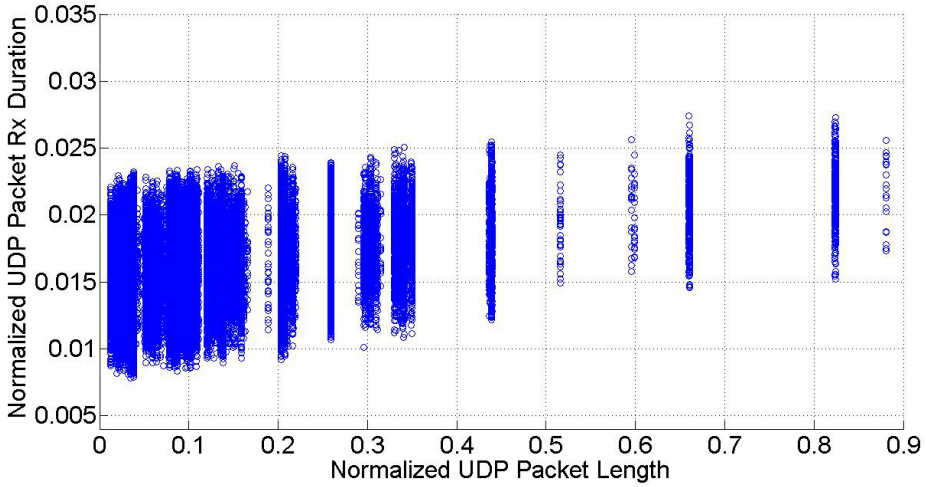

Figure 5.5: Scatter plot of UDP packet size to packet reception time for UWI data.

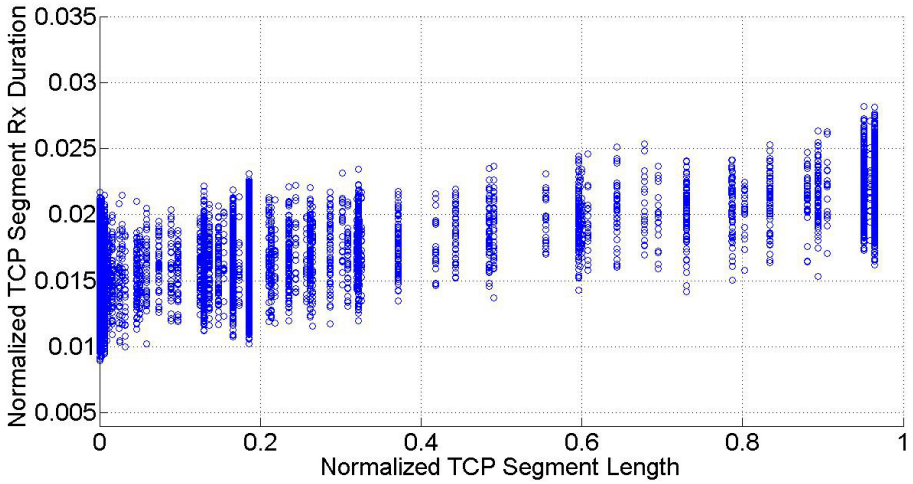

Figure 5.6: Scatter plot of TCP segment size to segment reception time for UWI data.

mation performance for various sampling strategies[6]. In such instances, it is still possible to temporally characterise occupancy for given users/networks. However, in general it would be extremely difficult to isolate and track users without some knowledge of the user. The frame–based random temporal sampling architecture is illustrated in Fig. 5.7.

[6]A 50% occupancy Poisson Process was used to generate wireless data on USRPs, in WILab, which was then collected using another USRP to assess the impact of different sampling strategies. Energy detection was used to determine the start and end of frames.

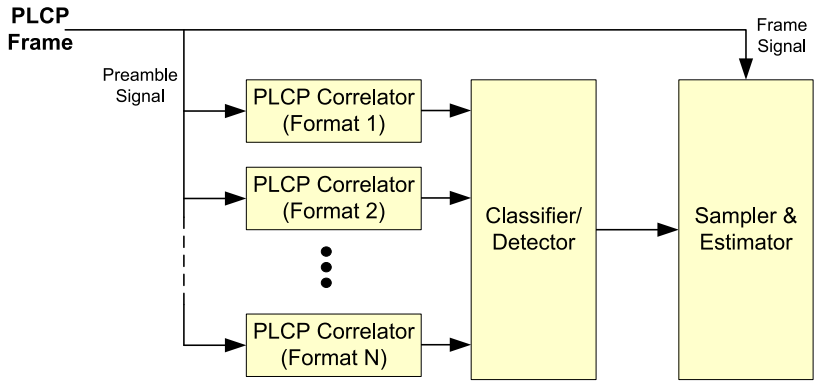

Figure 5.7: Frame–based random temporal sampler architecture, for a DSA scenario in which N possible frame formats can be used. Prior knowledge of frame formats is assumed. A detector/classifier is used to quickly determine which of the pre–defined MAC frames is being used. Based upon classification, frames are then decoded and sampled for estimation of temporal characteristics.

5.3.3 Frame Sampling

For the measurement interval of interest, $\boldsymbol{T} < \infty$, consider the frame arrival point process, $X(t)$,where arrivals are defined as the start of frame reception within the wireless medium. This is based upon the assumption that frames are used for exchanging higher layer protocol data units (PDUs), which are finite in length. Frame arrivals within $\boldsymbol{T}$ can be modelled as a finite point process[7], where there are N_o frames (*i.e.*, renewals) with frame lengths, $L_j, j \in [1, N_o]$, and inter–renewal times, $\tau_i, i \in [1, N_o - 1]$. N_o is random. Further, the nominal frame lengths, L_i, and the nominal data transmission rates, D_i, are assumed to be positive independent, identically distributed random variables, which are independent of the total number of renewals. A similar assumption is made for the inter–renewal times, τ_i. Sets of frames are considered to be related based upon common properties of interest(*e.g.*, source/destination addresses, protocols, connection ID). Based upon this concept, frame transmissions can be further defined as marked point processes, if discrimination is required for monitoring. Additionally, due to MAC protocol operation, it is assumed that frame transmissions from different processes are generally interleaved within the measurement interval.

[7]This requires careful consideration of special addresses (*e.g.*, broadcast/multi–cast) and frame types (*e.g.*, management/control frames).

In packet/flow sampling, the time instant at which each packet arrives at routers or other network devices triggers the sampling decision–making process. In contrast, for frame sampling, monitoring nodes need to detect the start of each frame. However, this would typically require dense sampling of each channel, which consumes resources and also limits the number of channels which can be monitored simultaneously. A time–slotted random channel sampling approach is thus used to define the start of the sampling instant, t_0, on any given channel. Sampling then proceeds for the measurement duration, $T < \infty$. Should a frame continue past the interval, the entire frame is received for the extra time, t_e[8], in order to ensure that the header is not in error and can be decoded. Therefore, sampling occurs during the interval, $\boldsymbol{T} = [t_0, t_0 + T + t_e]$, during which stationarity is assumed. In an N–channel scenario, randomly switching between channels using a simple random channel sampling approach such as described in Chapter 3, can allow for independent sampling of each channel, for approximate duration, $T + t_e$. Consider that channels are each sampled an average of J times for the total measurement interval.

An illustration of frame–based sampling for a single channel is given in Fig 5.8. During the measurement interval, $\mathbf{T}$, frames may not be detected, with probability of missed detection, p_m. This may be due to several factors such as fading, interference, low SNR or due to sampling design[9], among others. For simplicity, it is assumed that this probability is fixed, based upon aggregation of all factors, and missed frames are defined as events in which only a portion of a frame is received. By definition, this implies that the start–of–frame delimiter was missed, but some portion of the frame transmission was still detected. Let $N_m \in \{0, \ldots, N_o\}$ denote the number of missed frames in the measurement interval, $\mathbf{T}$. This gives rise to a modified point process, $X_m(t)$, where missed frames are ignored. For, $X(t)$, if an errored frame is detected but which cannot be corrected, the reception duration is recorded[10] and used for estimation of the missed–detection probability.

For detected frames in $X_m(t)$, the frame sampling decision-making process opts whether

[8] t_e is therefore of random duration.

[9] For example, sampling on one channel may not allow sampling simultaneously on all remaining channels of interest.

[10] Error events can occur, for example, because of intermittently low SNR or due to interference from multiple simultaneous transmissions. At this stage, differentiating between them is not studied based upon the aggregation of effects in the missed detection probability.

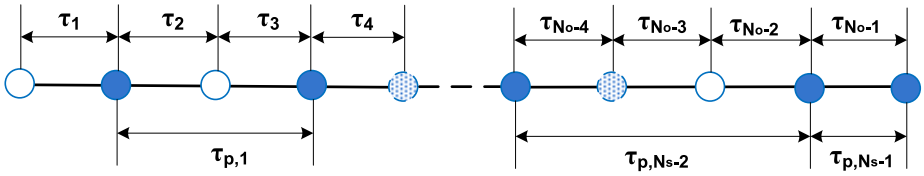

Figure 5.8: Frame–based random temporal sampling, with missed frames. Circles represent frame arrival events. Unfilled circles represent detected frame arrival events where the frames were not sampled. Filled circles represent detected and sampled frame events. Dashed outline, dotted circles represent undetected/missed frame arrival events.

or not to sample the frame being currently received, with sampling probability, p_s. This gives rise to the sampled process, $X_s(t)$. Frame sampling and the use of sampling inversion can then be used to recover statistics about the original process. A single process is considered for simplicity, but it is noted that the approach can be extended to more complex process models of interest. The randomly sampled frames form a sampled finite point process, where there are $N_s \in \{0, \ldots, N_o - N_m\}$ sampled frames (*i.e.*, renewals) with nominal lengths, $L_{p,j}, j \in [1, N_s]$, nominal data rates, $D_{p,j}$, and sampled inter–renewal times[11] $\tau_{p,i}$, $i \in [1, N_s - 1]$. The nominal frame lengths and data rates are obtained from the relevant PLCP fields[12]. Additionally, for each received frame the frame reception time, T_{Rx_j}, is measured. Note that N_o and N_s are not pre–determined for any measurement interval, $\mathbf{T}$. The subscript '$_p$' is used to refer to sampled data to distinguish from the original data it was taken from.

For temporal occupancy estimation for a given user/network, the estimation problem is then, based upon the N_s sampled frames obtained in each of J independent sampling intervals of approximate duration, T, according to the above frame–based sampling approach, to temporally characterise the process of interest. Chapter 4 presented several examples of characteristics can be investigated depending upon monitoring objectives.

[11] For sampled inter–renewal times it is understood that $N_s > 0$.

[12] It is assumed that frame headers are accessible. This is reasonably assumed in practice as encryption is typically done higher up the protocol stack.

5.4 Related Work

Frame–based spectrum sensing is based upon work being done in estimation of network flow[13] characteristics (*e.g.*, flow size - number of packets in a flow.). Network flow estimation forms an important aspect of network traffic measurement which is essential for traffic engineering and accounting. However, given that the generation of statistics does not scale well with link speeds, the network measurement community has increasingly researched traffic sampling techniques, (*e.g.*, [174–181]).

While many routers currently support packet sampling approaches such as '1–in–N' or Bernoulli sampling, these approaches are well known to have severe limitations such as flow length bias. Flow length bias dramatically obscures the details of small flows, which may make up a lot of the flows in a given router. Several enhancements have been proposed in the literature, such as flow sampling, in which all packets belonging to several randomly selected flows are sampled. The problem with this approach is that look–ups must be performed on every packet, which can be resource–intensive. Other enhancements, such as the use of TCP sequence numbers, have been used to improve estimation of TCP flows [176]. In that technique, the presence of unsampled packets can be inferred through the byte count given in sequence number fields of sampled packets.

In this chapter, a similar approach is proposed for estimation of temporal spectrum occupancy parameters, through use of PLCP frame semantics with random sampling techniques for temporal occupancy characterization of users/networks of interest. To the best of the author's knowledge, there has been little work in this area, for spectrum occupancy characterization of targeted users/wireless networks in a DSA setting. Additionally, the proposed approach has several advantages over work done in current network measurement techniques:

- There is less correlation between the spectrum occupancy and the protocol data unit (PDU) length, the higher up the one goes in the network stack [122]. There is a more direct relationship between the PLCP frame size and the frame transmission time, than that for higher layer PDUs [122].

[13] A flow is generally defined as a set of packets with the same 5–tuple (IP protocol, source address, destination address, source port, destination port), with a fixed maximum inter–packet time,T_0.

- At the PLCP level, less processing is required for decoding PDUs compared to higher layers. This is critical in high speed links.

- Relationships between PDU length are very complex and dependent upon the higher layer protocol mechanisms such as fragmentation. This increases the processing required for modelling the relationship between the two parameters. Further, there may be multiple protocols at a given layer, and all models would need to be estimated. While there may be several protocols which utilise OSA, the overall number of models to consider would be less, reducing the complexity of the problem.

5.4.1 Estimating Inter–renewal Times and Flow Lengths

The problem of estimating inter–renewal times and the number of frames in the original point process based upon the randomly sampled subset of frames as formulated in the previous section, is closely related to the problem of sampling inversion [174, 175]. As noted, the proposed frame–based sampling inversion approach further involves several aspects not present in previous work on sampling inversion. However, several elements of the work done in this area can be applied to this problem. Therefore related work in sampling inversion is presented in the following.

Sampling inversion problems have been motivated through data traffic analysis study of communication networks, where information is conveyed through packets which can be grouped into flows. In the literature, information from packet headers are assumed accessible, which can be used to reconstruct flow statistics. Knowledge of flow characteristics is important for network operations and research, as it allows better understanding of data traffic characteristics. However, large data rate links and limited storage and processing resources limit the ability to capture and decode all packets for characterization, therefore leading to the use of packet and flow sampling techniques. Using the probabilistically sampled packets, the inversion problem of flow reconstruction, follows from networking literature.

In the literature most of the work has focussed upon estimating the original flow size distribution (*e.g.*, [174, 177, 181]). A decompounding framework has been investigated where

inference of the distribution of inter–arrival times between packets, based upon sampled data, is determined as a function of known probability density function for the number of original renewals between the i^{th} and $(i+1)^{th}$ sampled renewals conditioned on the number of sampled renewals [182–186]. Antunes and Pipiras [175] further investigated inference of inter–arrival times between packets from sampled data where the probability distribution of the number of original renewals conditioned on the number of sampled renewals must also be estimated. In addition to statistical estimation of flow characteristics, there has also been work on sampling techniques. These include the sample–and–hold approach [179, 180] and dual sampling [178]. A framework for random sampling of alternating renewal processes has also been investigated in [166].

5.4.2 Estimating PDU Length Distribution

Current wireless networks support a multitude of voice and data services with different characteristics, making multi–service traffic modelling very challenging. The literature illustrates many approaches based upon analytical and empirically–fitted representations for various single–service and multi–service scenarios, (*e.g.*, [163, 164]). Frost [187] and [188] provide excellent overviews of several popular parametric models, such as Renewal Traffic models (*e.g.*, Poisson Processes, Bernoulli Processes, Phase–type Renewal Processes), Markov and Markov–Renewal Models, Markov–Modulated models (*e.g.*, Markov–Modulated Poisson Processes, Transition–Modulated Processes), Fluid Traffic models, Autoregressive Traffic models and Long–range Dependent Traffic Models. In the literature such parametric models are used to fit collected data.

While such models can be useful for network traffic, inclusive of PDU lengths, as shown in [189], distribution of Data Link PDU lengths may not fit these models. [189] presented analysis of enterprise network traffic and provided a comparison of changes in traffic composition over a decade. It was noted that traffic composition was not only non–parametric but had shifted from trimodal to bi–modal distributed frame lengths, based upon traffic composition. Data Link PDU length histograms of the captured network data from UWI and WPI were compared to those in [189]. The histograms of the collected data from this study, seen in Figs 5.9 and 5.10, were also bi–modal further supporting the results obtained

in [189]. A key implication of these measurements was that the use of simple parametric estimation techniques may not be suitable, and in fact use of empirical distributions of the data may provide simple estimates of the frame length distribution.

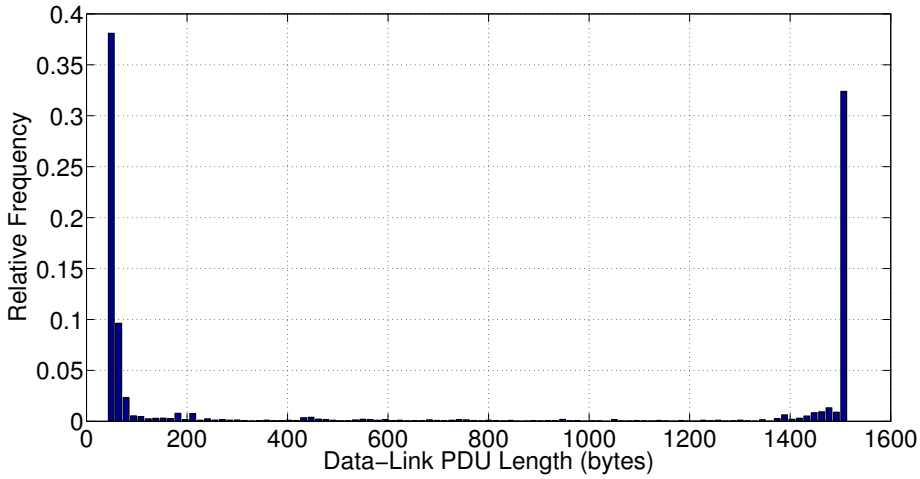

Figure 5.9: Histogram of Data–Link Layer PDU lengths for data collected at WPI from 8:00AM–4:10PM on 9^{th} December, 2013.

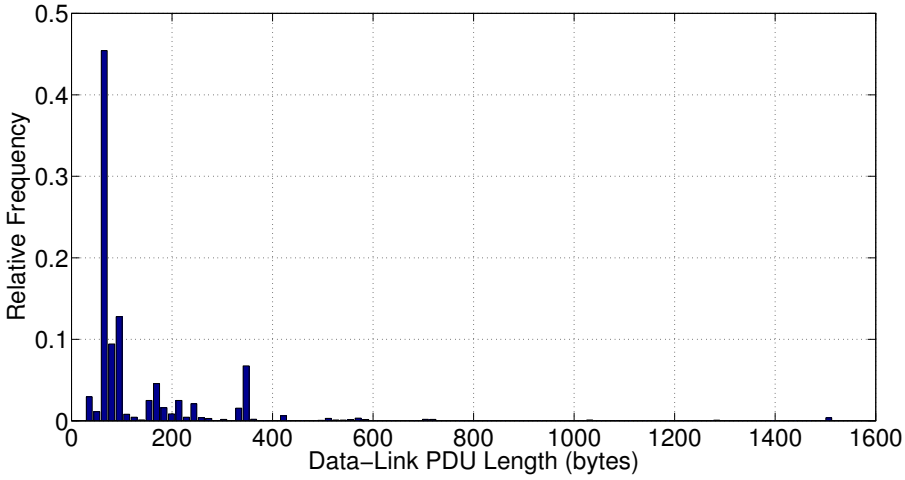

Figure 5.10: Histogram of Data–Link Layer PDU lengths for data collected at UWI from 9:00AM–5:05PM on 24^{th} January, 2013.

5.4.3 Estimating Frame Reception Model

A frame reception model is important, because it provides a probabilistic characterization of the impact of the channel on nominal transmission parameters. Therefore the actual time a user spends transmitting can be adjusted for channel effects, in estimating temporal occupancy characteristics. To the best of the author's knowledge, there is not much direct work into frame reception models, nor is there work on its use in temporal occupancy characterization. However, related work into estimating the reception model includes studies of the relationship between the PHY–layer frame length, data transmission rate and transmission time. Simple affine models can be used which assume constant bit rates in relating to frame lengths, (*e.g.*, [122]). Other RF propagation mechanisms such as multipath can also be incorporated into a suitable frame reception model [125]. These models also incorporate random effects, for example due to queueing and processing delays. In contrast to the assumption of a constant bit rate during the measurement interval, piece–wise constant bit–rate approximations such as the Markov–Modulated Fluid Traffic models [188], can be used. While such models are useful in variable bit–rate scenarios, such as expected in CR scenarios, in such studies the models focus upon the transition between data rates but do not specify relationships between the data rates, transmission times and frame lengths.

5.5 Frame–based Characterization of Temporal Occupancy

This section provides an overview of how frame sampling and sampling inversion techniques can be used for temporal characterization of occupancy for a given user. Specifically, frame sampling and sampling inversion, including the impact of missed start–of–frame delimiter detection is analysed. In demonstrating the concept of frame–based sampling, in this chapter several characteristics are investigated for temporal occupancy characterization:

1. The original distribution of the number of frames for the original frame arrival process (*i.e.*, associated with a given user/network);

2. The original distribution of the inter–renewal times, $F_{\tau_i} = P(\tau_i \leq t_i)$;

3. The frame reception model, which defines the relationship, $f(L_j, D_j)$, between nominal frame lengths, L_j, nominal data rates, D_j, and frame reception time, T_{Rx_j}.

The above characteristics facilitate estimation of the probability of the total "ON" time associated with a given user/network. Specifically, the frame length distribution, the frame reception model, and the distribution of the number of frames in the original frame arrival process can be used to estimate the distribution of the "ON" time of the transmitting device(s). The distribution of the difference between the inter–renewal time and the "ON" time can be used to estimate the "OFF" time of the transmitting device(s). It is noted, though, that some parameters can be alternatively obtained. For example, the duration between an end–of–frame delimiter and the next sampled start–of–frame delimiter can be used to estimate "OFF" times, or "ON" times could be estimated directly from the distribution of T_{RX_j}. However, use of the frame reception model provides a probabilistic characterization of the impact of the channel on frame reception, which can be used in assessing the confidence of the monitored device's behaviour based upon the the channel.

5.5.1 Original Number of Frames in T

The approach to estimation is adapted from [174, 175]. However, several adaptations are made to account for the missed detection of frames. First, consider the relationship between $X(t), X_m(t)$, and $X_s(t)$. Assuming stationarity, if $X(t)$ has rate λ, then if each frame can be independently missed with probability, p_m, $X_m(t)$ has rate $\lambda_m = \lambda(1 - p_m)$ [190, 191]. This is because the probability of retaining packets is given by $1 - p_m$. This implies that the rate of $X(t)$ can be recovered from $X_m(t)$ using:

$$\lambda = \frac{\lambda_m}{1 - p_m}. \tag{5.1}$$

The spectral densities of $X(t)$ and $X_m(t)$ are also related. If it is assumed that $X(t)$ is a simple and locally finite second order stationary point process, then:

$$\Gamma_{X_m}(\omega) = (1 - p_m)^2 \Gamma_X(\omega) + p_m(1 - p_m)\lambda, \tag{5.2}$$

where $\Gamma_X(\omega)$ and $\Gamma_{X_m}(\omega)$ are the spectral densities of $X(t)$ and $X_m(t)$, respectively. There-

fore, using Eqn (5.1) and (5.2):

$$\Gamma_X(\omega) = \frac{1}{(1-p_m)^2}\left(\Gamma_{X_m}(\omega) - p_m\lambda_m\right). \tag{5.3}$$

Using Eqn (5.3) it is therefore possible to recover the original process from the process which contains missed frames, assuming stationarity, and that frames are independently missed. Similarly, if the sampled process, $X_s(t)$, is now considered, then for simple random sampling:

$$\lambda_m = \frac{\lambda_s}{p_s}, \tag{5.4}$$

where λ_s is the rate of the sampled process. Further, if $X_m(t)$ is a locally finite second order stationary process, then the spectral densities of $X_m(t)$ and $X_s(t)$ are related as follows:

$$\Gamma_{X_m}(\omega) = \frac{1}{(p_s)^2}\left(\Gamma_{X_s}(\omega) - (1-p_s)\lambda_s\right), \tag{5.5}$$

where $\Gamma_{X_s}(\omega)$ is the spectral density of $X_s(t)$. Therefore, through Eqns (5.3)–(5.5), the original process can be recovered from the sampled process, and:

$$\Gamma_X(\omega) = \frac{1}{(1-p_m)^2(p_s)^2}\left(\Gamma_{X_s}(\omega) - (1-p_s)\lambda_s + p_m p_s\lambda_s\right). \tag{5.6}$$

This result demonstrates that useful information about the original arrival process can be obtained without any specific assumptions on the detailed structure of the original process, beyond the process being simple, locally finite, and second order stationary. Such assumptions can hold approximately for sufficiently short measurement intervals, $\mathbf{T}$.

5.5.2 Inter–arrival Time Estimation

The goal is to infer the distribution of the inter–renewal times from the sampled inter–renewal times. Since it is assumed that $X(t)$ is an inter–renewal process with interval distribution, $F_\tau(t)$, then it follows that $X_m(t)$ is also a renewal process with interval distribution, $F_{\tau_m}(t)$ being a random convolution of $F_\tau(t)$. The number of terms in the convolution is one more than the number of consecutively missed points, n. Clearly, $n \sim Geometric_0(p_m)$, (*i.e.*, $P(n=q) = p_m(1-p_m)^q$, $q = (0,1,\ldots)$). Therefore, $F_{\tau_m}(t)$ is given by:

$$F_{\tau_m}(t) = E\left[F_\tau^{(q+1)*}(t)\right] \tag{5.7}$$

where '^{q*}' specifies the q–fold convolution. The above result can be extended to the case of sampling by noting that a frame would not be used in estimation if the start–of–frame delimiter is either missed, or detected but the frame was not sampled. In this case the probability of these events is given by, $p = p_m + (1-p_m)(1-p_s)$. Thus, substitution of p for p_m in Eqn (5.7) gives the distribution of the inter–renewal times for both missed detection of start–of–frame delimiters and frame sampling. This result then allows for inversion of the observed inter–renewal times to determine the original distribution. First, taking the Laplace transform of Eqn (5.7) gives:

$$\begin{aligned} \tilde{F}_{\tau_m}(v) &= \sum_{q=1}^{\infty} p_m(1-p_m)^{q-1}\tilde{F}_{\tau}^{q}(v), \\ &= \frac{p_m\tilde{F}_{\tau}(v)}{1-(1-p_m)\tilde{F}_{\tau}(v)}, \end{aligned} \tag{5.8}$$

where $\tilde{F}_{\tau}(v)$ denotes the Laplace transform of $F_{\tau_m}(t)$. Therefore, inversion of Eqn (5.8) provides an estimate of the original inter–renewal time distribution with consideration of missed detection:

$$\tilde{F}_{\tau}(v) = \frac{\tilde{F}_{\tau_m}(v)}{p_m + (1-p_m)\tilde{F}_{\tau_m}(v)}. \tag{5.9}$$

Also, as before, substitution of p for p_m in Eqn (5.9) gives the distribution of the original inter–renewal times for both missed detection of start–of–frame delimiters and frame sampling. From Eqn (5.9), as well as the extensions for frame sampling, the relationships between the sampled and missed frames with the original frames are provided under the assumption of an infinite power series. In practice, the summation in Eqn (5.8) is not infinite, since $\mathbf{T} < \infty$. Therefore the finite series summation for a geometric series can be used:

$$\begin{aligned} \tilde{F}_{\tau_m}(v) &= \sum_{q=1}^{Q} p_m(1-p_m)^{q-1}\tilde{F}_{\tau}^{q}(v), \\ &= \frac{p_m\tilde{F}_{\tau}(v)\left(1-(1-p_m)^{Q}\tilde{F}_{\tau}^{Q}(v)\right)}{1-(1-p_m)\tilde{F}_{\tau}(v)}. \end{aligned} \tag{5.10}$$

For high frame detection rates or small sample rates the geometric series decays very quickly, and the finite approximation also holds. Such finite series approximations can be reverted to obtain expressions for the original frame statistics in term of the missed and

sampled frame statistics, for more complex process structures. In practice, series reversion algorithms can be used to obtain the series reversions of truncated forms of Eqns (5.8) and (5.10). An example is [192] which provides fast algorithms for power series reversion.

5.5.3 Frame Reception Model

Define the spectrum "ON" time, T_{Rx}, in terms of frame reception as a function of the frame length and frame transmission rate, L and D respectively:

$$T_{Rx} = f(L, D). \tag{5.11}$$

In the simplest case T_{Rx} can be defined in terms of the transmission time, T_{Tx}. For constant data rate, D *bps*, the time to transmit a frame of length L *bits* is given by: $T_{Tx} = \frac{L}{D}$ *s*. At the receiver, propagation effects such as multipath can cause signal spreading at the receiver [125]. Additionally, random frame processing times adds another delay to the frame reception time. Such effects are random in nature and add non–deterministic delays to the transmission time [122, 125]. Figs 5.3–5.6 presented examples of this, based upon collected data, for different levels in the network architecture. Denote this random delay for the j^{th} frame by V_j. Therefore, for the j^{th} frame, the frame reception time can be defined as follows:

$$T_{Rx_j} = T_{Tx_j} + V_j = \frac{L_j}{D_j} + V_j. \tag{5.12}$$

Considering data rate adaption mechanisms a piecewise formulation may be more appropriate for $N_o > 1$ frames, transmitted at different data rates to determine an average:

$$T_{Rx_{avg}} = \frac{1}{N_o} \sum_{i=1}^{N_o} \{T_{Tx_i} + V_i\} = \frac{1}{N_o} \sum_{i=1}^{N_o} \{\frac{L_i}{D_i} + V_i\}, \tag{5.13}$$

where L_i and D_i are the nominal length and data transmission rate for the i^{th} frame and V_i is the associated delay during propagation and processing. The length and rate information are typically found in protocol headers, and thus once decoded are known for a sampled frame. An estimate of the distribution of the nominal frame transmission time can be empirically derived from the sampled frames. Alternately, the empirically–derived joint distribution of the data rates and lengths could be used.

Given the 2–tuples, $(L_{p,i}, D_{p,i})$, obtained from the i^{th} of N_s randomly sampled frames, it is possible to estimate the prior PDF for the frame transmission time:

$$f_{T_{Tx}}\left(\frac{L_{p,i}}{D_{p,i}}\right) = P\left(T_{Tx} = \frac{L_{p,i}}{D_{p,i}}\right). \tag{5.14}$$

Using Eqn (5.13), it is easily seen that:

$$P\left(T_{Rx} = t\right) = P\left(T_{Rx} - \frac{L_{p,i}}{D_{p,i}} = t - \frac{L_{p,i}}{D_{p,i}}\right) = P\left(V_i = t - \frac{L_{p,i}}{D_{p,i}}\right) = f_V\left(t - \frac{L_{p,i}}{D_{p,i}}\right). \tag{5.15}$$

Therefore the problem reduces to estimation of the PDF for $V[i]$, $f_V(v)$. As discussed previously in Section 5.3, $f_V(v)$ can be approximated by uniform or normal distributions, among others.

In such cases, the distribution is defined using several parameters, and parametric estimation techniques such as maximum likelihood or Bayesian estimation can be used. If the form of the distributions are not known, then non–parametric techniques such as kernel density estimation or k–nearest neighbour estimation can be used. The performance of these techniques typically improves as observations increase. Since each sampled frame gives an observation of V, independently of which user is transmitting, it is reasonably assumed that the sample size would be sufficient for estimating $f_V(v)$.

Following determination of the frame reception model, probabilities of interest can be determined through the model. For example, based upon Eqn (5.13), for large N_o, by the Central Limit Theorem, the distribution of the total frame reception time for a finite renewal process is approximately normally–distributed (*i.e.*, $F_{T_{ON}} \sim N(\mu_{Rx}, \sigma^2_{Rx})$ [147]). $\mu_{Rx} = \sum_{j=1}^{N_o}\{E[T_{Tx_j}] + E[V_j]\}$ and $\sigma^2_{Rx} = \sum_{j=1}^{N_o}\{var[T_{Tx_j}] + var[V_j]\}$, where the sequences, $\{T_{Tx_j}\}$ and $\{V_j\}$ are independent and identically distributed[14]. Other temporal characteristics, such as those defined in Chapter 4, can be similarly determined. This data can be advantageous for spectrum management and compliance monitoring of non–deterministic CR networks.

[14]The Central Limit Theorem also specifies results similar to the i.i.d. case, but for non–identically distributed variables, and even further for dependent variables.

5.6 Experimental Results

This section summarises results obtained from investigating the proposed frame–based sampling inversion technique. The investigations were carried out via simulation using the previously measured data from WPI and UWI fit to an assumed Poisson Process model.

5.6.1 Effect of Sampling Ratio and Rate of Missed Detection on Process Rate Estimation

To investigate the effect of sampling ratio and the probability of missed detection on the simulated processes, $X(t)$, missed detection events were first simulated with varying probabilities, p_m, to create realizations of $X_m(t)$. The resulting realizations were then sampled with probability, p_s, to create $X_s(t)$. Using a group–based method, 1000 random samples were created from which the process rate was estimated for varying measurement durations, $\mathbf{T}$. The rate parameter was estimated based upon the observed average rate of packets, using Eqns (5.1)–(5.4). The variance of the estimates of the process rate was then determined. Fig 5.11 and Fig 5.12 illustrate the effect of the probability of missed detection and the sampling ratio, on the variance of the estimates obtained, when it was assumed that p_m was known[15]. The results suggest that performance in terms of the variance decreases for increasing rates of missed detection, p_m, and increases for increasing sampling ratios, p_s.

5.6.2 Effect of Sampling Ratio and Rate of Missed Detection on Distribution of Inter–renewal Times

The distribution of inter–renewal times was fit from the measured data. Following a similar approach to the previous set of experiments, the impact of missed frames and the sampling ratio were investigated. Figs 5.13–5.16 illustrate the comparisons for the UWI and WPI data, respectively. The graphs illustrated that the performance was comparable for estimating shorter inter–renewal probabilities, but that the tails of the distributions appeared to diverge from the actual value, for smaller effective sampling ratios. Given the

[15] p_s is known since it is the rate of sampling.

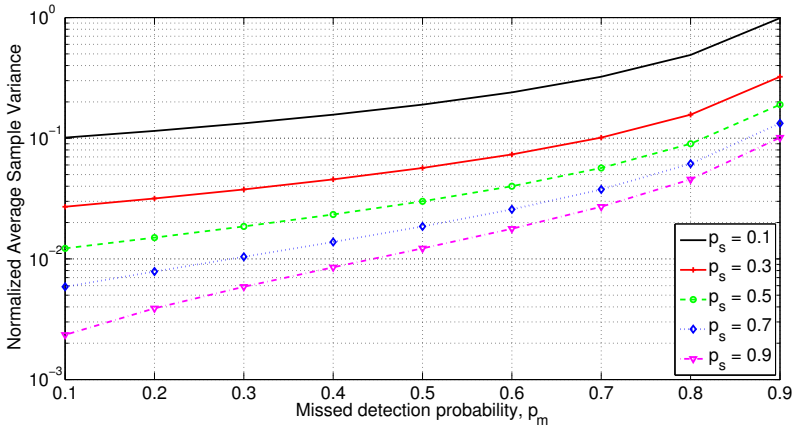

Figure 5.11: Effect of missed detection rate on estimation of the simulated Poisson process rate parameter for WPI, $\lambda = 45.215$ packets/sec, simulation time = 60 minutes, $|\mathbf{T}| = 2$ minutes. p_m is assumed known.

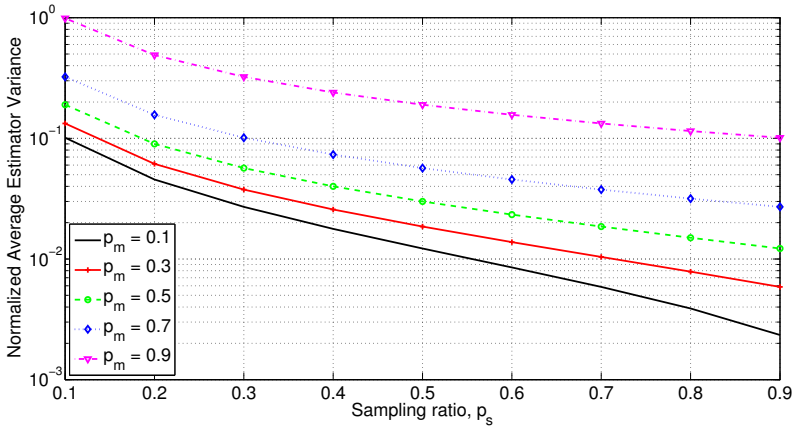

Figure 5.12: Effect of sampling ratio on estimation of the simulated Poisson process rate parameter for WPI, $\lambda = 45.215$ packets/sec, simulation time = 60 minutes, $|\mathbf{T}| = 2$ minutes. p_m is assumed known.

low probabilities for such events, these probabilities can reasonably be ignored.

5.6.3 Frame Reception Model

The frame reception model was estimated for the captured data for different effective sampling ratios. Fig 5.17 illustrates one realization at each effective sampling ratio, p_{eff} using 10 minutes of the UWI data, assuming a Gaussian distribution for the delays. As seen from the illustration, the variance decreased as the number of sampled frames increased.

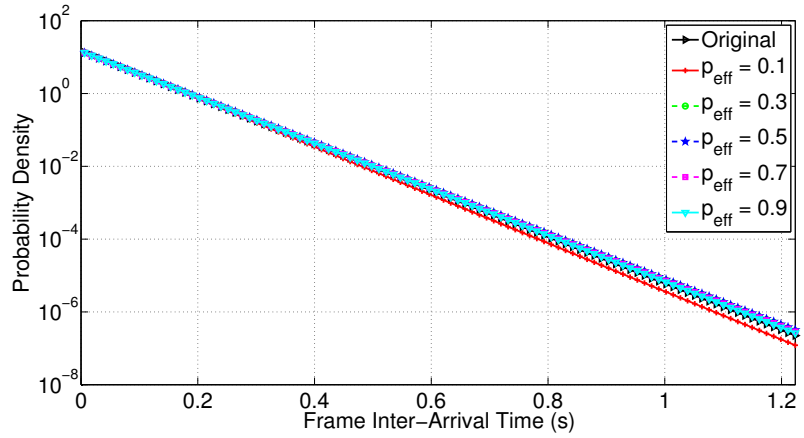

Figure 5.13: Effect of sampling ratio and missed detection on estimated inter–arrival time PDF for UWI data, effective sampling rate, $p_{eff} = p_s(1-p_m)$, simulation time = 60 minutes, $|\mathbf{T}| = 2$ minutes, binwidth = 12.3ms.

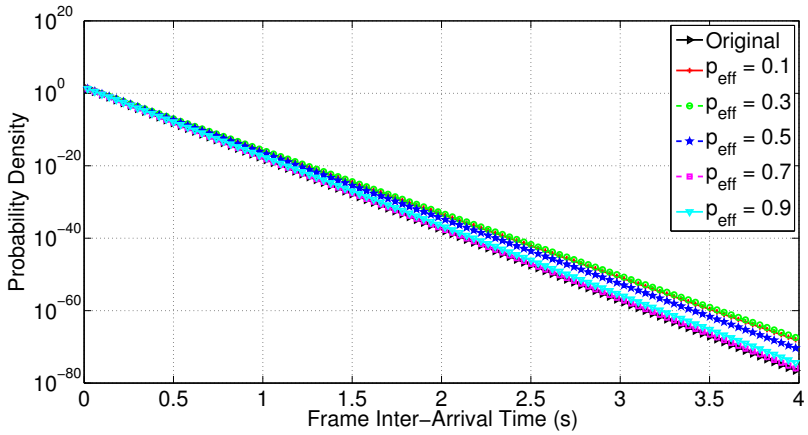

Figure 5.14: Effect of sampling ratio and missed detection on estimated inter–arrival time PDF for WPI data, effective sampling rate, $p_{eff} = p_s(1-p_m)$, simulation time = 60 minutes, $|\mathbf{T}| = 2$ minutes, binwidth = 40ms.

This suggests increased precision in the estimated frame reception model as the sample size increases, which is in line with sampling theory. Even for low effective sampling ratios, after about 100 frames, the variance decreased significantly. This demonstrates that after sufficiently sampled frames, the model approximation holds across the range of p_{eff}. Similar trends were observed for the WPI data.

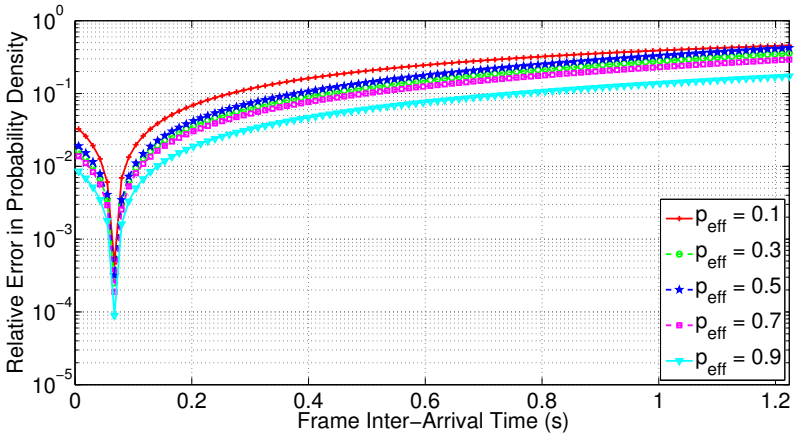

Figure 5.15: Relative error of estimated inter–arrival time PDF for UWI data, effective sampling rate, $p_{eff} = p_s(1 - p_m)$, simulation time = 60 minutes, $|\mathbf{T}| = 2$ minutes, binwidth = 12.3ms.

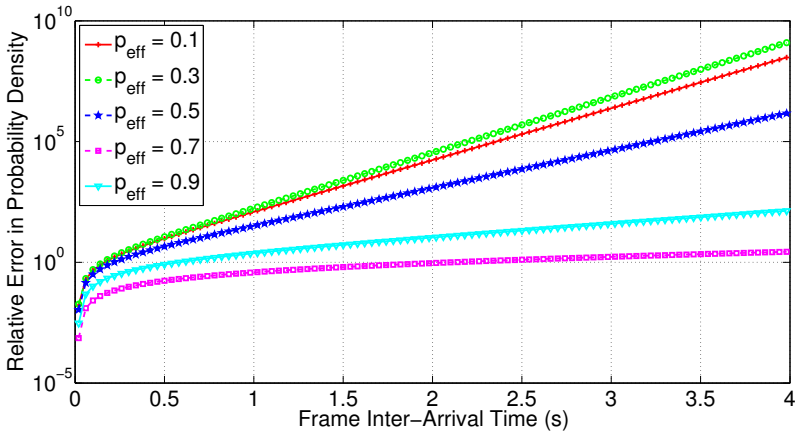

Figure 5.16: Relative error of estimated inter–arrival time PDF for WPI data, effective sampling rate, $p_{eff} = p_s(1 - p_m)$, simulation time = 60 minutes, $|\mathbf{T}| = 2$ minutes, binwidth = 40ms.

5.7 Conclusion

In this chapter, the frame–based random temporal sensing approach was introduced as a means of statistically modelling the temporal behaviour of users/networks of interest, identified through PLCP frame semantics. The approach was proposed as an alternative to existing techniques which have been proposed for spectrum security, such as primary user emulation, because of the need to probabilistically characterise the temporal behaviour in

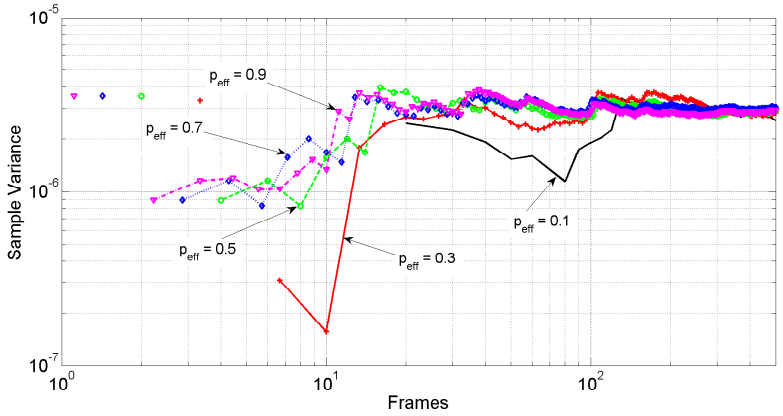

Figure 5.17: Convergence of frame reception model for different effective sampling ratios, p_{eff}, using UWI data, $|\mathbf{T}| = 10$ minutes.

coexistence DSA scenarios. This aspect of DSA coexistence is only now being explored by the DSA community, and thus there is limited work which focuses upon the aspects presented in this chapter.

In particular, the approach was investigated for estimating various temporal characteristics using simulations. Simulation parameters were derived from empirical measurements conducted at WPI and at UWI. The results illustrated the impact of missed detection and sampling ratios on the performance for estimation of various temporal parameters, under the assumption of Poisson process models. The results suggest that performance improved for higher sampling ratios. Further even for low sampling ratios, provided there were sufficient observations, the estimation of the models were very close.

Finally, a frame reception model was proposed for relating actual transmission times to frame reception times, to account for random channel effects in temporal characterisation. Results illustrated that with sufficient observations, the random temporal sensing approach performance improves as time elapses. Further, the estimator variances converges for all sample rates, if there are sufficient frame samples. This is therefore recommended for use in probabilistic characterisation of temporal occupancy, which is a key requirement for compliance monitoring in DSA networks.

Investigations utilised simulations for analysis. However, further work on this technique will demonstrate the application of this technique in actual DSA deployments, as DSA

technologies evolve and are deployed. The performance of the technique will also be investigated for other temporal occupancy models to provide a more diverse set of results on the performance in envisioned DSA scenarios.

Chapter 6

Distributed and Mobile Electrospace Sampling

6.1 Introduction

Cognitive radios are currently allowed to opportunistically operate within specified sub–bands, within geographically–specified regions. Monitoring networks therefore should be capable of monitoring across time, frequency, and spaces of interest. In the previous chapters in this dissertation, the investigated scenarios implicitly assumed sensor nodes: 1) did not cooperate; and 2) were stationary. In this chapter, those assumptions are removed, and random sensing approaches are expanded to include scenarios which involve both distributed and mobile spectrum sensing nodes. Further, scenarios are considered, in which the cognitive radios being sensed are also mobile. Specifically, random sensing in vehicular dynamic spectrum access (VDSA) networks is investigated.

Investigations in this chapter build upon research into convergence of distributed consensus algorithms, which aims to provide distributed mechanisms for distributed systems to arrive at similar estimates of a given parameter, as time elapses. The intent of such approaches is to provide a mechanism through which the techniques of the previous chapters can be improved through collection of spatial diversity. In this chapter, the approach is demonstrated through application to random spectral sensing. However, the approach can

be similarly applied to the other techniques studied for temporal characterization. While there has been much research into consensus algorithms, there has been limited investigation of realistic mobility models, and analysis has been focussed upon less realistic mobility models which are analytically tractable.

Work presented in this chapter, therefore contributes to the literature on distributed consensus algorithms through investigation of more realistic mobility models enabled through the use of bi–directionally–coupled simulators [193]. Additionally, current work into consensus algorithms is based upon consensus under conditions which may not hold within vehicular networks, particularly for where nodes travelling at typical vehicular speeds [1]. Therefore a distance–based approach is proposed, under which consensus is investigated.

Several aspects of this chapter also appear in publications developed for this dissertation: [88, 90, 95, 96].

6.2 Motivation

Distributed sensing techniques have been proposed in the spectrum sensing literature for several years, particularly to introduce spatial diversity. Spatial diversity is typically recommended for improving detection and estimation performance, by mitigating RF propagation effects such as fading. Additionally, through collaborative mechanisms, load sharing can be realised, in addition to reduced energy consumption per node, faster spectrum scanning, and increased accuracy. Much of the literature on collaborative spectrum sensing currently focuses upon one–hop collaboration, which typically implies high node density networks for distributed sensing across regions of interest. In [58], distributed fusion techniques were developed for multi–hop large networks, which used consensus–based techniques to derive distributed mechanisms to converge to globally–optimal solutions using one–hop communications.

In contrast, mobile sensing has not been as extensively researched, even though it has been used in spectrum management strategies for some time. The use of distributed, but fixed, monitoring nodes has been regarded as insufficient for the spectrum management re-

[1] Also mobile nodes can be either sensed or sensing nodes.

quirements of emerging wireless technologies, including OSA–based technologies for several reasons [24, 194]:

- Many modern communication services are deployed in higher frequency bands, up to 6 GHz, which have shorter propagation ranges, thus requiring denser fixed node deployment.
- For duplex communications such as GSM, UMTS and WiMAX, it is typically very difficult to monitor the uplink frequencies.
- It is difficult to detect directional transmissions, as well as technologies which use techniques such as sectorization and beam–forming.
- Cellular technology and frequency reuse techniques imply lower transmit powers and smaller cell sizes, which further decrease the ease of transmission detection.
- Local communications such as wireless LANs and UWB are currently unable to be detected with the current network.

A fixed network would need to be very dense in areas of interest in order to detect transmissions such as those listed above. The non–deterministic behaviour of CR networks presents another challenge for detection. However, strategic deployment of mobile networks offers an opportunity to achieve monitoring objectives for cases including those above [24, 35, 36, 194]. Even with deployment of mobile and fixed monitoring nodes, one emerging area of importance, which would represent a challenge to current monitoring paradigms is that of intelligent transportation systems (ITS). ITS are currently being developed and deployed with increasing functionality, and demand for wireless spectrum for service delivery.

Consequently, ITS have recently attracted considerable interest from both academia and industry. Research conducted by the wireless networking and transportation communities has highlighted the potential of vehicular networks to revolutionise transportation systems through the provision of a communications infrastructure that can facilitate the future deployment of applications for accident avoidance/mitigation, traffic efficiency, and infotainment. In response to the increasing ubiquity envisioned in vehicular communications, wireless spectrum has also been allocated in support of ITS. For example, roughly 75

MHz and 30 MHz of spectrum have been allocated at around 5.9 GHz in the United States and Europe, while 10 MHz of spectrum at around 700MHz has been allocated in Japan for ITS applications.

However, the range of potential vehicular applications [195] and recent investigations (*e.g.*, [196]) suggest the inability of the current allocations to support the significant increase in the bandwidth requirements from prospective ubiquitous vehicular communications applications in the envisioned ITS infrastructure [197]. ITS applications will most likely use a complement of two or more of the following vehicular communications categories: Vehicle-to-Vehicle (V2V), Vehicle-to-Roadside (V2R) and Vehicle-to-Infrastructure (V2I). Of the three, V2V is the most challenging, and is generally supported via wireless spectrum allocated for DSRC. While it is still too early to determine if DSRC would provide sufficient spectrum for the growing demand for V2V applications, it is envisioned that it would be relatively difficult to obtain additional wireless spectrum allocations dedicated to vehicle communications.

Consequently, vehicular dynamic spectrum access (VDSA) [198, 199] was proposed as a possible approach to identify wireless spectrum opportunities for offloading some of the non–safety–related bandwidth demands from dedicated channels for vehicle communications. VDSA is based upon a DSA paradigm for dynamically obtaining additional spectrum to be used in vehicular communications. VDSA represents perhaps one of the more complex use cases for CR operation. Considering the dynamic topologies in combination with the non–deterministic radio operation, traditional monitoring systems may not offer the level of flexibility and adaptability required for such highly dynamic and stochastic vehicular environments [198–200].

In this chapter focus is thus upon the use of both distributed and mobile spectrum sensing for monitoring such CR networks. Specific contributions are as follows:

1. A framework for distributed random spectral sensing is presented for analysis of spectrum occupancy estimation in heterogeneous wireless access networks, such as in envisioned DSA scenarios.

2. A theoretical performance bound on spectrum occupancy estimation is derived for

random spectral sensing, and extended to distributed random spectral sensing.

3. Average consensus algorithms are presented for use in distributed and mobile random spectrum sensing, and a distance–based approach is proposed for use in average consensus in vehicular networks.

4. Experimental results are presented for several compliance monitoring scenarios for DSA networks, including extension of work into mobile consensus analysis using bi–directionally coupled simulations. To the best of the author's knowledge, there has been limited work using models representing realistic scenarios for investigation of average consensus.

The rest of this chapter is organised as follows: In Section 6.3 an overview of the sensing signal model for distributed monitoring for compliance monitoring is provided, followed by a performance analysis of distributed spectrum sensing based upon misclassification errors in Section 6.4. Next, Section 6.5 presents mobile spectrum sensing and introduces the distance–based approach for consensus in vehicular networking. Experimental results are presented in Section 6.6, for use of the distributed and mobile sensing in several envisioned compliance monitoring tasks for DSA networks. Finally there are concluding remarks in Section 6.7.

6.3 Sensing Signal Model

Consider a wide frequency band heterogeneous radio access scenario in which there are both primary and secondary users potentially operating. There are also L spatially distributed spectrum sensors which constitute the spectrum monitoring network. Each spectrum sensor has time and frequency sensing resolutions specified by Δ_t and Δ_f respectively. For a single sensor, the sensing objective is to statistically model the spectrum occupancy for spectrum $F = [f_0, f_0 + N_f\Delta_f]$ for time $T = [t_0, t_0 + MN_t\Delta_t]$, where time is slotted into N_t frames with m time samples per time slot, $\Delta_f \ll F$ and $\Delta_t \ll T$. Consider a slotted frequency segmentation structure, where F is divided into N_f non–overlapping narrowband subchannels, with center frequencies $\{f_i\}_{i=1}^{N_f-1}$.

Now assume that there are K_p active primary users and K_s active secondary users during the measurement interval, with transmitted signals given by $s_k(t),\ k \in \{1, \ldots, K_p + K_s\}$. The signal from the k^{th} transmitter propagates to the l^{th} sensor through a wireless fading channel with channel impulse, $h_{k,l}(t), l \in \{1, \ldots, L\}$. $h_{k,l}(t)$ may be frequency selective over F. However, it is assumed that the channel slowly varies over the measurement interval and can thus be treated as time–invariant during the measurement time. The discretised signal received by the l^{th} sensor can therefore be expressed as an $M \times 1$ vector, $\mathbf{r}_l = [r_l[1], \ldots, r_l[M]]^T$, such that:

$$r_l[m] = \sum_{k=1}^{K_p+K_s} h_{k,l}[m] * s_k[m] + w_l[m] \tag{6.1}$$

where '$*$' indicates convolution, $m \in \{1, \ldots, M\}$, and $w_l(t) \sim \mathcal{N}(0, \sigma^2)$. The received signal can be represented in the spectral domain using the Discrete Fourier Transform (DFT) matrix, $\mathbf{W}_{N_f}$ [121]:

$$\tilde{\mathbf{r}}_l = \mathbf{W}_{N_f}\mathbf{r}_l = \sum_{k=1}^{K_p+K_s} \tilde{\mathbf{h}}_{k,l} \circ \tilde{\mathbf{s}}_k + \tilde{\mathbf{w}}_l \tag{6.2}$$

where the 'tilde' operator denotes the DFT transformed equivalents of the time signals in Eqn (6.1) and '$\circ$' represents the Hadamard product. In general, for the DFT, although $M \neq N_f$, the vector lengths can be appropriately adjusted using zero–padding or truncation of the time signals [121]. The general received signal model can therefore be written as:

$$\tilde{\mathbf{r}}_l = \tilde{\mathbf{H}}_l\tilde{\tilde{\mathbf{s}}}_l + \tilde{\mathbf{w}}_l \tag{6.3}$$

Two cases of the general signal model in Eqn (6.3) can be considered: 1) Known channel state information (CSI) and 2) Unknown CSI. Generally the channel information is unknown, so signals are lumped together:

$$\tilde{\mathbf{H}}_l = \mathbf{I}_{N_f} \tag{6.4}$$

$$\tilde{\tilde{\mathbf{s}}}_l = \sum_{k=1}^{K_p+K_s} \tilde{\mathbf{h}}_{k,l} \circ \tilde{\mathbf{s}}_k \tag{6.5}$$

where I_{N_f} is the $N_f \times N_f$ identity matrix. If the channel information is known then:

$$\tilde{\mathbf{H}}_l = \left[diag(\tilde{\mathbf{h}}_{1,l}), \ldots, diag(\tilde{\mathbf{h}}_{K_p+K_s,l}) \right] \tag{6.6}$$

$$\tilde{\tilde{\mathbf{s}}}_l = [\tilde{\mathbf{s}}_1, \ldots, \tilde{\mathbf{s}}_1] \tag{6.7}$$

Therefore each sensor is tasked with estimating $\tilde{\tilde{\mathbf{s}}}_l$ given $\tilde{\mathbf{r}}_l$ as shown in Eqn (6.3). This signal model forms the basis for the work presented in this chapter. Estimation of $\tilde{\tilde{\mathbf{s}}}_l$ provides the basis for spectrum characterization. Earlier chapters described investigations of several characterization tasks based upon the above signal model, from the perspective of individual sensor operation. The following sections describe the use of spatial diversity in accomplishing characterization, particularly for use in monitoring DSA operation.

6.4 Collaborative/Distributed RSS

Under the random spectral sampling framework from Chapter 3, in order to benefit from spatial diversity, first assume that no CSI is available, (*i.e.*, Eqns (6.4)–(6.5) are applicable). Each of the L spectrum monitoring devices locally estimates the spectrum occupancy using RSS:

$$\hat{u}_l = u + \epsilon_l, l \in \{1, \ldots, L\}, \tag{6.8}$$

where ϵ_l represents the mis–classification error (*i.e.*, bias), primarily due to sampling and detection errors, while u and $\hat{u}$ are the true and estimated bandwidth occupancies. The bias can be estimated by considering the probability of classification errors for the DFT of the received signal vector, $\tilde{\mathbf{r}}_l$. Denote the classification vector as $\mathbf{c}_l \in \{0,1\}^{N_f \times 1}$. Each element in the classification vector is 1 if the sub–channel is occupied, and 0 if it is not. Detection approaches in the literature, such as Neyman Pearson detection, or use of fixed thresholding, can be used to obtain $\mathbf{c}_l$ from $\tilde{\mathbf{r}}_l$.

The performance of each detection approach can be compared through the false alarm and missed detection probabilities, p_{fa} and p_{md}, respectively. For a given spectrum occu-

pancy, μ, the number of unoccupied sub–channels mis–classified as occupied:

$$N_- \sim Binomial(N_f(1-\mu), p_{fa}). \tag{6.9}$$

Similarly, the number of occupied sub–channels mis–classified as unoccupied:

$$N_+ \sim Binomial(N_f\mu, p_{md}). \tag{6.10}$$

Thus, using Eqn (3.1), the bias resulting from mis–classification errors is given by, $\epsilon_l = \frac{N_- - N_+}{N_f}$. For sufficiently large N_f, the distribution of the mis–classification errors is approximately Normal [147]. Based upon this, it therefore follows that $\epsilon_l \sim \mathcal{N}(\mu_\epsilon, \sigma_\epsilon^2)$, where:

$$\mu_{\epsilon_l} = E\left[\epsilon_l\right] = E\left[\frac{N_- - N_+}{N_f}\right] = (1-\mu)p_{fa} - \mu p_{md}, \tag{6.11}$$

and

$$\sigma_{\epsilon_l}^2 = var\left(\epsilon_l\right) = var\left(\frac{N_- - N_+}{N_f}\right) = \frac{(1-\mu)(1-p_{fa})p_{fa} - \mu p_{md}(1-p_{md})}{N_f}. \tag{6.12}$$

Taking the global average gives:

$$\hat{u}_{Global} = \sum_{l=1}^{L} \hat{u}_l = u + \sum_{l=1}^{L} \epsilon_l = u + \epsilon_{Global}. \tag{6.13}$$

If there is correlation between the sensors, then averaging over L sensors implies that [147]:

$$\epsilon_{Global} \sim \mathcal{N}\left(\frac{1}{L}\sum_{l=1}^{L}\mu_{\epsilon_l}, \frac{\sum_{l=1}^{L}\sigma_{\epsilon_l}^2}{L^2} + \frac{1}{L^2}\sum_{l=1}^{L}\sum_{k>l}^{L} cov(\epsilon_l, \epsilon_k)\right). \tag{6.14}$$

If independence is assumed, then $cov(\epsilon_l, \epsilon_k) = 0$ and averaging over L sensors gives a lower bound on the variance under independent sampling. The resulting global mis–classification error is thus:

$$\epsilon_{Global} \sim \mathcal{N}\left(\frac{1}{L}\sum_{l=1}^{L}\mu_{\epsilon_l}, \frac{\sum_{l=1}^{L}\sigma_{\epsilon_l}^2}{L^2}\right). \tag{6.15}$$

Therefore through spatial diversity, the global average can reduce the variance and bias components due to mis–classification. Generalizations to the above formulation can be

used for analysis of more complex scenarios. For example, it was assumed that the false alarm and missed detection probabilities are independent and identically distributed over the classification vector. In practice, these probabilities may not be identically distributed across the sub–channels. Also, for wideband channels, sub–channels may be dependent. For non–identical distribution of p_{fa} and p_{md} in each interval, the Poisson Binomial distribution may be alternatively used [201]. This defines the probability distribution for the sum of independent, non–identically distributed Bernoulli trials. Similarly, bounds such as the Chernoff bound can be used for dependent and non–identically distributed probabilities. In each case, through spatial diversity, global averaging improves the estimates.

One way to achieve the global averaging function is via a centralised approach, whereby a designated sensing unit collects local estimates and then computes the global value. However, such a topology is sensitive to node failure and may further incur heavy communication costs in transmitting to the central node. If the network is a multihop sensing network, extra routing information may also be required, which makes the situation even worse.

An alternative approach proposed in the literature, involves the use of the average–consensus technique [202], which is useful for distributed coordination of mobile autonomous agents. This technique was used in [58] for collaborative compressed wideband sensing. Similarly, average consensus techniques can be used for random sensing. The goal is to design a distributed and decentralised occupancy estimation approach which is scalable to the monitoring network size, L, and where multi–hop routing is avoided through one–hop broadcasting among neighbouring sensor nodes.

Adopting notation from [202], the average consensus problem can be used to describe the problem as follows. Let $\mathcal{G} = (\mathcal{V}, \mathcal{E})$ be an undirected connected graph, with node set $\mathcal{V} = \{1, \ldots, L\}$ and edge set $\mathcal{E}$, where each edge $\{k, l\} \in \mathcal{E}$ is an unordered pair of distinct nodes which are within one–hop communications range of each other. Now, let $\hat{u}_l(0)$ be the occupancy estimate associated with the l^{th} sensor node at time, $t = 0$. Then the (distributed) average consensus problem is to compute the average, $\frac{1}{L}\sum_{l=1}^{L} \hat{u}_l(0)$ at every node, through local communication and computation on the graph, $\mathcal{G}$. Each sensor node broadcasts $\hat{u}_l(t)$ to its neighbours, $\mathcal{N}_l := \{k : (k, l) \in \mathcal{E}\}$, and further updates itself each time step by addition of a weighted sum of local discrepancies [202]:

$$\hat{u}_l(t+1) = \hat{u}_l(t) + \sum_{k \in \mathcal{N}_l} w_{kl}(\hat{u}_k(t) - \hat{u}_l(t)), \tag{6.16}$$

where w_{kl} is a weight associated with the edge (k, l). Since $\mathcal{G}$ represents an undirected graph, $w_{kl} = w_{lk}$. In [202] design rules are discussed which can provide values for the weights. Properly chosen weights guarantee that:

$$\lim_{t \to \infty} \hat{u}_l(t) = \frac{1}{L} \sum_{k=1}^{L} \hat{u}_k(0), \forall l \in \{1, \ldots, L\}. \tag{6.17}$$

Eqn (6.17) implies that local one–hop communications can guarantee that each sensor node obtains the averaged bandwidth occupancy of the multi–hop network represented by $\mathcal{G}$. The above approach can further be extended to the stratification technique proposed for RSS. To accomplish this, consider the distance matrix, $\mathbf{D}$, calculated in Section 3.5.1 using the DistMat algorithm. Due to symmetry, and noting that the distance along the main diagonal is always 0, the lower triangular portion of $\mathbf{D}$, (*i.e.*, excluding the main diagonal) uniquely defines the distance matrix. Therefore consider the distance vector formed by stacking columns from the lower triangular portion:

$$\mathbf{d} = [D(2,1), \ldots, D(N_f,1), D(3,2), \ldots, D(N_f,2), \ldots, D(N_f, N_f-1)]^T. \tag{6.18}$$

Clearly, $\mathbf{d} \in \mathbb{R}^{0.5(N_f-1)^2 \times 1}$. Using the average consensus technique described previously, each node can obtain the averaged distance matrix for the multi–hop network represented by $\mathcal{G}$. Each node can then locally compute spectral strata using the MatSearch algorithm described in Section 3.5.1. Following this, each node can then compute bandwidth occupancy using RSS and use average consensus, to obtain the global average. However, this approach increases the communication overhead, and thus a cost–benefit analysis would be necessary to evaluate if the gain achieved justifies the extra overhead.

6.5 Mobile RSS

Mobile sensing builds on the work in the previous section. In mobile sensing, consensus can be investigated in the context of a dynamic topology. Mobile RSS builds on

work presented in [203], as well as more recent work presented in [204]. Average consensus was investigated in a network with dynamically changing topology, where it was shown that use of suitably–defined weights guarantees convergence of time–varying communication graphs which are jointly connected [203]. In general, for mobile networks such as vehicular networks, this condition may not hold and there would therefore be no guarantee of convergence. Further, in much of the research into average consensus, it is assumed that the initial measurements used for average consensus do not change. This may not be the case for monitoring a dynamic CR network, particularly when the sensor network is multi–hop in nature. In such cases, convergence is also not guaranteed.

In [204] theoretical analysis of the convergence speed of gossip algorithms for random mobility models, was investigated using Markov chain analysis. It was seen that different mobility patterns can have different effects on the convergence behaviour of the network. However, mobility models for more realistic node motions such as in vehicular networks, need to be considered. In particular, vehicle motion is usually constrained to roadways within a geography, which can impact the manner in which messages are propagated through the network. To address vehicular scenarios, a distance–based approach is investigated for constraining the network size for convergence. In such realistic cases, analytical investigation may not be tractable. Therefore, analysis is performed using a bi–directionally coupled vehicular simulator to analyze convergence along a portion of the I–90 in Massachusetts. The simulation draws upon previously collected spectrum occupancy data.

The problem is similarly described as in the distributed case, but with consideration of time–varying aspects. In this case, consider the representation of the time–varying communication monitoring network. Let $\mathcal{G}(t) = (\mathcal{V}, \mathcal{E}(t))$ be an undirected connected graph, with monitoring nodes $\mathcal{V} = \{1, \ldots, L\}$ and edge set $\mathcal{E}(t)$, where each edge $\{k, l\} \in \mathcal{E}(t)$ is an unordered pair of distinct nodes which are within one–hop communications range of each other at time t. Let $\mathcal{N}_l(t) = \{k \in \mathcal{V} | \{k, l\} \in \mathcal{E}(t)\}$ denote the set of neighbours of the l^{th} node at time t. Define $d_l(t) = |\mathcal{N}_l(t)|$ be defined as the degree of the l^{th} measurement node at time t. $\mathcal{G}_i = (\mathcal{V}, \mathcal{E}_i), i \in \{1, \ldots, r\}$ defines a finite collection of graphs with common vertex set, $\mathcal{V}$. If the union $\mathcal{G} = \bigcup_{i=1}^{r} \mathcal{G}_i = (\bigcup_{i=1}^{r} \mathcal{E}_i, \mathcal{V})$, is a connected graph[2], then $\{\mathcal{G}_i\}_{i \in \{1,\ldots,r\}}$ is

[2]A graph, $\mathcal{G} = (\mathcal{V}, \mathcal{E})$, is connected if for any pair of vertices, k and l, there exists a sequence of edges

defined as jointly connected [203].

At $t = 0$, the l^{th} measurement node has state, $x_l(0)$. After each step, nodes update their state according to the distributed linear iterative combination of its own state with those of its instantaneous neighbour set:

$$x_l(t+1) = W_{ll}(t)x_l(t) + \sum_{k \in \mathcal{N}_l(t)} W_{kl}(t)x_k(t), l \in \{1, \ldots, L\}, \tag{6.19}$$

where $W_{kl}(t)$ is the linear weight on $x_k(t)$ at the l^{th} node. If we set $W_{kl}(t) = 0$ for $k \notin \mathcal{N}_l(t)$, then the iterative procedure can be expressed in vector form as follows:

$$\mathbf{x}(t+1) = \mathbf{W}(t)\mathbf{x}(t), \tag{6.20}$$

where $\mathbf{x}(0) = [x_1(0), \ldots, x_L(0)]^T$ is the initial condition, $\mathbf{x}(t) = [x_1(t), \ldots, x_L(t)]^T$, and $\mathbf{W}(t) \in \mathbb{R}^{L \times L}$. The t–step transition matrix is then defined as $\mathbf{\Phi}(t) = \prod_{\tau=0}^{t-1} \mathbf{W}(\tau)$. Therefore, $\mathbf{x}(t) = \mathbf{\Phi}(t)\mathbf{x}(0)$. [203] discusses the use of maximum–degree weights or Metropolis weights to guarantee convergence, provided that the time–varying communication graphs are jointly connected. For a general mobile network this may not be the case, given the possibly infinite possible set of graphs. A distance–based approach is suggested to establish joint connectivity within a bounded region, for convergence.

The distance–based approach is part of a distance–based knowledge management approach proposed in [88] for vehicular dynamic spectrum access. The main principle behind this approach is that RF propagation at frequencies of interest, (*e.g.*, UHF/VHF), implies similar occupancy across a bounded geographical extent. Within this bounded region, there may be both mobile and fixed monitoring nodes, which form a bounded–size network. In this network, mobile nodes are constrained to move along various routes, (*i.e.*, representative of road networks). Fig 6.1 illustrates the distance–based concept.

Along these routes, the paths are discretised in space, such that each location on any road is one of a finite amount number of locations that mobiles can be located at. While a vehicle transits within the bounded region, the occupancy is assumed to be stationary. Under these constraints, it can reasonably be assumed that networks inclusive of mobile

(*i.e.*, a path) $\{(k, k_1), (k_1, k_2), \ldots, (k_{s-1}, k_s), (k_s, l)\} \in \mathcal{E}$.

nodes are jointly connected. It is also assumed that the rate at which mobile nodes enter and exit the region is, on average, constant. A consequence of this is that the set of fixed nodes $\{\beta_j\}$ plus possible locations of mobile nodes, $\{\theta_j\}$, represent a finite set, $\mathcal{V}$ of measurement nodes.

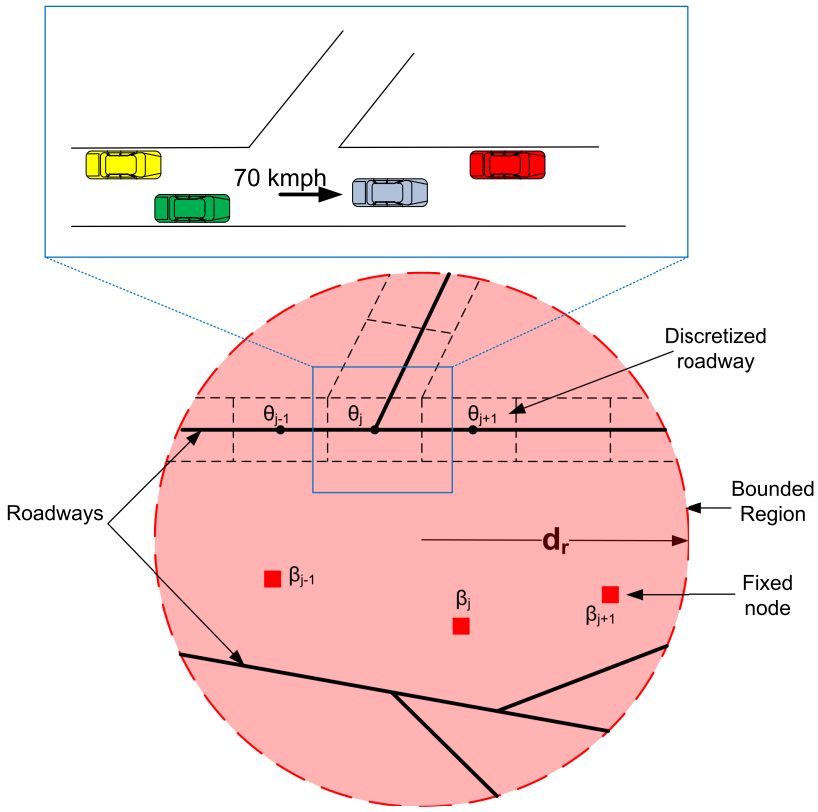

Figure 6.1: Distance–based bounding of sensing network for distributed mobile spectrum sensing. Nodes are assumed to be possibly connected only to other nodes within the bounded region. $\{\theta_i\}$, the centroids of the road segments, represent the possible locations of mobile nodes within the bounded region. $\{\beta_j\}$ are the fixed node locations.

Hence, there are only a total of r possible communications graphs, $\{\mathcal{G}_i\}_{i\in\{1,\ldots,r\}}$. If it is assumed that they are jointly connected within the bounded region, then as shown in [203], convergence is guaranteed for use of maximum–degree weights:

$$W_{kl} = \begin{cases} \frac{1}{L}, & if\ \{k,l\} \in \mathcal{E}(t), \\ 1 - \frac{d_l(t)}{L}, & if\ k = l, \\ 0, & otherwise, \end{cases} \tag{6.21}$$

or use of Metropolis weights:

$$W_{kl} = \begin{cases} \frac{1}{1+max\{d_k(t),d_l(t)\}}, & if\ \{k,l\} \in \mathcal{E}(t), \\ 1 - \sum_{\{l,m\} \in W_{lm}}, & if\ k = l, \\ 0, & otherwise. \end{cases} \tag{6.22}$$

6.6 Experimental Results

In this section, results are presented for CRSS and mobile RSS. First CRSS, is examined via simulations and evaluated in terms of the mis–classification error random variable, which provides an estimate of RSS performance. Next, CRSS was used for estimating the tail distribution of the amplitude power distribution (APD) for use in compliance monitoring for DSA. Finally, results on the use of mobile RSS are presented, based upon a study of VDSA.

6.6.1 CRSS Mis–classification Performance

CRSS was examined for $K_p = 32$ and $K_s = 32$ primary and secondary users respectively, across 32 equal–bandwidth channels. The users were randomly located within a $1kmkm$ grid. Frequency–selective fading was modelled using time-delayed taps with independent Rayleigh fading gains on the taps. Additionally, a path loss exponent of 4 was assumed under a free space path loss model. Different occupancy profiles were randomly assigned to the users to create different RF environment scenarios for testing RSS. $L \in \{1, 2, \ldots, 10\}$ sensors were randomly deployed in the grid for sensing. Each sensor used RSS individually to estimate the bandwidth occupancy in the presence of white Gaussian noise. The estimated occupancies were then compared to the true occupancy for each scenario. Mis–classification errors were investigated by varying the decision thresholds for determining the classification vectors, $\mathbf{c}_l$, for each sensor. This was repeated 1000 times for each scenario, and the resulting data was used to compare the performance of CRSS. Figs 6.2–6.7 illustrate results of the investigations.

In Figs 6.2–6.3 the average mis–classification error, μ_{ϵ_l}, was compared for different band-

width occupancy scenarios, for various false alarm and missed detection probabilities. The results demonstrated that μ_{ϵ_l} was fairly constant across different occupancy scenarios. However, performance improved as either false alarm or missed detection probabilities decreased. A similar trend was observed for the variance of the mis–classification error, as shown in Figs 6.4–6.5.

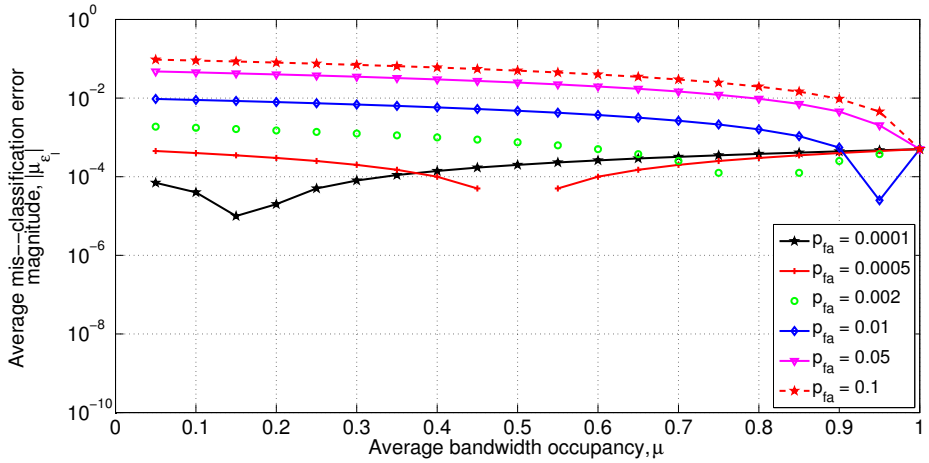

Figure 6.2: Average mis–classification error for RSS sensor, $p_{md} = 0.0005$.

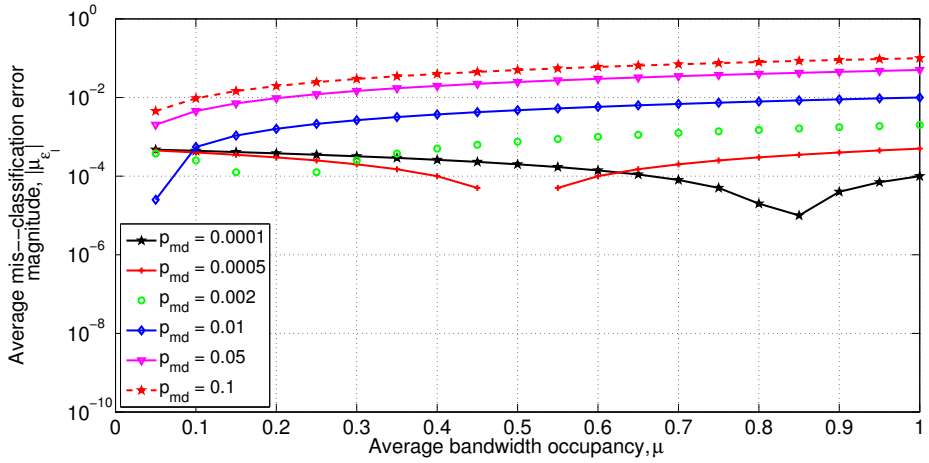

Figure 6.3: Average mis–classification error for RSS sensor, $p_{fa} = 0.0005$.

Figs 6.6–6.7 illustrated the impact of using the average consensus algorithm on the RSS estimates. The results suggest that use of average consensus reduces the variance of the

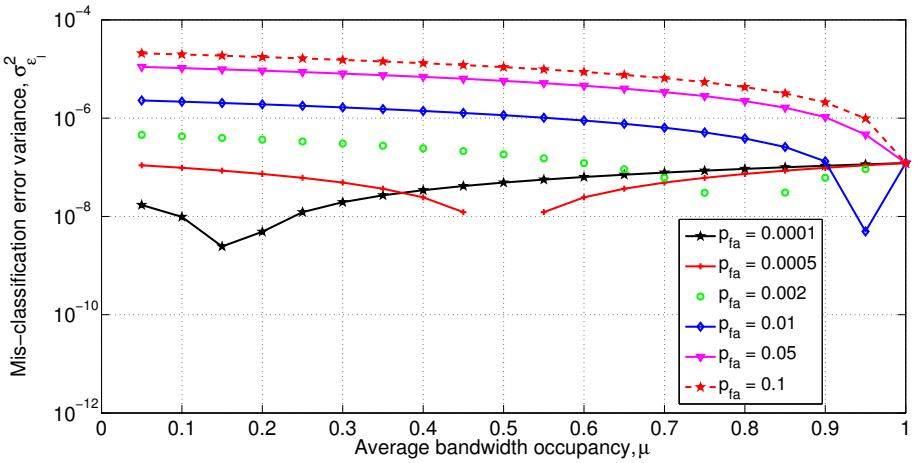

Figure 6.4: Variance of mis–classification error for RSS sensor, $p_{md} = 0.0005, N_f = 4096$.

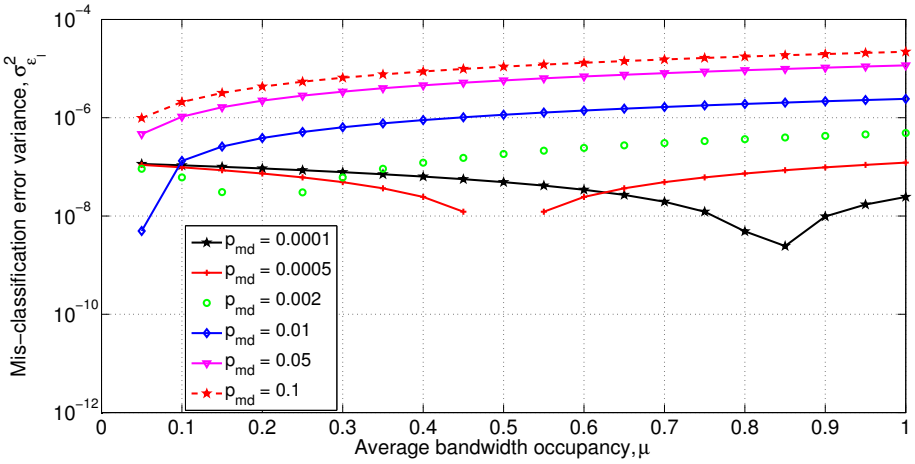

Figure 6.5: Variance of mis–classification error for RSS sensor, $p_{fa} = 0.0005, N_f = 4096$.

mis–classification error, which in turn improves the precision of the bandwidth occupancy estimate achieved via RSS. the results further support the analysis which shows that the precision increases with more sensors. However, increasing L would also increase the network size, consequently increasing the convergence time for the algorithm. The results also show that the variance is greater than the theoretical bound attainable through independent sampling. The additional variance is due to covariance between the occupancy estimates for the sensors.

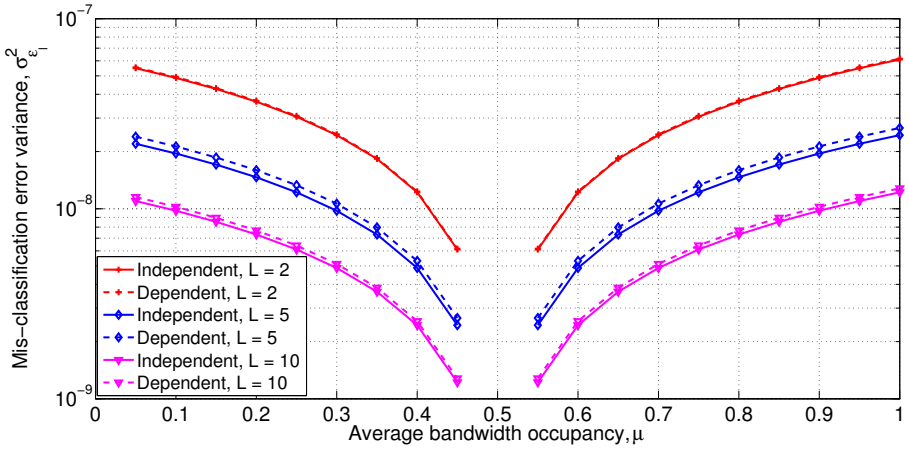

Figure 6.6: Impact of average consensus on mis–classification error for RSS, $p_{fa} = 0.0005, p_{md} = 0.0005, N_f = 4096$.

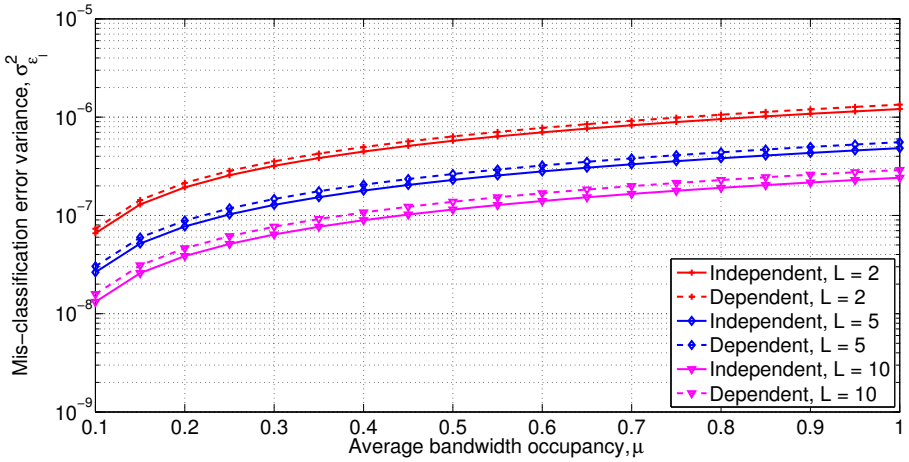

Figure 6.7: Impact of average consensus on mis–classification error for RSS, $p_{fa} = 0.0005, p_{md} = 0.01, N_f = 4096$.

6.6.2 CRSS in a Practical Scenario: Estimating APD tail distribution for Compliance Monitoring

In this set of experiments, the use CRSS was investigated for use in estimating the tail distribution for the APD. The APD is very useful in compliance monitoring since it gives an estimate of the probability that a signal transmission exceeds a given power level, given that it is over a particular threshold. It provides a way of estimating the probability that a given transmitter exceeds its spectral mask power, either in some subset or across the entire

channel. In this experiment, the use of CRSS was investigated via realistic simulations based upon spectrum measurements which were obtained from a measurement campaign to characterise spectrum occupancy across four mid-sized US cities. The measurements spanned frequencies between $88MHz - 2686MHz$ at twenty geographically separated sites, with five sites per city. Further details of the measurements can be obtained in [2]. Figs 6.8–6.10 present summary characteristics of the measurement data, used in the investigation.

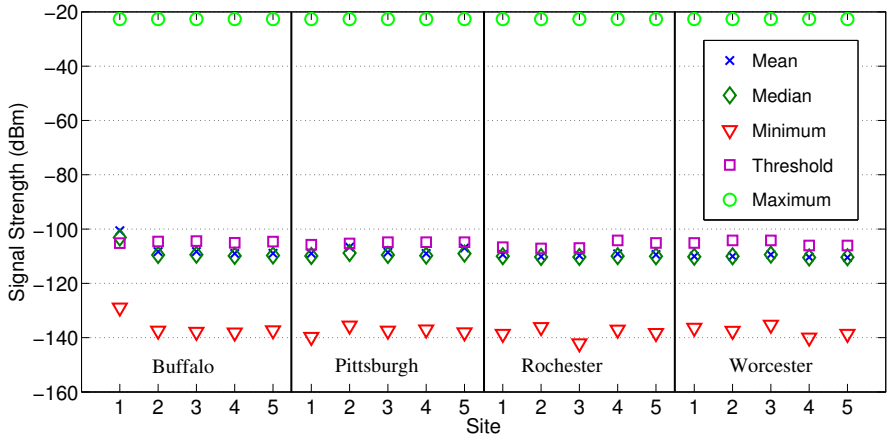

Figure 6.8: First–order statistic summary for measurement sites, illustrating the mean, median, maximum and minimum values of the measured power for the measurement interval. The threshold was the Otsu threshold obtained for the overall set of measurements at the site.

The illustrations additionally present further insights into the distribution of occupancy parameters across space and frequency. As seen in Fig 6.8 and Fig 6.9, at most sites the span of spectral occupancy variations at each site is similar, even though the percentile distributions are different. This can be explained by noting the different histograms at each site. When aggregated by city, the distributions exhibit less variation. This is notable since the measurements were all taken within mid–sized US cities. When compared by bands, (*i.e.*, Fig 6.10), the variation across sites is considerable. This can be explained by the geographic variation of spectrum usage for each sub–band.

RSS was used on the measurement data to investigate the impact of random sampling upon the estimation of the tail distribution via average consensus. Sensors were randomly placed within the grid representing the region within the measurements were taken. The

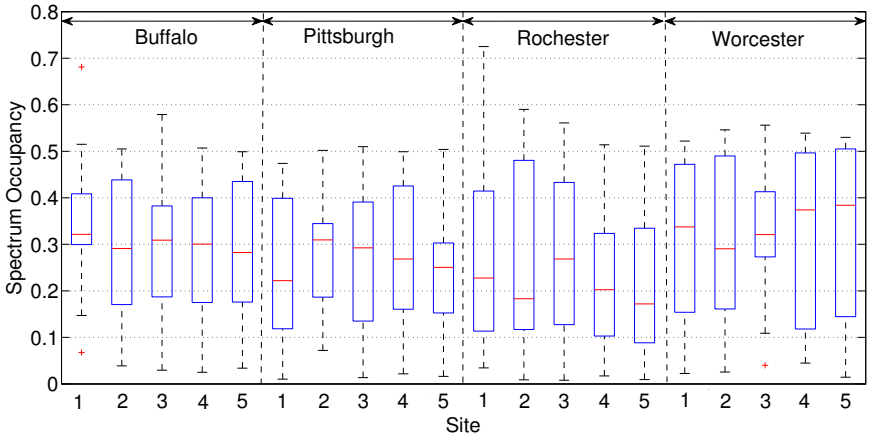

Figure 6.9: Overall occupancy for measurement sites, based upon the use of Otsu thresholding method for separating signal and noise signals.

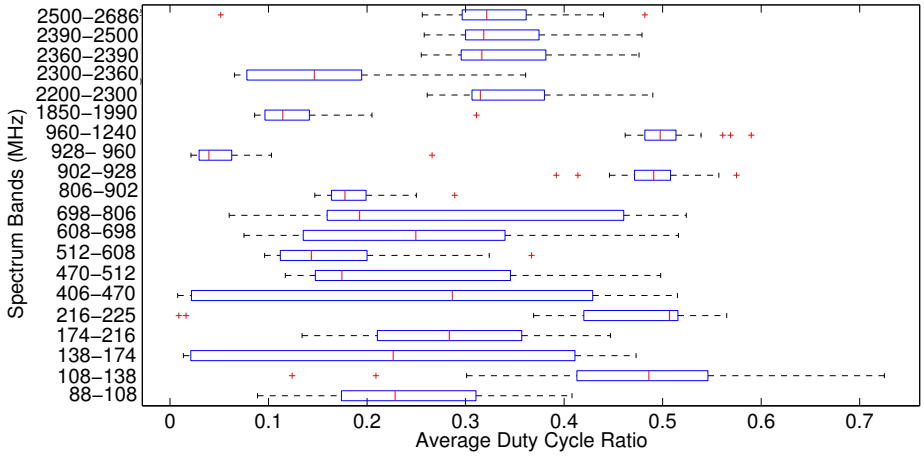

Figure 6.10: Overall occupancy by service bands, based upon the use of Otsu thresholding method for separating signal and noise signals.

measurement data was stratified according to service band. At each site, RSS was used to randomly select sub–intervals from which power measurements were obtained. To account for fading and path loss effects, the signals at each randomly placed sensor was based upon use of a path loss model which took into account the distance between the sensor and the actual measurement locations of the measurement data. Sensors were assumed to have the same resolution bandwidth, and amplitude errors due to calibration or other such effects were not considered.

For each sensor, the power measurements collected, were used to determine the overall

APD across all bands measured. L–moments were estimated for each sensor using the approach presented in [90]. Figs 6.11–6.14 illustrate the L–moment ratio diagrams of sample L–Skewness, τ_3, and L–Kurtosis, τ_4, for the simulated sensors at the 4 cities investigated in the measurement study. L–moment ratio curves of various distributions, as well as the overall lower bound of τ_4 as a function of τ_3, were overlaid on the diagram. The distributions selected were those typically used in the analysis of points over threshold and maxima. As seen, in each case the distribution of the extreme values was best approximated by the General Pareto distribution (GPD) curve.

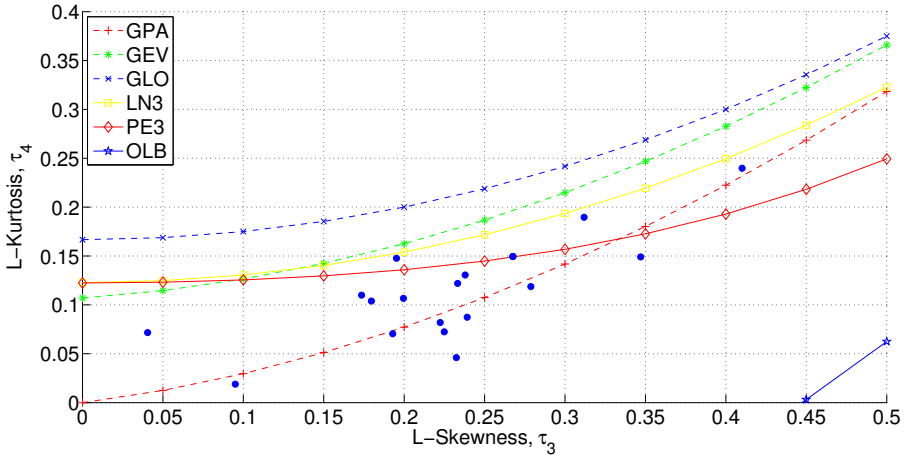

Figure 6.11: L–moment ratio diagram showing sample L–skewness (τ_3) and L–Kurtosis (τ_4) for 20 sites in Buffalo using RSS. Key to curves: general pareto (GPA), generalised extreme value (GEV), pearson type III (PE3), generalised logistic (GLO), log normal (LN3) and overall lower bound (OLB).

Finally, the average consensus was used to produce site–averaged L–moment ratios, which were then used to estimate the GPD parameters for the tail distribution. The method for estimating the GPD parameters from τ_3 and τ_4 were described in [90]. Figs 6.15–6.18 illustrate the results for the 4 cities based upon average consensus, using the GDP approximation. These were compared to the actual empirical data at each measurement site, in each city. The results suggest that CRSS can be used to further characterise the APD, which can then be used in probabilistic characterization of the probability of a transmitter violating its spectral mask, or some subset of it.

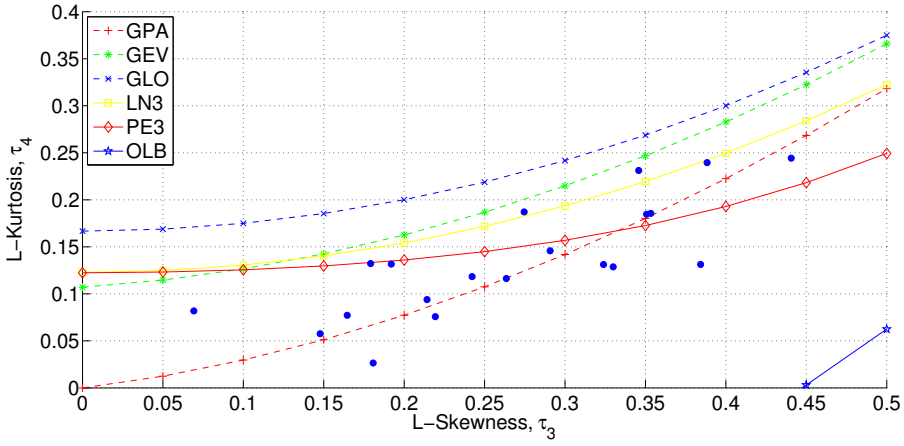

Figure 6.12: L–moment ratio diagram showing sample L–skewness (τ_3) and L–Kurtosis (τ_4) for 20 sites in Pittsburgh using RSS. Key to curves: general pareto (GPA), generalised extreme value (GEV), pearson type III (PE3), generalised logistic (GLO), log normal (LN3) and overall lower bound (OLB).

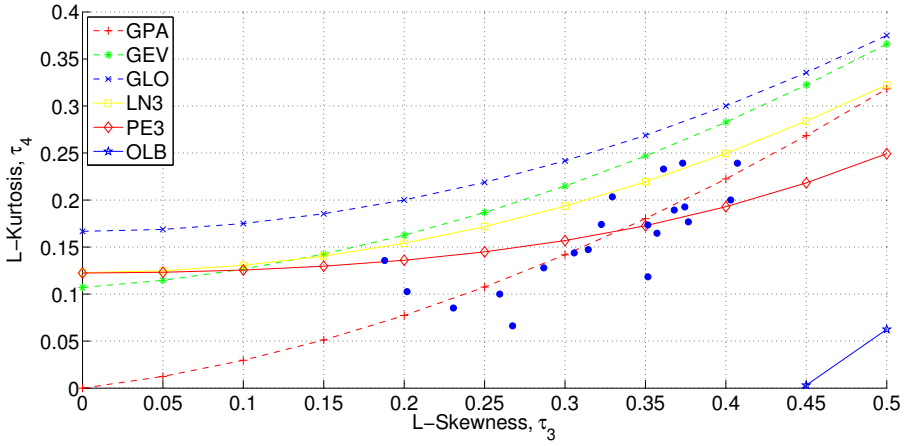

Figure 6.13: L–moment ratio diagram showing sample L–skewness (τ_3) and L–Kurtosis (τ_4) for 20 sites in Rochester using RSS. Key to curves: general pareto (GPA), generalised extreme value (GEV), pearson type III (PE3), generalised logistic (GLO), log normal (LN3) and overall lower bound (OLB).

6.6.3 Mobile CRSS

The work presented in this section is derived from work done as part of a research project with Toyota ITC. Further details of the system implementation used for this study can be found in [88]. A highway communications scenario is considered for investigation of Mobile RSS, to determine the impact of the proposed distance technique for average consensus on

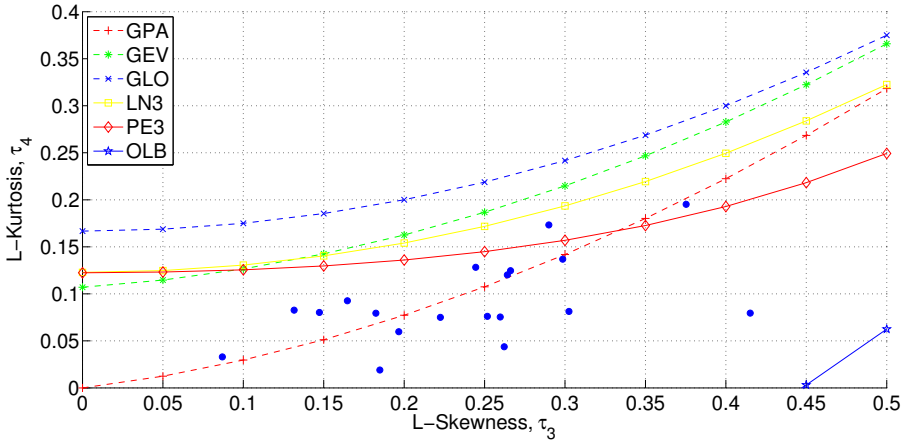

Figure 6.14: L–moment ratio diagram showing sample L–skewness (τ_3) and L–Kurtosis (τ_4) for 20 sites in Worcester using RSS. Key to curves: general pareto (GPA), generalised extreme value (GEV), pearson type III (PE3), generalised logistic (GLO), log normal (LN3) and overall lower bound (OLB).

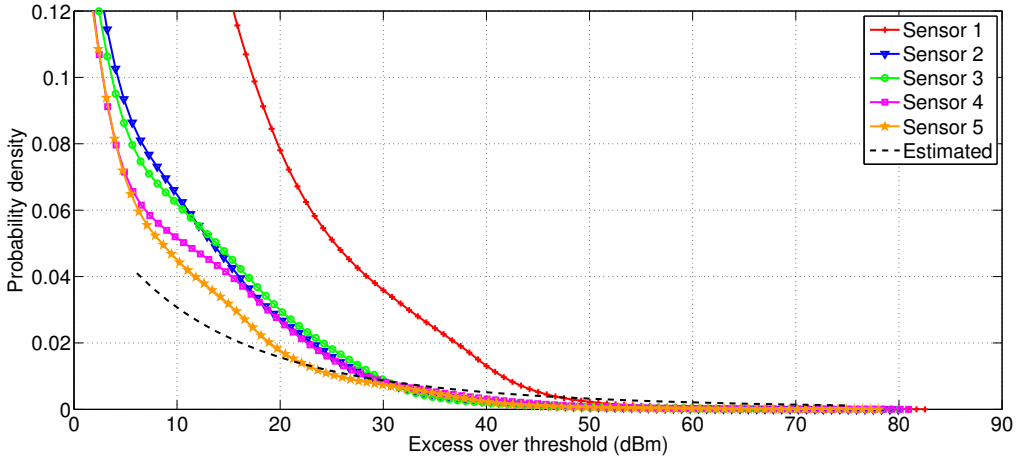

Figure 6.15: Comparison of APD tails for measurement data with GPD estimate in Buffalo using CRSS.

vehicles knowledge of sensed spectrum. This represents a spectrum monitoring approach in which vehicles need to better understand spectrum usage for use in channel selection for VDSA. Further details of this requirement and the application of the knowledge in VDSA can be found in [88, 198, 199].

Data collected via vehicle measurements along I–90 in Massachusetts [205] was used to create a realistic simulation environment for investigation. Artificial secondary TV whitespace device signals were superimposed on signals generated based upon measurement statis-

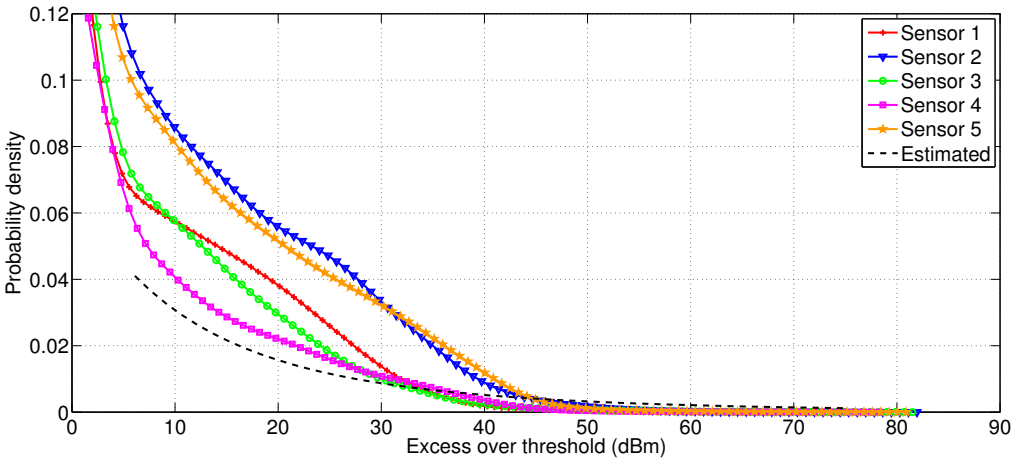

Figure 6.16: Comparison of APD tails for measurement data with GPD estimate in Pittsburgh using CRSS.

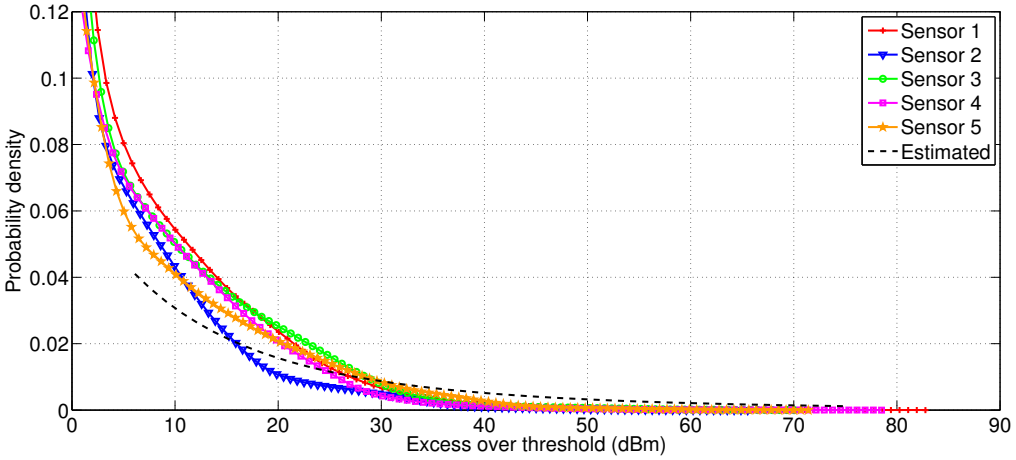

Figure 6.17: Comparison of APD tails for measurement data with GPD estimate in Rochester using CRSS.

tics for digital TV signals. For the simulation, there were 10 TV channels from channel 36 to channel 45. Artificial primary user signals are generated based upon the model in [199]. The Okumura–Hata model was used to calculate the actual received signal strength at a vehicle. Using road data for the study area, (Fig. 6.19), several routes were created offering vehicles alternate paths to transit between the given origin–destination pair. Alternate routes were all within 5 km of the primary I–90 route. Signal sources consisting of both fixed base–stations and mobile devices were randomly distributed within the region under consideration. Vehicles were assumed to have a random speed not exceeding 40m/s on the

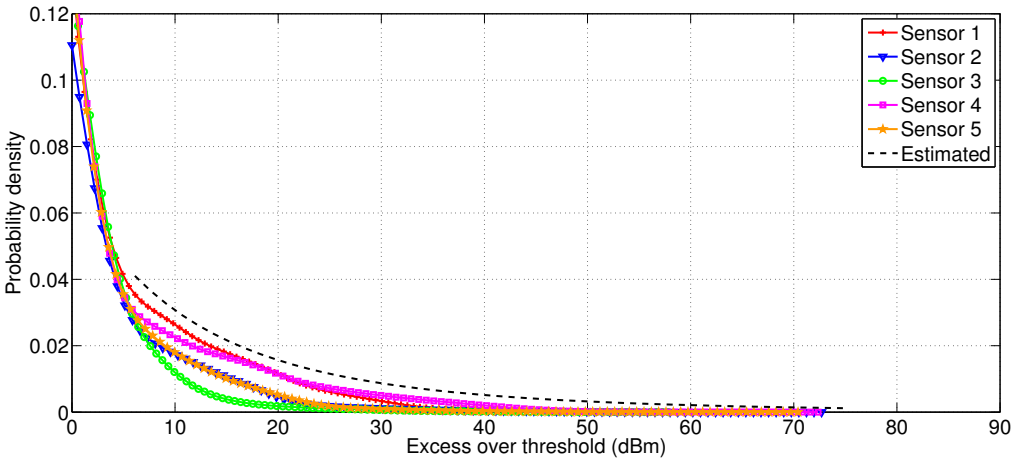

Figure 6.18: Comparison of APD tails for measurement data with GPD estimate in Worcester using CRSS.

I–90 and 25m/s on the alternate routes.

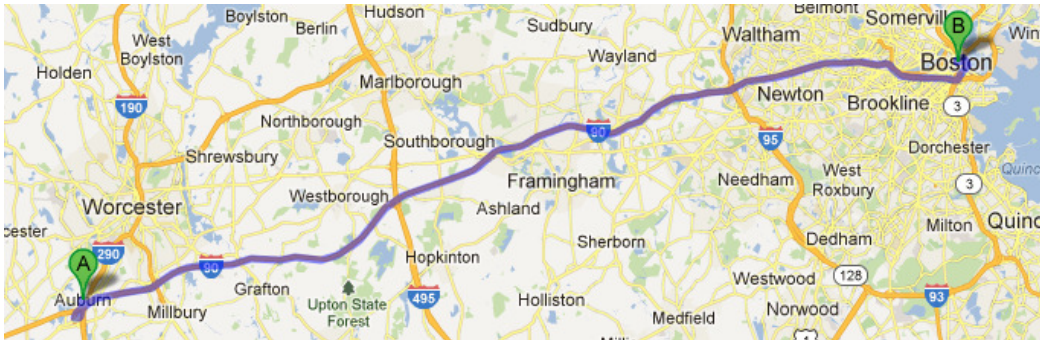

Figure 6.19: Map of study area.

Fig 6.20 illustrates the impact of MRSS on channel switching availability in VDSA. The results suggest that use of MRSS reduces the effective false alarm rate for occupancy detection. This therefore reduces the likelihood that a vehicle would switch channels unnecessarily. For this scenario, MRSS used $d_r = 2500$m. Fig. 6.21 illustrates the effect of varying d_r on the channel switching likelihood. The results suggest that increasing the range for consensus adversely affects averaging consensus performance. As the range is increased, the chances of a vehicle reporting an unoccupied channel as occupied is increased. An interesting result is that the channel switching would also be expected to increase with vehicular density as there are expected to be more attempts of using vacant channels for

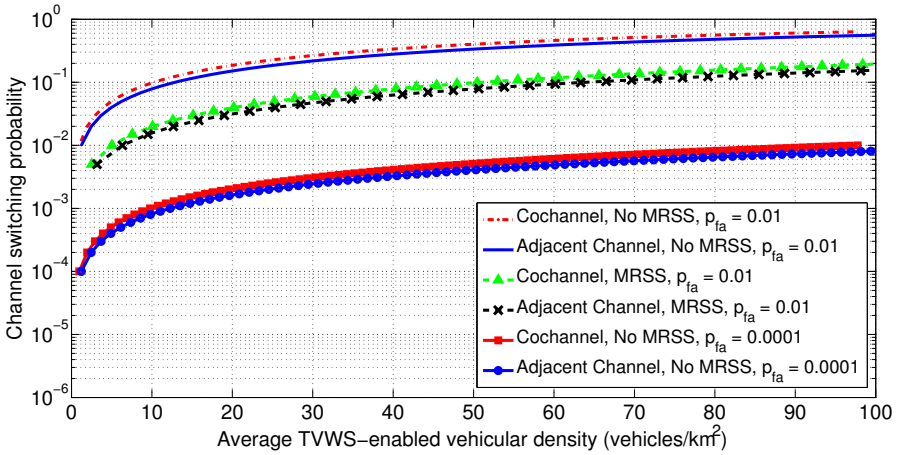

Figure 6.20: Impact of MRSS on channel switching probability. MRSS reduces the misclassification of occupied channels, reducing the effective false alarm rate for a given detector.

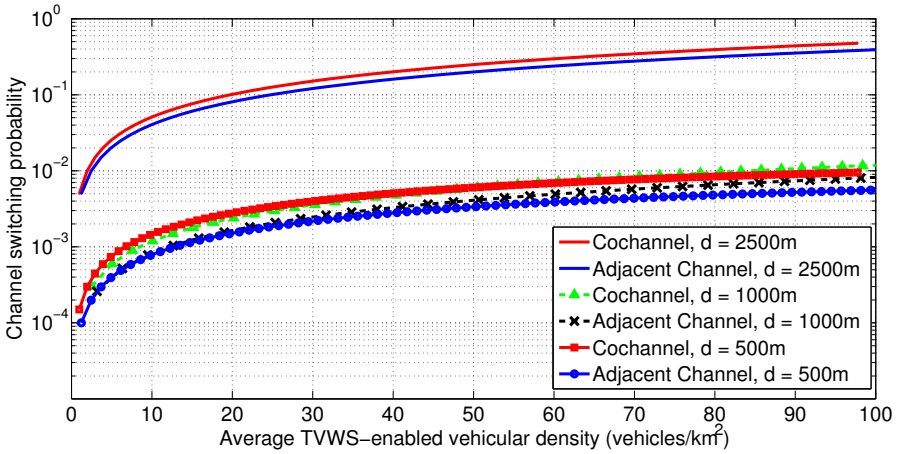

Figure 6.21: Impact of d_r on channel switching probability for MRSS, $p_{fa} = 0.01$. Increasing the d_r increases the chance of falsely detecting a channel as occupied.

VDSA. However, in the scenarios examined the occupancy profiles used for VDSA were low occupancy, to reduce the effect of this demand. However, the key results observed were that MRSS reduced the effective false alarm probability, and increasing the mobile network size for MRSS reduced MRSS performance.

6.7 Conclusion

In this chapter, the use of distributed and mobile randomised spectral sensing was investigated for occupancy estimation in several different scenarios. A framework for performance analysis of distributed sensing using the mis–classification error was presented for the task of bandwidth occupancy estimation using RSS. A lower bound on sensing performance in terms of mis–classification errors was derived. The lower bound was seen to be approximately normally–distributed, with decreasing variance as the number of sensors increased. The impact of incorporating spatial diversity was further considered in performance.

The use of average consensus algorithms was then investigated for two important compliance monitoring tasks in DSA: bandwidth occupancy classification and estimation of the APD for use in compliance monitoring. Both applications were observed to benefit from the use of CRSS, which improved the accuracy in estimating spectrum occupancy characteristics in various scenarios. Results demonstrated that performance was bounded across different occupancy levels: a) in terms of the mis–classification error performance and b) using actual measurements across several service bands from 4 mid–sized US cities to estimate the tail distributions of the APD at the measurement locations. This method is therefore recommended for statistical occupancy characterisation for various occupancy levels.

Mobile RSS was then considered and a distance–based approach was proposed for use in average consensus algorithms in vehicular networks, where convergence may be difficult at vehicular speeds. An implementation mobile random sensing using bi–directionally coupled simulation tools was then used for exploring average consensus performance in VDSA scenarios. The simulation platform was used to investigate the impact of MRSS on channel switching probabilities in VDSA networks. Channel switching was reduced through the use of MRSS. Further results for the proposed distance–based technique for bounding network size in mobile networks, was demonstrated to improve performance for VDSA.

While user discrimination was not considered in this chapter, the use of CRSS and MRSS for characterisation provides another opportunity for further work in incorporating spatial diversity for improvement of spectrum characterisation in DSA networks.

Chapter 7

Conclusions and Future Research

7.1 Conclusions

This dissertation presented various perspectives on the use of random sampling techniques for probabilistic characterisation of wireless spectrum occupancy across time, frequency, and space. Probabilistic characterisation was motivated by the potentially non–deterministic behaviour of cognitive radios in typical market–based spectrum access models, both those implemented and those currently being contemplated through regulatory interventions.

The state–of–the–art for spectrum monitoring was presented in this problem space, and several challenges were examined for spectrum management and compliance enforcement functions in emerging DSA networks. Probabilistic characterisation was seen as essential for occupancy estimation and compliance verification in DSA deployment scenarios, given the increased spectrum agility and learning abilities of cognitive radios. Therefore in this dissertation, a thesis is presented for the use of random sampling techniques in characterisation of probabilistic spectrum etiquette. This is in line with probabilistic approaches currently used in network management, for specification of technical and operational parameters and subsequently these specifications are met.

Four aspects of random sampling were examined in this dissertation: random spectral sampling for bandwidth occupancy classification, PHY–based random temporal sampling

and frame–based random temporal sampling for temporal occupancy characterisation, and distributed and mobile random spectral sampling. Random spectral sampling and PHY–based random temporal sampling techniques were implemented using the USRP2 hardware and experimented with, to explore different envisioned DSA scenarios. The benefits of the approaches were demonstrated for these cases. Frame–based random temporal sampling as well as distributed and mobile random spectrum sampling were also investigated in a simulation environment which was developed for this dissertation. This was used to provide a proof of concept and to further explore these methods using DSA technologies which are still under development. The parameters for the simulation environment were derived from various spectrum measurements taken within Massachusetts as well as in Trinidad and Tobago, during the course of this dissertation.

In support of wideband spectrum occupancy characterisation in heterogeneous radio access scenarios, such as those envisioned for future DSA networks, the NCSS concept was introduced as an alternative way of simultaneously sensing noncontiguous subbands. Based upon the presented framework bandwidth occupancy estimation using stratified sampling techniques and random spectral sampling was proposed and investigated using hardware and techniques developed as part of this dissertation. Experimental results demonstrate the effectiveness of this proposed technique for occupancy estimation, emphasizing the need for appropriate stratification techniques.

To achieve online stratification, a distancebased approach to automatic stratification was proposed for use with random spectral sampling for characterisation of bandwidth occupancy in spectrum monitoring networks. The proposed approach was validated via simulations, USRP hardware and through use of spectrum measurements. The results illustrated that the technique provides an automatic stratification approach and additionally exhibits similar performance in spectrum occupancy estimation, compared to established clustering approaches which are ill–suited for online use. The suitability of the technique for various occupancy levels was also demonstrated, motivating its use as a compressed sensing alternative for use in congested scenarios (*i.e.*, where the spectrum sparsity assumption which leads compressed sensing does not hold). The results support the thesis that random spectral sampling can be used in online wideband occupancy characterisation.

In support of temporal occupancy characterisation in heterogeneous access scenarios where there is no need to isolate specific users, PHY–based random temporal sensing techniques were proposed. In addition to the derivation of theoretical performance bounds for temporal occupancy estimation using the proposed techniques, a proof of concept was developed using USRP2 hardware upon which investigations were carried out. Results demonstrated that randomised temporal sensing can outperform periodic sensing, and indicated that random sampling performance approaches the theoretical lower bound using larger sample sizes, or through sparser sampling, for processes with decaying autocorrelation functions. Results further showed that cyclostationary detection techniques improved estimation performance over energy detection in low SNR scenarios. An added benefit of cyclostationary feature detection was for use in coarse discrimination between users with different cyclostationary features.

Random temporal sampling techniques were also demonstrated to perform better than compressed sensing techniques in medium to high occupancy scenarios. Therefore, compressed sensing approaches were seen to be less suited for use in temporal occupancy estimation in scenarios where spectrum congestion may occur. Further, the CSbased approach first reconstructs the signal prior to occupancy estimation. The reconstruction stage is avoided entirely in the random sampling approaches presented. Therefore, although specific comparisons of computational cost would be implementation specific, it can be said that the random approaches would be lower cost compared to CSbased techniques, all things being equal, since they do not have to reconstruct the signal for temporal occupancy estimation. The random sampling approach was therefore seen to offer a lower complexity alternative to existing techniques for characterisation of temporal spectrum occupancy.

Framebased random temporal sensing was then introduced as a means of statistically modelling the temporal behaviour of users/networks of interest, identified through PLCP frame semantics. The technique was explored for estimating the probabilistic distribution of several temporal occupancy parameters. Further, the impact of missed frame detection was examined for the proposed technique. Simulations using measured data were used to provide proof of concept for the presented technique. Results demonstrated the performance of the technique in estimating various occupancy parameters was dependent upon the sampling

ratios used. The technique was able to recover the approximate distribution of the number of frames as well as their inter–arrival times using the sampling inversion techniques, with better performance for higher sampling ratios.

Results further demonstrated that a probabilistic model relating nominal transmission times to frame reception times could also be estimated. This model provided essential information for determining the probability of particular transmission times, accounting for random channel effects in temporal occupancy characterisation, which is an important aspect of assessing temporal compliance in DSA networks. Through simulations, the model was determined to converge to bounded performance for all sampling ratios as the number of sampled frames increases.

Finally, distributed and mobile spectrum sensing were explored within the random sampling framework. A theoretical lower bound on random spectral sampling performance was derived for distributed sampling, which demonstrated that performance improved with increased spatial diversity, assuming average consensus algorithms were used. The use of average consensus algorithms was then investigated for two important compliance monitoring tasks in DSA: bandwidth occupancy classification and estimation of the APD for use in compliance monitoring. Investigations involved the use of bi–directionally–coupled vehicular network simulation tools for generation of more realistic mobility scenarios.

Results demonstrated that both applications benefit from the use of distributed random spectral sampling, which improved the accuracy in estimating spectrum occupancy characteristics in various scenarios. Results demonstrated that performance was bounded across different occupancy levels: a) in terms of the mis–classification error performance and b) using actual measurements across several service bands from 4 mid–sized US cities to estimate the tail distributions of the amplitude power distributions at the measurement locations. However, it was observed that in mobile sensing scenarios performance declined when average consensus approaches were used at typical vehicular speeds. Distance–based stratification was used to bound the size of the network used for convergence, which was observed to improve performance. This method is therefore recommended for statistical occupancy characterisation for various occupancy levels.

7.2 Future Work

In advancing the theory of random sampling approaches for compliance monitoring in DSA networks several challenges must still be addressed.

First, the techniques presented in this dissertation were for the purpose of demonstrating proof of concept for random sampling in statistical occupancy characterisation in emerging DSA networks. In some cases, it was possible to build hardware implementations, while in others it was reasonably practical to resort to simulations for analysis. Given the need for such techniques for compliance monitoring and verification in emerging DSA deployments, the contributions of this dissertation are only the beginning. Extended investigations should be carried out as DSA deployments and regulatory practices evolve to address the needs of spectrum management.

Also, further work would involve the use of the random techniques in more realistic scenarios, involving various occupancy models not examined in this dissertation. Also, theoretical performance bounds were established under certain scenarios. Tighter performance bounds can be established through relaxation of several assumptions made in this dissertation. In such cases, techniques such as Chernoff bounds can be used for establishing distributions of probabilistic characteristics with stronger guarantees of compliance to operational and technical specifications. Such tighter bounds would of particular use in dispute resolution and compliance enforcement processes.

Additionally, using the presented framework for analysis, investigation of higher order characteristics (*i.e.*, for time frequency, and space), as well as those not investigated in this dissertation should be carried out. The theory can additionally be advanced through investigation of improving sampling performance through use of alternative allocation techniques that are more sensitive to the variance and measurement 'cost' of the sampling technique (*e.g.*, cost–based, Neyman, optimal allocation).

Bibliography

[1] Spectrum Efficiency Working Group, "Report of the Spectrum Efficiency Working Group," et docket no. 02-135, Federal Communications Commission (FCC), Nov. 2002.

[2] S. Pagadarai and A. Wyglinski, "A quantitative assessment of wireless spectrum measurements for dynamic spectrum access," in *Proc. 4th Int. CROWNCOM Conf.*, pp. 1–5, Jun. 2009.

[3] R. Chiang, G. Rowe, and K. Sowerby, "A quantitative analysis of spectral occupancy measurements for cognitive radio," in *Proc. IEEE 65th Veh. Tech. Conf. - Spring*, pp. 3016–3020, Apr. 2007.

[4] S. Contreras, G. Villardi, R. Funada, and H. Harada, "An investigation into the spectrum occupancy in japan in the context of tv white space systems," in *2011 Sixth International ICST Conference on Cognitive Radio Oriented Wireless Networks and Communications*, pp. 341 –345, Jun. 2011.

[5] Shared Spectrum Company, "Spectrum Occupancy Reports." `http://www.sharedspectrum.com/papers/spectrum-reports/`, 2012.

[6] T. Taher, R. Bacchus, K. Zdunek, and D. Roberson, "Long-term spectral occupancy findings in chicago," in *IEEE DySPAN*, pp. 100 –107, May 2011.

[7] K. Patil, R. Prasad, and K. Skouby, "A survey of worldwide spectrum occupancy measurement campaigns for cognitive radio," in *2011 International Conference on Devices and Communications*, pp. 1 –5, Feb. 2011.

[8] V. N. Q. Bao, L. Q. Cuong, L. Q. Phu, T. D. Thuan, N. T. Quy, and L. M. Trung, "Vietnam spectrum occupancy measurements and analysis for cognitive radio applications," in *2011 International Conference on Advanced Technologies for Communications*, pp. 135 –143, Aug. 2011.

[9] K. Qaraqe, H. Celebi, A. Gorcin, A. El-Saigh, H. Arslan, and M.-s. Alouini, "Empirical results for wideband multidimensional spectrum usage," in *Proc. of IEEE 20th International Symposium on Personal, Indoor and Mobile Radio Communications*, pp. 1262 –1266, Sept. 2009.

[10] M. Lopez-Benitez, A. Umbert, and F. Casadevall, "Evaluation of spectrum occupancy in spain for cognitive radio applications," in *Proc. IEEE 69th Vehicular Technology Conference - Spring.*, pp. 1 –5, Apr. 2009.

[11] M. Lopez-Benitez, F. Casadevall, A. Umbert, J. Perez-Romero, R. Hachemani, J. Palicot, and C. Moy, "Spectral occupation measurements and blind standard recognition sensor for cognitive radio networks," in *Proc. 4th Int. CROWNCOM Conf.*, pp. 1 –9, Jun. 2009.

[12] M. Islam, C. Koh, S. Oh, X. Qing, Y. Lai, C. Wang, Y.-C. Liang, B. Toh, F. Chin, G. Tan, and W. Toh, "Spectrum survey in singapore: Occupancy measurements and analyses," in *Proc. 3rd Int. CROWNCOM Conf.*, pp. 1 –7, May 2008.

[13] IEEE, "IEEE Standard Definitions and Concepts for Dynamic Spectrum Access: Terminology Relating to Emerging Wireless Networks, System Functionality, and Spectrum Management," *IEEE Std 1900.1-2008*, pp. c1–48, Sep. 2008.

[14] W. I. Forum, "Quantifying the Benefits of Cognitive Radio," winnf-09-p-0012, Wireless Innovation Forum, 2010.

[15] J. Peha, "Sharing Spectrum through Policy Reform and Cognitive Radio," *Proc. of the IEEE*, vol. 97, pp. 708–719, Apr. 2009.

[16] C. Kim, C. Leem, S. Kang, and J. Lee, "Policy and Technology of Dynamic Spectrum Access in Korea," *Proc. 3rd Int. CROWNCOM Conf.*, pp. 1–4, May 2008.

[17] J. Bernthal, T. Brown, D. hatfield, D. Sicker, P. Tenhula, and P. Weiser, "Trends and Precedents Favoring a Regulatory Embrace of Smart Radio Technologies," *IEEE DySPAN*, pp. 633–648, Apr. 2007.

[18] M. El-Moghazi, F. Digham, and E. Azzouz, "Radio Spectrum Reform in Developing Countries," *IEEE DySPAN*, pp. 1–8, Oct. 2008.

[19] S. Delaere and P. Ballon, "Flexible Spectrum Management and the Need for Controlling Entities for Reconfigurabel Wireless Systems," *IEEE DySPAN*, pp. 347–362, Apr. 2007.

[20] A. Gad and F. Digham, "Impact of DSA on Current Regulatory Regimes," *IEEE DySPAN*, pp. 1–6, Oct. 2008.

[21] T. Hazzlett, "The wireless craze, the unlimited bandwidth myth, the spectrum faux pas, and the punchline to Ronald Coase's big joke: An essay on airwave allocation policy," *Harvard Journal of Law and Technology*, vol. 14, pp. 335–567, 2001.

[22] E. Hakanen, "On Autopilot inside the Beltway:Orgainzational Failure, the Doctrine of Localism, and the Case of Digital Audio Broadcasting," *Telematics and Informatics*, vol. 12, no. 1, pp. 11–20, 1995.

[23] W. Melody, "Radio spectrum allocation: role of the market," *American Economic Review*, vol. 70, no. 1, pp. 393–397, 1980.

[24] R. Schiphorst and C. Slump, "A Monitoring Network for Spectrum Governance," *Journal of RF Engineering and Telecommunications*, vol. 64, pp. 236–239, Nov./Dec. 2010.

[25] P. Kolodzy, "Dynamic Spectrum Policies: Promises and Challenges," *CommLaw Conspectus*, 2004.

[26] J. Brito, "The Spectrum Commons in Theory and Practice," *Stanford Technology Law Review*, Feb. 2007.

[27] R. Berger, "Open spectrum: A path to ubiquitous connectivity," *Queue*, vol. 1, no. 3, pp. 60–68, 2003.

[28] M. Buddhikot, "Understanding dynamic spectrum access: Models,taxonomy and challenges," in *IEEE DySPAN*, pp. 649–663, Apr. 2007.

[29] C. Evci and B. Fino, "Spectrum Management, Pricing, and Efficiency Control in Broad–band Wireless Communications," *Proc. of the IEEE*, vol. 89, pp. 105–115, Jan. 2001.

[30] C. Bazelon, "Next Generation Frequency Coordinator," *Telecommunications Policy*, vol. 27, no. 7, pp. 517–525, 2003.

[31] Microsoft Research, "Microsoft Research White Space Finder." `http://whitespaces.msresearch.us/WSWebGUI/whitespaces.aspx`.

[32] M. Mueck, M. Di Renzo, M. Debbah, and T. Renk, "Combination of centralized amp; decentralized database and terminal-based spectrum sensing for secondary spectrum access," in *Proc. IEEE Intnl Conf. on Wireless Information Technology and Systems*, pp. 1 –4, Sept. 2010.

[33] A. Stirling, "Exploiting hybrid models for spectrum access: Building on the capabilities of geolocation databases," in *Proc. IEEE DySPAN Conf.*, pp. 47 –55, May 2011.

[34] ITU-R, "Tasks of a monitoring service," ITU-R SM.1050-2, International Telecommunications Union, 2004.

[35] ITU-R, "Handbook on Spectrum Monitoring," tech. rep., International Telecommunications Union, 2011.

[36] ITU-R, "Mobile spectrum monitoring unit," ITU-R SM.1723-1, International Telecommunications Union, 2005.

[37] ITU-R, "Essential requirements for a spectrum monitoring system monitoring system for developing countries," ITU-R SM.1392-2, International Telecommunications Union, 2011.

[38] CFRS, "CFRS Website." `http://www.cfrs.com/`, 2013.

[39] CFRS, "Multi–User, Multi–Misson Remote Real–Time Spectrum Monitoring," *Microwave Journal*, Aug. 2012.

[40] FCC, "Second memorandum opinion and order: Federal Communication Commission," document 10-174, Federal Communications Commission, Sept. 2010.

[41] FCC, "CFR Title 47: Telecommunications, Part 15, Subpart H Television Band Devices," tech. rep., Federal Communications Commission, 2013.

[42] OFCOM, "Consultation document: Digital dividendcognitive access," tech. rep., The Office of Communications, Feb. 2009.

[43] OFCOM, "Digital dividend: Cognitive access; A statement on licence exempting cognitive devices using interleaved spectrum," tech. rep., The Office of Communications, Jul. 2009.

[44] ECMA, "Standard ECMA 392, MAC and PHY for Operation in TV White Space (2nd Edition)," tech. rep., ECMA International, Jun. 2012.

[45] IEEE, "IEEE Standard for Wireless Regional Area Networks Part 22: Cognitive Wireless RAN Medium Access Control (MAC) and Physical Layer (PHY) specifications: Policies and procedures for operation in the TV Bands," tech. rep., IEEE, Jul. 2011.

[46] IEEE, "Draft Standard for Information Technology - Telecommunications and Information Exchange Between Systems - Local and Metropolitan Area Networks - Specific Requirements - Part 11: Wireless LAN Medium Access Control (MAC) and Physical Layer (PHY) Specifications; Amendment: TV White Spaces Operation," tech. rep., IEEE, Jun. 2011.

[47] T. Baykas, "Workshop on TV White Space Coexistence: IEEE 802.19.1 Overview," tech. rep., IEEE, Jul. 2010.

[48] IEEE, "PAR: Radio Interface for White Space Dynamic Spectrum Access Radio Systems Supporting Fixed and Mobile Operation," tech. rep., IEEE, Jun. 2011.

[49] IEEE, "IEEE Recommended Practice for the Analysis of In-Band and Adjacent Band Interference and Coexistence Between Radio Systems," *IEEE Std 1900.2-2008*, pp. c1–94, Sep. 2008.

[50] IEEE, "IEEE Standard for Architectural Building Blocks Enabling Network-Device Distributed Decision Making for Optimized Radio Resource Usage in Heterogeneous Wireless Access Networks ," *IEEE Std 1900.4-2009*, pp. c1–119, 2009.

[51] IEEE, "IEEE Standard for Policy Language Requirements and System Architectures for Dynamic Spectrum Access Systems ," *IEEE Std 1900.5-2011*, pp. c1–51, 2011.

[52] IEEE, "IEEE Standard for Spectrum Sensing Interfaces and Data Structures for Dynamic Spectrum Access and other Advanced Radio Communication Systems," *IEEE Std 1900.6-2011*, pp. c1–168, 2011.

[53] H. Harada, P. Houze, L. Grande, and K. Moessner, "Ieee scc 41 standards for dynamic spectrum access networks." `https://mentor.ieee.org/802-sg-whitespace/dcn/09/sg-whitespace-09-0057-01-0000-ieee-scc41-standards-for-dynamic-spectrum-access-net pdf`, Mar. 2009.

[54] T. Yucek and H. Arslan, "A survey of spectrum sensing algorithms for cognitive radio applications," *IEEE Commun. Surveys Tuts.*, vol. 11, no. 1, pp. 116–130, 2009.

[55] J. Li, Z. Tan, S. Xu, and H. Wang, "Cooperative correlation based spectrum sensing for dmb-t systems," in *IEEE Vehicular Technology Conference, Spring*, pp. 1 –5, May 2010.

[56] D. Cabric, S. Mishra, and R. Brodersen, "Implementation issues in spectrum sensing for cognitive radios," in *38th Asilomar Conference on Signals, Systems and Computers*, vol. 1, pp. 772–776, Nov. 2004.

[57] J. Lunden, V. Koivunen, A. Huttunen, and H. V. Poor, "Spectrum sensing in cognitive radios based on multiple cyclic frequencies," in *Proc. 2nd Int. CROWNCOM Conf.*, pp. 37 –43, Aug. 2007.

[58] Z. Tian, "Compressed wideband sensing in cooperative cognitive radio networks," in *IEEE GLOBECOM*, pp. 1–5, Dec. 2008.

[59] Y. Polo, Y. Wang, A. Pandharipande, and G. Leus, "Compressive wide-band spectrum sensing," in *IEEE International Conference on Acoustics, Speech and Signal Processing*, pp. 2337 –2340, Apr. 2009.

[60] Y. Hur, J. Park, K. Kim, J. Lee, K. Lim, C.-H. Lee, H. Kim, and J. Laskar, "A cognitive radio (cr) testbed system employing a wideband multi-resolution spectrum sensing (mrss) technique," in *Proc. IEEE VTC–Fall*, pp. 1 –5, Sept. 2006.

[61] P. Wang, Z. Zhang, and G. Yu, "A wideband multi-resolution spectrum sensing method based on belief propagation," in *Fourth International Conference on Communications and Networking in China (ChinaCOM)*, pp. 1 –5, Aug. 2009.

[62] A. Ghasemi and E. Sousa, "Collaborative spectrum sensing for opportunistic access in fading environments," in *IEEE DySPAN*, pp. 131 –136, Nov. 2005.

[63] H. Moussavinik, W. Guibene, and A. Hayar, "Centralized collaborative compressed sensing of wideband spectrum for cognitive radios," in *International Congress on Ultra Modern Telecommunications and Control Systems and Workshops (ICUMT)*, pp. 246 –252, Oct. 2010.

[64] J. Meng, W. Yin, H. Li, E. Houssain, and Z. Han, "Collaborative spectrum sensing from sparse observations using matrix completion for cognitive radio networks," in *IEEE International Conference on Acoustics Speech and Signal Processing (ICASSP)*, pp. 3114 –3117, Mar. 2010.

[65] S. Hong, "Multi-resolution bayesian compressive sensing for cognitive radio primary user detection," in *IEEE GLOBECOM*, pp. 1 –6, Dec. 2010.

[66] F. Zeng, Z. Tian, and C. Li, "Distributed compressive wideband spectrum sensing in cooperative multi-hop cognitive networks," in *Proc. IEEE ICC*, pp. 1 –5, May 2010.

[67] Z. Tian and G. Giannakis, "Compressed sensing for wideband cognitive radios," in *IEEE ICASSP*, vol. 4, pp. 1357–1360, Apr. 2007.

[68] Z. Tian and G. Giannakis, "A wavelet approach to wideband spectrum sensing for cognitive radios," in *Cognitive Radio Oriented Wireless Networks and Communications, 2006. 1st International Conference on*, pp. 1–5, Jun.

[69] R. Chen and J.-M. Park, "Ensuring trustworthy spectrum sensing in cognitive radio networks," in *IEEE Workshop on Networking Technologies for Software Defined Radio Networks*, pp. 110–119, 2006.

[70] Z. Yuan, D. Niyato, H. Li, and Z. Han, "Defense against primary user emulation attacks using belief propagation of location information in cognitive radio networks," in *IEEE WCNC*, pp. 599–604, 2011.

[71] R. Chen, J.-M. Park, and J. Reed, "Defense against primary user emulation attacks in cognitive radio networks," *IEEE JSAC*, vol. 26, no. 1, pp. 25–37, 2008.

[72] G. Jakimoski and K. P. Subbalakshmi, "Denial-of-service attacks on dynamic spectrum access networks," in *IEEE ICC Workshops*, pp. 524–528, 2008.

[73] C. Sorrells, L. Qian, and H. Li, "Quickest detection of denial-of-service attacks in cognitive wireless networks," in *Proc. IEEE Conference on Technologies for Homeland Security*, pp. 580–584, 2012.

[74] A. Sethi and T. Brown, "Hammer model threat assessment of cognitive radio denial of service attacks," in *Proc. IEEE DySPAN Conf.*, pp. 1–12, 2008.

[75] T. Newman, T. Clancy, M. McHenry, and J. Reed, "Case study: Security analysis

of a dynamic spectrum access radio system," in *Proc. IEEE GLOBECOM*, pp. 1–6, 2010.

[76] Z. Gao, H. Zhu, S. Li, S. Du, and X. Li, "Security and privacy of collaborative spectrum sensing in cognitive radio networks," *IEEE Wireless Communications*, vol. 19, no. 6, pp. 106–112, 2012.

[77] G. Polyzos, G. Marias, S. Arkoulis, P. Frangoudis, M. Fiedler, A. Popescu, H. De Meer, R. Herkenhoner, A. Fischer, and J. Oberender, "Aspects: Agile spectrum security," in *EURO-NGI Conference on Next Generation Internet*, pp. 1–2, 2011.

[78] S. Arkoulis, L. Kazatzopoulos, C. Delakouridis, and G. Marias, "Cognitive spectrum and its security issues," in *International Conf. on Next Generation Mobile Applications, Services and Technologies*, pp. 565–570, 2008.

[79] H. Mao and L. Zhu, "An investigation on security of cognitive radio networks," in *Proc. International Conf. on Management and Service Science*, pp. 1–4, 2011.

[80] Y. Sixing, L. Shufang, and Y. Jixin, "Temporal-spectral data mining in anomaly detection for spectrum monitoring," in *Proc. International Conf. on Wireless Communications, Networking and Mobile Computing*, pp. 1–5, 2009.

[81] S. A. Kyriazakos, *Practical Radio Resources Management in Wireless Systems*. Artech House, Inc., 2004.

[82] Spectrum Bridge Inc., "Spectrum Bridge - Technology." `http://www.spectrumbridge.com/Technology/Technology.aspx`, 2013.

[83] J. Wang and V. Gaddam, "Feasibility study of sensing tv whitespace with local quiet zone," in *Proc. IEEE Int. Conf. on Systems, Man and Cybernetics*, pp. 2287 –2292, Oct. 2009.

[84] S. Y. Lee, M. K. Kwon, and S. H. Lee, "Transmit power control scheme for tv white space wireless system," in *Proc. ICACT*, pp. 1025 –1029, Feb. 2011.

[85] FCC, "FCC spectrum dashboard." `http://reboot.fcc.gov/reform/systems/spectrum-dashboard/`.

[86] S. Rocke and A. Wyglinski, "Wideband spectrum occupancy estimation using random spectral sampling in heterogeneous radio access environments," *IEEE Transactions on Vehicular Technology, Submitted*, 2013.

[87] S. Rocke and A. Wyglinski, "Randomized temporal spectrum sensing using periodic sampling sdr platforms," *IEEE Transactions on Vehicular Technology, Submitted*, 2013.

[88] S. Rocke and A. Wyglinski, "Knowledge-based dynamic channel selection in vehicular networks," *IEEE VNC 2012*, 2012.

[89] S. Rocke and A. Wyglinski, "Estimation of spectrum occupancy in heterogeneous radio access environments using random spectral sampling," in *Proc. 35th IEEE Sarnoff Symposium*, pp. 1 –6, May 2012.

[90] S. Rocke and A. Wyglinski, "Geo-statistical analysis of wireless spectrum occupancy using extreme value theory," in *Communications, Computers and Signal (PACRIM), 2011 IEEE Pacific Rim Conference on*, pp. 1–6, Aug. 2011.

[91] S. Rocke and A. Wyglinski, "Spectrum monitoring in dynamic access networks: Challenges and opportunities," *IEEE Communications Magazine, In Preparation*, 2013.

[92] S. Rocke and A. Wyglinski, "Non-uniform wideband spectrum sensing for spectrum monitoring in dynamic spectrum access networks," *Eurasip JWNC, In Preparation*, 2013.

[93] S. Rocke and A. Wyglinski, "Knowledge-based, non-contiguous, multi-resolution wideband spectrum sensing in heterogeneous radio access environments," *IET Signal Processing Special Issue, Submitted*, 2013.

[94] S. Rocke and A. Wyglinski, "Frame–based sampling inversion technique for spectrum occupancy estimation for dsa compliance verification," *IEEE Transactions on Wireless Communications, In Preparation*, 2013.

[95] S. Rocke and A. Wyglinski, "Knowledge-based dynamic channel selection for vehicular communications," *IEEE Vehicular Technology Magazine, In Preparation*, 2013.

[96] S. Rocke and A. Wyglinski, "On vehicular communications in tvws: Challenges and opportunities," *IEEE Communications Magazine, In Preparation*, 2013.

[97] ABI Research, "Research database." `http://www.abiresearch.com/research/databases/`.

[98] ITU, "ITU World Telecommunication/ICT Indicators Database." `http://www.itu.int/ITU-D/ict/statistics/`.

[99] J. W. Burns, "Measuring spectrum efficiency - the art of spectrum utilization metrics," in *Proc. of IEE Conf. on getting the most out of radio spectrum*, (London, UK), Oct. 2002.

[100] L. Berry, "Spectrum metrics and spectrum efficiency: Proposed definitions," *IEEE Trans. on Electromagn. Compat.*, vol. EMC-19, pp. 254–260, Aug. 1977.

[101] M. Cave, C. Doyle, and W. Webb, *Essentials of Modern Spectrum Management*. Cambridge University Press, 2007.

[102] M. McHenry, K. Steadman, and M. Lofquist, "Determination of detection thresholds to allow safe operation of television band "white space" devices," in *Proc. IEEE DySPAN Conf.*, pp. 1–12, Oct. 2008.

[103] J. T. MacDonald and D. A. Roberson, "Spectrum occupancy estimation in wireless channels with asymmetric transmitter powers," in *Proc. 2nd Int. CROWNCOM Conf.*, pp. 245–249, Aug. 2007.

[104] S. Jones, E. Jung, X. Liu, N. Merheb, and I.-J. Wang, "Characterization of spectrum activities in the u.s. public safety band for opportunistic spectrum access," in *Proc. IEEE IEEE DySPAN Conf.*, pp. 137–146, Apr. 2007.

[105] P. Marshall, *Quantitative Analysis of Cognitive Radio and Network Performance*. Norwood, MA: Artech House, 2010.

[106] T. W. Rondeau and C. W. Bostian, *Artificial Intelligence in Wireless Communications*. Norwood, MA: Artech House, 2009.

[107] H. N. Tran, M. Hasegawa, Y. Murata, and H. Harada, "Representation of user satisfaction and fairness evaluation for user-centric dynamic spectrum access," *Proc. of IEEE 20th Int. Symp. on Personal, Indoor and Mobile Radio Commun.*, pp. 838–842, Sep. 2009.

[108] C. Ghosh, S. Pagadarai, D. Agrawal, and A. Wyglinski, "A framework for statistical wireless spectrum occupancy modeling," *IEEE Trans. on Wireless Commun.*, vol. 9, pp. 38–44, Jan. 2010.

[109] C. Ghosh, S. Pagadarai, D. Agrawal, and A. Wyglinski, "Queueing theory representation and modeling of spectrum occupancy employing radio frequency measurements," in *Proc. IEEE VTC–Fall*, pp. 1–5, Sept. 2009.

[110] G. Hardin, "The tragedy of the commons," *Science*, vol. 162, pp. 1243–1248, 1968.

[111] E. Hossain, D. Niyato, and Z. Han, *Dynamic Spectrum Access and Management in Cognitive Radio Networks*. Cambridge, UK: Cambridge University Press, 2009.

[112] J. Mitola and J. Maguire, G.Q., "Cognitive radio: Making software radios more personal," *IEEE Personal Communications*, vol. 6, no. 4, pp. 13–18, 1999.

[113] S. Mangold, Z. Zhong, K. Challapali, and C.-T. Chou, "Spectrum agile radio: Radio resource measurements for opportunistic spectrum usage," in *IEEE GLOBECOM*, vol. 6, pp. 3467–3471, 2004.

[114] L. Berlemann, S. Mangold, and B. H. Walke, "Policy–based reasoning for spectrum sharing in radio networks," in *IEEE DySPAN*, pp. 1–10, 2005.

[115] S. Haykin, "Cognitive radio: Brain-empowered wireless communications," *IEEE Journal on Selected Areas in Communications*, vol. 23, no. 2, pp. 201–220, 2005.

[116] ITU-R, "Definitions of Software Defined Radio (SDR) and Cognitive Radio System (CRS)," ITU-R SM.2152, International Telecommunications Union, 2009.

[117] ETSI, "Reconfigurable Radio Systems (RRS); Cognitive Radio System Concept," etsi tr 102 802, ETSI, 2009.

[118] B. Fette, *Cognitive Radio Technology*. Newnes, 2006.

[119] S. Russell and P. Norvig, *Artificial Intelligence: A Modern Approach*. Prentice Hall, 3 ed., 2010.

[120] Infodev/ITU, "ICT Regulation Toolkit - Module 5: Radio Spectrum Management." `http://www.ictregulationtoolkit.org/en/Section.1247.html`.

[121] J. G. Prokis and D. K. Manolakis, *Digital Signal Processing (4th Edition)*. Prentice Hall, 4 ed., 2006.

[122] J. Kurose and K. Ross, *Computer Networking: A Top-Down Approach*. Addison-Wesley, 5 ed., 2009.

[123] H. Sizun, *Radio Wave Propagation for Telecommunications Applications*. Springer-Verlag, 2003.

[124] N. Blaunstein and C. ChristoDoulou, *Radio Propagation and Adaptive antennas for Wireless Communications Links: Terrestrial, Atmospheric, and Ionospheric*. Wiley, 2007.

[125] S. Saunders and Zavala, *Antennas and Propagation for Wireless Communication Systems*. Wiley, 2 ed., 2007.

[126] S. Kumar, *Foundations of Coverage for Wireless Sensor Newtorks*. PhD thesis, Ohio State University, 2006.

[127] S. Meguerdichian, F. Koushanfar, M. Potkonjak, and M. Srivastava, "Coverage problems in wireless ad-hoc sensor network," in *Proc. IEEE ICC*, pp. 1380–1387, 2001.

[128] S. Meguerdichian, F. Koushanfar, G. Qu, and M. Srivastava, "Exposure in wireless ad-hoc sensor network," in *Proc. IEEE International Conference on Mobile Communications*, pp. 139–150, 2001.

[129] L. Gueguen and B. Sayrac, "Traffic prediction from wireless environment sensing," in *Proc. IEEE Wireless Commun. and Netw. Conf.*, pp. 1–5, Apr. 2009.

[130] FCC, "Spectrum Analysis: Options for Broadcast Spectrum, OBI Tech. Paper No. 3." `http://download.broadband.gov/plan/fcc-omnibus-broadband-initiative-(obi)-technical-paper-spectrum-analysis-options-for-broadband-spectrum.pdf`.

[131] H. Palaiyanur, K. Woyach, R. Tandra, and A. Sahai, "Spectrum zoning as robust optimization," in *Proc. IEEE DySPAN Conf.*, pp. 1–12, Apr. 2010.

[132] T. Reddy, B. Manoj, and R. Rao, "On the accuracy of sampling schemes for wireless network characterization," in *IEEE WCNC*, pp. 3314 –3319, Apr. 2008.

[133] L. Gueguen, B. Sayrac, and D. Depierre, "Spectogram reconstruction from random sampling: Application to the gsm band sensing," in *IEEE Int. Conf. on Commun.*, pp. 1–5, Jun. 2009.

[134] ITU-R, "Spectrum Occupancy Measurement," ITU-R SM.1880, International Telecommunications Union, 2011.

[135] B. Farhang-Boroujeny and R. Kempter, "Multicarrier communication techniques for spectrum sensing and communication in cognitive radios," *IEEE Communications Magazine*, vol. 46, pp. 80 –85, Apr. 2008.

[136] D. Thomson, "Spectrum estimation and harmonic analysis," *Proceedings of the IEEE*, vol. 70, pp. 1055 – 1096, sept. 1982.

[137] B. Farhang-Boroujeny, "Filter bank spectrum sensing for cognitive radios," *IEEE Transactions on Signal Processing*, vol. 56, pp. 1801 –1811, May 2008.

[138] K. Jaiswal, "Spectral sensing of adaptive frequency hopping signal for cognitive radio," in *IEEE International Performance, Computing and Communications Conference*, pp. 360 –365, Dec. 2008.

[139] D. W. K. Andrews, "An empirical process central limit theorem for dependent non-identically distributed random variables," *Journal of Multivariate Analysis*, vol. 38, Aug. 1991.

[140] N. Guillotin-Plantard and C. Prieur, "Central limit theorem for sampled sums of dependent random variables," *ArXiv e-prints*, Dec. 2007.

[141] R. M. d. Jong, "Central limit theorems for dependent heterogeneous random variables," *Econometric Theory*, vol. 13, pp. pp. 353–367, Jun. 1997.

[142] S. L. Lohr, *Sampling: Design and Analysis*. Duxbury Press, 1 ed., Dec. 1999.

[143] S. J. Saeed and R. A. Shellhammer, *TV White Space Spectrum Technologies: Regulations, Standards, and Applications*. CRC Press, May 2011.

[144] N. Otsu, "A threshold selection method from gray-level histograms," *IEEE Trans. on Systems, Man and Cybernetics*, vol. 9, pp. 62–66, Jan. 1979.

[145] M. Steinbach, P.-N. Tan, and V. Kumar, *Introduction to data mining*. Addison-Wesley, us ed ed., May 2005.

[146] P. Vaidyanathan, "Multirate digital filters, filter banks, polyphase networks, and applications: a tutorial," *Proc. of the IEEE*, vol. 78, pp. 56 –93, Jan. 1990.

[147] J. A. Gubner, *Probability and Random Processes for Electrical and Computer Engineers*. Cambridge University Press, 2006.

[148] S. Rocke and A. Wyglinski, "Randomized temporal spectrum sensing in dynamic spectrum access networks," *IET Communications, In Preparation*, 2013.

[149] M. Steenstrup, "Opportunistic use of radio-frequency spectrum: a network perspective," in *IEEE DySPAN 2005*, pp. 638 –641, Nov. 2005.

[150] C. Cordeiro, K. Challapali, and M. Ghosh, "Cognitive phy and mac layers for dynamic spectrum access and sharing of tv bands," in *Proceedings of the first international workshop on Technology and policy for accessing spectrum*, TAPAS '06, (New York, NY, USA), ACM, 2006.

[151] H. Kim and K. Shin, "Efficient discovery of spectrum opportunities with mac-layer sensing in cognitive radio networks," *IEEE Transactions on Mobile Computing*, vol. 7, pp. 533 –545, may 2008.

[152] H. Kim and K. Shin, "Fast discovery of spectrum opportunities in cognitive radio networks," in *IEEE DySPAN*, pp. 1–12, Oct. 2008.

[153] H. Du, Z. Wei, Y. Yang, and D. Yang, "Sensing overhead and average detection time mitigation for sensing scheduling algorithm," in *18th International Conference on Telecommunications (ICT)*, pp. 216 –220, May 2011.

[154] S. Kandeepan, A. Giorgetti, and M. Chiani, "Periodic spectrum sensing performance and requirements for detecting legacy users with temporal and noise statistics in cognitive radios," in *IEEE GLOBECOM Workshops*, pp. 1 –6, Dec. 2009.

[155] R. Xu, M. Chen, C. Tian, X. Lu, and C. Diao, "On the periodic scheduling of spectrum sensing for cognitive radio," in *International Conference on Wireless Communications and Signal Processing (WCSP)*, pp. 1 –6, Nov. 2011.

[156] D. Donoho and Y. Tsaig, "Recent advances in sparsity-driven signal recovery," in *IEEE ICASSP*, vol. 5, pp. 713–716, 2005.

[157] D. Donoho, "Compressed sensing," *IEEE Trans. on Information Theory*, vol. 52, no. 4, pp. 1289–1306, 2006.

[158] E. Candes, J. Romberg, and T. Tao, "Robust uncertainty principles: exact signal reconstruction from highly incomplete frequency information," *IEEE Trans. on Information Theory*, vol. 52, no. 2, pp. 489–509, 2006.

[159] Q. Liang, M. Liu, and D. Yuan, "Channel estimation for opportunistic spectrum access: Uniform and random sensing," *IEEE Transactions on Mobile Computing*, vol. PP, no. 99, p. 1, 2011.

[160] X. Wang, Z. Zhao, N. Zhao, and H. Zhang, "On the application of compressed sensing in communication networks," in *Proc. CHINACOM'10*, pp. 1 –7, Aug. 2010.

[161] Z. Tian, "Cyclic feature based wideband spectrum sensing using compressive sampling," in *Proc. IEEE ICC*, pp. 1–5, 2011.

[162] E. Rebeiz, V. Jain, and D. Cabric, "Cyclostationary-based low complexity wideband spectrum sensing using compressive sampling," in *Proc. IEEE ICC*, pp. 1619–1623, 2012.

[163] D. Zou, X. Zhang, and W. Wang, "Multi-service traffic models of heterogeneous wireless communication networks," in *7th World Congress on Intelligent Control and Automation*, pp. 495 –498, Jun. 2008.

[164] M. Stasiak, P. Zwierzykowski, and J. Wiewiora, "Wcdma interface in umts network carrying a mixture of multi-rate traffic with different priorities," in *International Conference on Telecommunications*, pp. 254 –259, May 2009.

[165] S. M. Ross, *Stochastic Processes*. Wiley, 2 ed., Jan. 1995.

[166] D. R. Cox, *Renewal Theory*. Wiley, 1962.

[167] S. Castellanos-Lopez, F. Cruz-Perez, and G. Hernandez-Valdez, "Performance of cognitive radio networks under on/off and poisson primary arrival models," in *IEEE PIMRC*, pp. 609–613, 2011.

[168] J. Heo, J. Shin, J. Nam, Y. Lee, J.-G. Park, and H.-S. Cho, "Mathematical analysis of secondary user traffic in cognitive radio system," in *Proc. IEEE VTC–Fall*, pp. 1–5, 2008.

[169] V. Pla, J.-R. Vidal, J. Martinez-Bauset, and L. Guijarro, "Modeling and characterization of spectrum white spaces for underlay cognitive radio networks," in *Proc. IEEE ICC*, pp. 1–5, 2010.

[170] D. Pacheco-Paramo, V. Pla, and J. Martinez-Bauset, "Optimal admission control in cognitive radio networks," in *Proc. 4th Int. CROWNCOM Conf.*, pp. 1–7, 2009.

[171] T. Baykas, M. Kasslin, M. Cummings, H. Kang, R. Paine, A. Reznik, R. Saeed, and S. Shellhammer, "Developing a standard for tv white space coexistence: Technical

challenges and solution approaches," in *IEEE Wireless Communications*, pp. 10–22, Feb. 2012.

[172] S. Kawade, "Long-range communications in licence-exempt tv white spaces: An introduction to soft-licence concept," in *Proc. 6th Int. CROWNCOM Conf.*, pp. 141 –146, Jun. 2012.

[173] J. Mwangoka, P. Marques, and J. Rodriguez, "Exploiting tv white spaces in europe: The cogeu approach," in *IEEE DYSPAN*, pp. 608 –612, May 2011.

[174] N. Hohn and D. Veitch, "Inverting sampled traffic," *IEEE/ACM Trans. Netw.*, vol. 14, pp. 68–80, Feb. 2006.

[175] N. Antunes and V. Pipiras, "Probabilistic sampling of finite renewal processes," *Bernoulli*, vol. 17, no. 4, pp. 1285–1326, 2011.

[176] N. Duffield, C. Lund, and M. Thorup, "Properties and prediction of flow statistics from sampled packet streams," in *Proc. ACM SIGCOMM Workshop on Internet measurment*, IMW '02, (New York, NY, USA), pp. 159–171, ACM, 2002.

[177] L. Yang and G. Michailidis, "Sampled based estimation of network traffic flow characteristics," in *IEEE INFOCOM*, pp. 1775–1783, 2007.

[178] P. Tune and D. Veitch, "Towards optimal sampling for flow size estimation," in *Proc. ACM SIGCOMM Conf. on Internet Measurement*, IMC '08, (New York, NY, USA), pp. 243–256, ACM, 2008.

[179] C. Estan and G. Varghese, "New directions in traffic measurement and accounting," *SIGCOMM Comput. Commun. Rev.*, vol. 32, pp. 323–336, Aug. 2002.

[180] R. Clegg, R. Landa, H. Haddadi, M. Rio, and A. Moore, "Techniques for flow inversion on sampled data," in *IEEE INFOCOM Workshops*, pp. 1–6, 2008.

[181] N. Duffield, C. Lund, and M. Thorup, "Estimating flow distributions from sampled flow statistics," in *Proceedings of the 2003 Conference on applications, tech-*

nologies, architectures, and protocols for computer communications, SIGCOMM '03, (New York, NY, USA), pp. 325–336, ACM, 2003.

[182] M. Bogstead and S. Pitts, "Decompounding random sums: A nonparametric approach," *Annals of the Institute of Statistical Math*, vol. 62, no. 5, pp. 855–872, 2010.

[183] B. Buchmann and R. Grubel, "Decompounding: An estimation problem for poisson random sums," *The Annals of Statistics*, vol. 31, no. 4, pp. 1054–1074, 2003.

[184] B. Buchmann and R. Grubel, "Decompounding poisson random sums: Recursively truncated estimates in the discrete case," *The Annals of the Institute of Statistical Math*, vol. 56, no. 4, pp. 743–756, 2004.

[185] P. Hall and J. Park, "Nonparametric inference about service time distribution from indirect measurement," *ournal of the Royal Statistical Society. Series B. Statistical Methodology*, vol. 66, no. 4, pp. 861–875, 2004.

[186] M. Hansen and S. Pitts, "Nonparametric inference from the m/g/1 workload," *Bernoulli*, vol. 12, no. 4, pp. 737–759, 2006.

[187] V. Frost and B. Melamed, "Traffic modeling for telecommunications networks," *IEEE Communications Magazine*, vol. 32, no. 3, pp. 70–81, 1994.

[188] A. Adas, "Traffic models in broadband networks," *IEEE Communications Magazine*, vol. 35, no. 7, pp. 82–89, 1997.

[189] D. Murray and T. Koziniec, "The state of enterprise network traffic in 2012," in *Proc. of 18th Asia-Pacific Conf. on Communications*, pp. 179–184, 2012.

[190] D. R. Cox and V. Isham, *Point Processes*. Chapman and Hall, 1980.

[191] A. F. Carr, *Point Processes and their Statistical Inference*. Marcel Dekker, Inc, 1991.

[192] F. Johansson, "A fast algorithm for reversion of power series," 2011.

[193] C. Sommer and F. Dressler, "Progressing Toward Realistic Mobility Models in VANET Simulations," *IEEE Communications Magazine*, vol. 46, pp. 132–137, November 2008.

[194] R. Schiphorst and C. Slump, "Evaluation of Spectrum Occupancy in Amsterdam Using Mobile Monitoring Vehicles," *Proc. IEEE VTC–Spring*, pp. 1–5, May 2010.

[195] R. Popescu-Zeletin, I. Radusch, and M. Rigani, *Vehicular-2-X Communication: State-Of-The-Art and Research in Mobile Vehicular Ad Hoc Networks*. Springer, 2010.

[196] A. J. Ghandour, K. Fawaz, and H. Artail, "Data delivery guarantees in congested vehicular ad hoc networks using cognitive networks.," in *IEEE IWCMC*, pp. 871–876, 2011.

[197] ERTICO, "Cooperative vehicle-infrastructure systems (CVIS) EU FP-7 project," 2006-2010.

[198] S. Chen, R. Vuyyuru, O. Altintas, and A. Wyglinski, "Learning in vehicular dynamic spectrum access networks: opportunities and challenges," in *2011 International Symposium on Intelligent Signal Processing and Communications Systems*, pp. 1–6, Dec. 2011.

[199] S. Chen, R. Vuyyuru, O. Altintas, and A. Wyglinski, "On optimizing vehicular dynamic spectrum access networks: Automation and learning in mobile wireless environments," in *IEEE VNC*, pp. 39–46, Nov. 2011.

[200] K.-S. Huang, C.-H. Lin, and P.-A. Hsiung, "A space-efficient and multi-objective case-based reasoning in cognitive radio," in *2010 IET International Conference on Frontier Computing. Theory, Technologies and Applications*, pp. 25 –30, Aug. 2010.

[201] M. Fernandez and S. Williams, "Closed-form expression for the poisson-binomial probability density function," *IEEE Trans. on Aerospace and Electronic Systems*, vol. 46, no. 2, pp. 803–817, 2010.

[202] L. Xiao, S. Boyd, and S.-J. Kim, "Distributed average consensus with least–mean–square deviation," in *Journal of Parallel and Distributed Computing*, vol. 67, pp. 33–46, 2007.

[203] L. Xiao, S. Boyd, and S. Lall, "A scheme for robust distributed sensor fusion based on average consensus," in *Fourth International Symposium on Information Processing in Sensor Networks*, pp. 63–70, 2005.

[204] A. Sarwate and A. Dimakis, "The impact of mobility on gossip algorithms," *IEEE Trans. on Information Theory*, vol. 58, no. 3, pp. 1731–1742, 2012.

[205] S. Pagadarai, A. Wyglinski, and R. Vuyyuru, "Characterization of vacant uhf tv channels for vehicular dynamic spectrum access," *IEEE VNC*, pp. 1–8, Oct. 2009.